UNIVERSIDAD YACHAY TECH

UNIVERSIDAD DE INVESTIGACIÓN DE TECNOLOGÍA EXPERIMENTAL YACHAY

Escuela de Ciencias Biológicas e Ingeniería

Título: Chemical and Biological Characterization of Saline Soil from Santa Catalina of Salinas, Imbabura Province- Ecuador

Trabajo de integración curricular presentado como requisito para la obtención del título de Biomedicina

Autora:
JAZMÍN ALEXANDRA GONZÁLEZ FLORES
jazmin.gonzalez@yachaytech.edu.ec

Tutor:
PH. D NELSON SANTIAGO VISPO
nvispo@yachaytech.edu.ec

Co- tutores:

PH. D HORTENSIA RODRIGUEZ
hmrodriguez@yachaytech.edu.ec

PH. D YANIEL VÁZQUEZ
yvazquez@yachaytech.edu.ec

Urcuquí, agosto 2021

SECRETARÍA GENERAL
(Vicerrectorado Académico/Cancillería)
ESCUELA DE CIENCIAS BIOLÓGICAS E INGENIERÍA
CARRERA DE BIOMEDICINA
ACTA DE DEFENSA No. UITEY-BIO-2021-00031-AD

A los 13 días del mes de agosto de 2021, a las 15:00 horas, de manera virtual mediante videoconferencia, y ante el Tribunal Calificador, integrado por los docentes:

Presidente Tribunal de Defensa	Dr. GUDIÑO GOMEZJURADO, MARCO ESTEBAN , Ph.D.
Miembro No Tutor	Dr. GONZALES ZUBIATE, FERNANDO ALEXIS , Ph.D.
Tutor	Dr. SANTIAGO VISPO, NELSON FRANCISCO , Ph.D.

El(la) señor(ita) estudiante **GONZALEZ FLORES, JAZMIN ALEXANDRA**, con cédula de identidad No. **1803272606**, de la **ESCUELA DE CIENCIAS BIOLÓGICAS E INGENIERÍA**, de la Carrera de **BIOMEDICINA**, aprobada por el Consejo de Educación Superior (CES), mediante Resolución **RPC-SO-43-No.496-2014**, realiza a través de videoconferencia, la sustentación de su trabajo de titulación denominado: **CHEMICAL AND BIOLOGICAL CHARACTERIZATION OF THE SALINAS OF THE PARISH OF SANTA CATALINA PROVINCE OF IMBABURA -ECUADOR**, previa a la obtención del título de **INGENIERO/A BIOMÉDICO/A**.

El citado trabajo de titulación, fue debidamente aprobado por el(los) docente(s):

Tutor	Dr. SANTIAGO VISPO, NELSON FRANCISCO , Ph.D.

Y recibió las observaciones de los otros miembros del Tribunal Calificador, las mismas que han sido incorporadas por el(la) estudiante.

Previamente cumplidos los requisitos legales y reglamentarios, el trabajo de titulación fue sustentado por el(la) estudiante y examinado por los miembros del Tribunal Calificador. Escuchada la sustentación del trabajo de titulación a través de videoconferencia, que integró la exposición de el(la) estudiante sobre el contenido de la misma y las preguntas formuladas por los miembros del Tribunal, se califica la sustentación del trabajo de titulación con las siguientes calificaciones:

Tipo	Docente	Calificación
Miembro Tribunal De Defensa	Dr. GONZALES ZUBIATE, FERNANDO ALEXIS , Ph.D.	9,8
Tutor	Dr. SANTIAGO VISPO, NELSON FRANCISCO , Ph.D.	10,0
Presidente Tribunal De Defensa	Dr. GUDIÑO GOMEZJURADO, MARCO ESTEBAN , Ph.D.	10,0

Lo que da un promedio de: **9.9 (Nueve punto Nueve)**, sobre 10 (diez), equivalente a: **APROBADO**

Para constancia de lo actuado, firman los miembros del Tribunal Calificador, el/la estudiante y el/la secretario ad-hoc.

Certifico que *en cumplimiento del Decreto Ejecutivo 1017 de 16 de marzo de 2020, la defensa de trabajo de titulación (o examen de grado modalidad teórico práctica) se realizó vía virtual, por lo que las firmas de los miembros del Tribunal de Defensa de Grado, constan en forma digital.*

GONZALEZ FLORES, JAZMIN ALEXANDRA
Estudiante

MARCO ESTEBAN GUDINO GOMEZJURADO
Firmado digitalmente por MARCO ESTEBAN GUDINO GOMEZJURADO
Fecha: 2021.08.13 16:42:59 -05'00'

Dr. GUDIÑO GOMEZJURADO, MARCO ESTEBAN , Ph.D.
Presidente Tribunal de Defensa

Dr. SANTIAGO VISPO, NELSON FRANCISCO , Ph.D.
Tutor

Dr. GONZALES ZUBIATE, FERNANDO ALEXIS , Ph.D.
Miembro No Tutor

ALARCON FELIX, KARLA ESTEFANIA
Secretario Ad-hoc

Autoría

Yo, **Jazmín Alexandra González Flores**, con cédula de identidad 1803272606, declaro que las ideas, juicios, valoraciones, interpretaciones, consultas bibliográficas, definiciones y conceptualizaciones expuestas en el presente trabajo; así cómo, los procedimientos y herramientas utilizadas en la investigación, son de absoluta responsabilidad de el/la autora (a) del trabajo de integración curricular. Así mismo, me acojo a los reglamentos internos de la Universidad de Investigación de Tecnología Experimental Yachay.

Urcuquí, agosto 2021.

JAZMIN
ALEXANDRA
GONZALEZ
FLORES

Firmado
digitalmente por
JAZMIN
ALEXANDRA
GONZALEZ FLORES
Fecha: 2021.08.24
15:54:47 -05'00'

_____
Jazmín Alexandra González Flores
1803272606

AUTORIZACIÓN DE PUBLICACIÓN

Yo, **Jazmín Alexandra González Flores**, con cédula de identidad 1803272606, cedo a la Universidad de Investigación de Tecnología Experimental Yachay, los derechos de publicación de la presente obra, sin que deba haber un reconocimiento económico por este concepto. Declaro además que el texto del presente trabajo de titulación no podrá ser cedido a ninguna empresa editorial para su publicación u otros fines, sin contar previamente con la autorización escrita de la Universidad.

Asimismo, autorizo a la Universidad que realice la digitalización y publicación de este trabajo de integración curricular en el repositorio virtual, de conformidad a lo dispuesto en el Art. 144 de la Ley Orgánica de Educación Superior

Urcuquí, agosto 2021

JAZMIN ALEXANDRA GONZALEZ FLORES

Firmado digitalmente por JAZMIN ALEXANDRA GONZALEZ FLORES
Fecha: 2021.08.24 15:55:39 -05'00'

Jazmín Alexandra González Flores
1803272606

This page is intentionally left blank.

Dedicatory

This thesis is in honor of my entire family.

To my parents Vilma Flores and Luis Alberto González, thank you for showing me how to overcome adversity. To my loving uncle Fernando Muñoz, who has always guided me in the right direction. Leonardo and Patricia González, my siblings, for their unfaltering affection. Finally, I'd want to thank my dear Iván Goottman, who helped me deal with day-to-day issues with his advice.

Thank you so much from the bottom of my heart

to each and every one of you.

Jazmín González

Acknowledgements

"Make a point to continually search for a better way of doing things, even when things are going well, to ensure that a better alternative has not been overlooked and to keep your creative talents in practice."

John Maxwell

I want to express my gratitude to God, who with his blessing always fills my life.

To begin, I would like to express my gratitude to my tutor Nelson Santiago Vispo Ph. D, who accompanied me through this research and helped me obtain the outcomes I desired. To my co-tutors Hortensia Rodriguez Ph. D and Yaniel Vázquez Ph. D., for their unwavering support throughout the process, especially Vázquez Ph. D., who remained committed to the research work at all times. I would also like to express my gratitude to Edward Vila, Ph.D., and Lola De Lima, Ph.D., who guided me in their different fields of expertise.

My gratitude also goes out to the Faculty of Chemical Sciences and Engineering and the Faculty of Biological Sciences and Engineering for providing me with all of the information and skills I needed to complete this research project effectively.

I would also like to express my gratitude to Yachay Tech Technology Research University for providing me with all of the materials and tools I needed to complete the research. I would not have been able to attain my goals without your continuous support.

Finally, I would want to thank my family and coworkers for their steadfast support during this process., even when my spirits were down. In particular, I would like to thank my uncle Fernando Patricio Muñoz, who was always there to provide me words of encouragement and a comforting hug to renew my energy.

Jazmín González

This page is intentionally left blank.

Resumen

Este trabajo analiza el material de la sal extraída de las montañas ya que desde las épocas pre colombinas era un preciado artículo, debido a su escasez y a su alto contenido en yodo. Al realizar el proceso de extracción de sal en la parroquia de Santa Catalinas de Salinas Ibarra, desde hace algún tiempo un subproducto ha tenido origen. El sub producto es un linimento el cual es conocido por los habitantes de este sector como solución yodada. Esta solución se caracteriza por ser de color marrón oscuro, la cual al dejarlo reposar por aproximadamente siete meses se torna aceitosa. Los habitantes del sector usan este linimento como un anti inflamatorio, además de un antiséptico el cual se aplica después de las picaduras de mosquitos. Por ello, este estudio busca una caracterización preliminar del linimento y de las muestras recogidas de las tolas, estas se caracterizan por sus propiedades higroscópicas. Para facilitar el estudio, las tolas fueron divididas en tres partes, superior medio y base del mismo modo el linimento. Este primer enfoque se logró a través de un proceso integral que incluyó (1) la extracción de las fracciones polares y no polares de las muestras, (2) la evaluación mineralógica y el estudio semicuantitativo de los compuestos utilizando un XRD difractómetro y SEM, y (3) actividad antibacteriana utilizando la prueba de difusión en agar o la técnica de prueba de Kirby-Bauer. Este estudio busca potenciar las capacidades locales además de respaldar este conocimiento empírico con aportes científicos.

Palabras clave: linimento, anti inflamatorio, antiséptico, tolas, propiedades higroscópicas, actividad antibacteriana.

Abstract

This study examines mountain salt, which has been a valuable commodity since pre-Columbian times due to its rarity and high iodine concentration. In Santa Catalina of Salinas-Ibarra, it gives from of salt extraction process, a by-product has originated, for some time. People in this sector recognize this liniment as an ionized solution. This solution is dark brown and turns oily after sitting for about seven months. The inhabitants of Santa Catalina de Salinas-Ibarra, use liniment as an anti-inflammatory and antiseptic; the latter is applied after mosquito bites. As a result, the goal of this research is to get a preliminary characterization of the liniment and the tolas samples which have hygroscopic characteristics. To make the study easier the tolas were split into three sections: top, middle, and base, similar to how the liniment was divided. This first approach was achieved through a comprehensive process that included (1) extracting the polar and non-polar fractions of the samples, (2) mineralogical assessment and semi-quantitative study of the compounds using an XRD-diffractor and SEM, and (3) antibacterial activity using the agar diffusion test or Kirby-Bauer test technique. This study seeks to enhance local capacities in addition to supporting this empirical knowledge with scientific contributions.

Key Words: liniment, hygroscopic properties, tolas, antiseptic, anti- inflammatory, antibacterial activity.

Table of Content

List of Figures

List of Tables

List of Annex

Chapter 1. Introduction and Field Area

1.1 General Introduction

Ethnohistorians of Latin America have recorded the influential role of salts, such as in the culture, economy, diet, and medicine, using colonial records of the period (1). The salt is a starting point to focus on a community, and as such, it is different in each town. In other words, the salt produced by Latin America's indigenous community has an inherent meaning within each community (2). For this reason, it is essential to know its history and thus extrapolate ourselves to the pre-Columbian period to conceive of salt as a cultural feature.

The salt mines' production and its importance due to its high iodine content have been mentioned in Ecuadorian ethnographic history (3). According to the ethnographic records, some of the extraction sites in the Sierra Andina of Ecuador have been determined, such as Salinas de Bolívar and Salinas de Imbabura (4).

Salt consumption habits were used as ethnic markers in the settlements of the highlands of Ecuadorian. This tells us, Pomeroy (1986), in his book 'Salt in Andean Cultures, where the salt extraction works were coordinated at the family level, and women were piece important at this activity. The processing tasks were a traditional female specialty that required relatively labor-intensive grinding techniques. However, they only produced small salt-perhaps between 300 and 500 tons per year (5).

In the 16th century, salt was sold and promoted throughout the Andes of Ecuador and its lowlands (5). The salt of the mountains and sea salt was not relatively dispersed in all Ecuadorian areas. Despite this, mineral salt has been observed in the northern, central highlands and in portions of the eastern and coastal lowlands (1). By the 1570s, however, sea salt's trading sphere covered most of the Ecuadorian highlands (5,6). This is because the Spaniards preferred the sea salt that frequently arrived in Quito at the time of colonization. After all, the salt from the mine or the first conquerors as "La Salinas" salt was brown and bitter (2).

In the mountainous region, cultural differences from the nineteenth century in salt were notable, causing Quichua prejudices. The pre-Hispanic indigenous society, for instance, judged individuals who did not eat salt every day, branding them as uncivilized. The Ecuadorian highlands considered salt and chili's use in meals to be a privilege that distinguishes an adequate livelihood from deprivation (7). This explains why the "Sichos Angamarcas Indians," located

in the west of the current province of Cotopaxi, exchanged salt for gold (5,8). This led to the fact that salt was seen as a central point in whole trade networks, that is to say, as a "standard Exchange item" or currency (9).

It should be noted that the Andean people have been favored by mineral salt not only for culinary use but also as a medicinal agent for human and animal organisms since the 16th century (1,5,9). It was used in the latter, La Salinas de Bolivar, as a herd's diarrhea medication. For instance, in the book 'Salt in Andean Cultures' a farmer from the Salinas region comments that this salt relieved his Glander-sick horses, a bacterial disease that affects Equidae (5,10). No experiments to validate iodized salt as a medication against Burkholderia mallei bacteria have been identified at present. However, an investigation of the Epidemiology, Control, and Prevention of Equine Glanders carried out in 2016 mentions that iodine has proven to be very used to disinfect B. mallei (11).

Moreover, it is said that when added to the body of cattle, salt from La Salina makes it fatter and gives it more strength (9). In his book 'Iodine for Livestock,' Corrie (1929) shows us that one of the iodine's roles in an animal's body is to stimulate growth and prevent causes that affect livestock development. In winter, one of the tests conducted to test this claim was to isolate the animals. Thus, 179 kgs more were obtained by the group that received iodized salt than the group that received only the basic ration. Consequently, Corrie states that there would be no physical growth if there is a significant iodine deficiency, but it indicates an inadequate diet if this deficiency is mild (12). Therefore, not only in animals but also in humans, iodine deficiency has caused severe complications.

Iodine deficiency disabilities (DDI) have become an issue that has led to seeing patients with goiter and severe neurological defects that impair their sight, voice, their way of walking(13). The literature shows us that the endemic goiter-cretin was a widespread disease in all countries in the 1930s, were in various periods, the incidence of goiter was more than 50% (14). In the Ecuadorian case, the nutritional importance of iodine salt is also a matter of its iodine content. Sea salt contains virtually no iodine, whereas montane salt is high in iodine. According to the 1957 study undertaken by the National Institute of Nutrition in Ecuador at the end of the decade, it was shown that endemic goiter was a significant issue of public health (15). According to historical literature, since the 18th century, the local community has treated this disease with the "odiferous salt flats of the Andes" (16).

Furthermore, it is essential to mention that since the 1500s BC in ancient Egypt, the administration of iodized salt served as prophylaxis for goiter. The same happened in the 1950s when Switzerland successfully implemented salt iodization to prevent goiter and endemic

cretinism (13). However, this disease continues to be a health problem that currently affects a high percentage of the world's population, 741 million individuals (17).

Even though unrefined sea salt is cheaper and more beneficial, Santa Catalina de Salinas follows the tradition of providing artisanal salt. Besides, this by-product is in great demand by this sector's inhabitants due to reduces body swelling and acts as an antiseptic after mosquito bites.

1.2 Problem Statement

Natural medicinal products contain active principles: chemical compounds with antioxidant, antibacterial, anti-inflammatory capabilities, among other bioactivities. These properties are used as a raw material for non-sterile pharmaceuticals, nutritional supplements, and dietary supplements (18). For a long time, Mrs. Ney Canpusino Torres, current connoisseur of the benefits given by ointment that is derived as a by-product of the salt extraction process in the Santa Catalina de Salinas parish of the Ibarra canton. From this ointment or liniment has precipitated a solution known as an iodized solution among the residents of this parish. After a few months of rest, this solution is used to treat inflammatory processes and natural mosquito repellent. This research aims to characterize the solution obtained through various extraction processes chemically using Fourier Transform infrared spectroscopy (FTIR), HPLC, X-ray diffraction analysis (XRD), and Scanning Electron Microscopy (SEM).

1.3 General and specific objectives

1.3.1 General objective

To carry out a preliminary investigation of a saline solution acquired by the salt extraction process in the parish of Santa Catalina de Salinas, Ibarra, utilizing extraction methods and characterization processes in order to determine the chemical compounds in the samples.

1.3.2 Specific objectives

1. To separate chemical molecules of the samples obtained by determining the organic composition using polar and non-polar fractions.

2. To perform the fractions' characterization using Fourier Transform infrared spectroscopy (FTIR), High-Performance Liquid Chromatography (HPLC), X-ray diffraction analysis (XRD), and Scanning Electron Microscopy (SEM).
3. To evaluate the antibacterial biological activity

1.4 Motivation

Remedies are as old as humanity itself (19). Numerous written testimonies from various civilizations and cultures document man's use of these natural products as alternative medicine (20). However, scholars and medical science practitioners have only recently become more involved in this field due to increased awareness of the natural health benefits. The World Health Organization (WHO) has supported the use of traditional and alternative medicine since 1976, providing that the benefits and existence of minimal risk for the patient have been proved through scientific rigor (20,21).

On the other hand, traditional medicine has been used to treat and care for patients with ailments that cause inflammatory processes in natural antibacterial products.
In this sense, traditional medicine today is widely used in the world; for example, in Africa, its use is above 80%, in China around 40%, while in Asia and Latin America, populations continue to use traditional medicine, as a result of historical circumstances and cultural beliefs, including many developed countries. They use traditional medicine, complementary and alternative medicine like this: 75% in France, 70% in Canada, 48% in Australia, 42% in the USA, and 38% in Belgium (22).

1.5 Field Area

The Santa Catalina de Salinas parish, located in the Imbabura province's Ibarra canton (**Figure 1**), is one of the Imbabura Geopark's geological and cultural sites of interest, as it helps us to learn about the region's geological history and events that have shaped its socio-cultural characteristics (23). The Imbabura Geopark aims to research, visualize, and promote geological heritage as a long-term territorial growth approach based on education and geo-tourism (24).
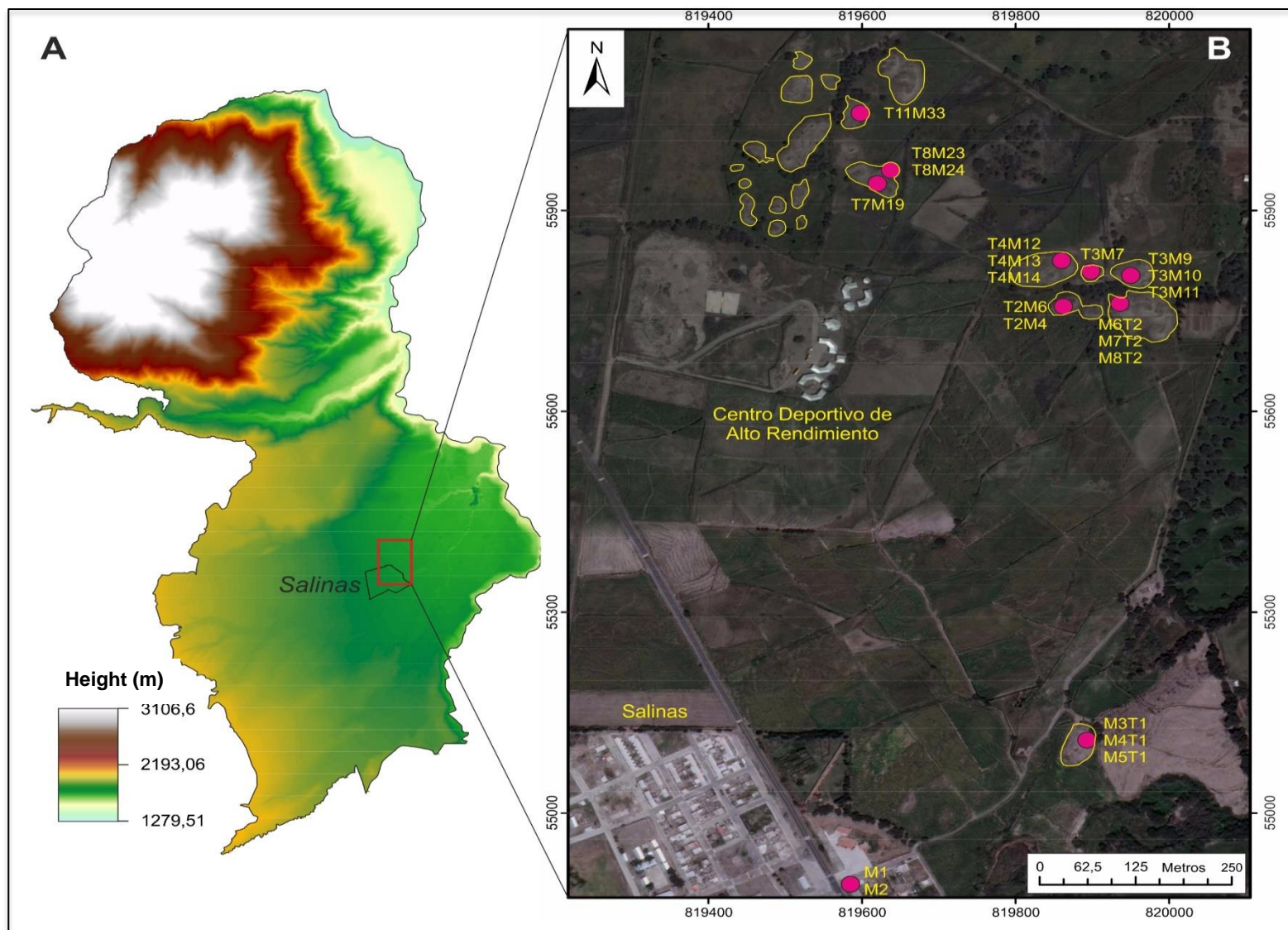
Figure 1. *Elevation model of the parish's terrain (A) and the location (B) of the Tolas and samples under investigation.*

The research area is part of the Chota-Salinas ancestral territory. In the XVII century, a group of African-Americans arrived in this village; a place where indigenous people had previously populated. This occurred as a result of the first Spanish landlords around 1550. The landlords wanted to increase the number of indigenous people who served in agricultural activities sowed grapes, cotton, olive trees, and sugar cane. However, indigenous exploitation failed, and as a result, black slaves were brought into the Salinas sector, giving rise to the current Afro-Ecuadorian population (25).

The parish of Santa Catalina de Salinas adopts its name due to salinized soils and the salt extraction process's historical link (25). As a result, salt production emerged as a new economic activity. The most plentiful residue has been leached soil that has traditionally been stacked up or piled up in mounds called Tolas during the extraction process. (**Figure 1B.**). Because Santa Catalina of Salinas has tangible and intangible assets registered as Cultural Heritage with Ecuador's National Institute of Cultural Heritage, the parish is currently considered an archaeological site in Ecuador (INPC). The Tolas, are considered a tangible heritage because it is associated with ancient wisdom in medicine, popular legends, and artisan legacy (26,27).

Santa Catalina of Salinas is located approximately 25.5 km north of the provincial capital (28).It limits to the north with the La Carolina parish of the Ibarra canton, to the south with the Urcuquí parishes of the San Miguel de Urcuquí and San Miguel of Ibarra of the Ibarra canton, to the east with the Juan Montalvo and Mira parishes of the Mira canton, belonging to the Province del Carchi, and the west with the parishes of Cahuasquí, Pablo Arenas and Tumbabiro of the San Miguel of Urcuquí canton (**Figure 2.**). The parish covers an area of 77.79km^2 (26). The parish's main rivers are: the Salinas, which originates near Tumbabiro; the Palacara, which rises in the Piñán paramos above Cahuasqui; and the Amarillo, Salado, and Jerónimo, which all originate in the same paramo; the Amarillo, Salado, and Jerónimo rivers, all began in the same moors. The minor rivers, such as Guallupe, San Pedro, Buenavista, Chinambi, Paramba, and Cachiyacu, are situated in the north and descend from the Chilluro branch (29). These rivers drain the surface waters of the highlands and are part of the Mira River's watershed (30).
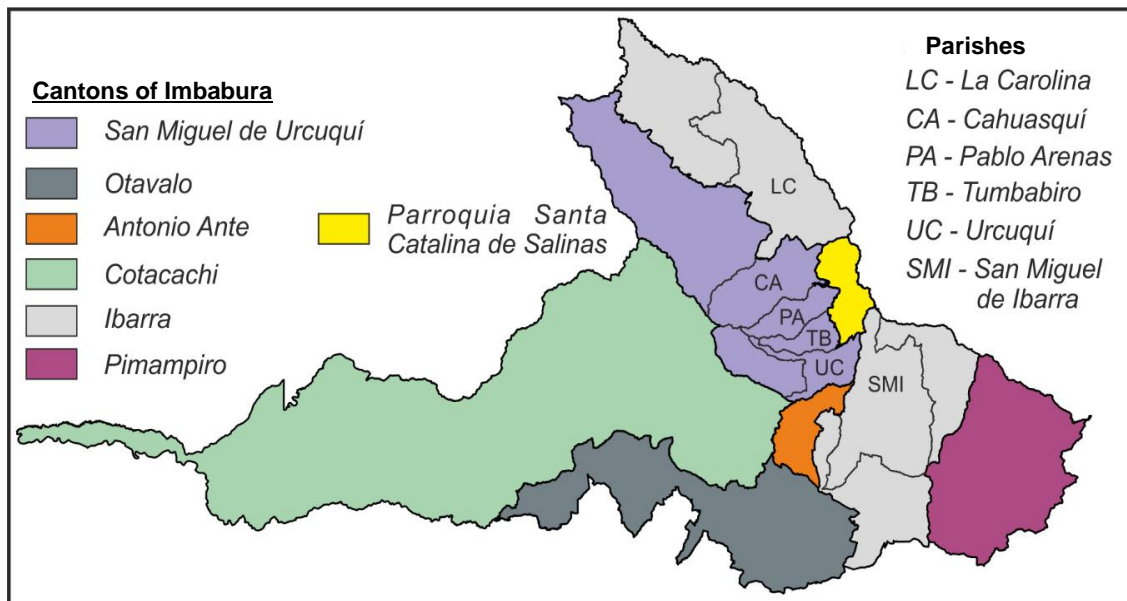
Figure 2. *The province of Imbabura, its six cantons, the research area (parish of Salinas), and the parish limits in general.*

Salinas' warm climate is primarily due to its location within the Andean Cordillera and its orography. The primary factors that control the climate in alpine systems, such as the Andes, are variations in height or altitude, distance to the oceans, and orographic barriers (31–33). Salinas is part of the Inter Andean Valley, an elongated depression with an NNE-SSW course that runs between the Ecuadorian Sierra's Real and Occidental mountain ranges (34). Like the rest of Ecuador, this region has two separate climatic seasons: the winter from January to May, with average temperatures of 19°C, and the summer from June to December, with average temperatures of 25°C. Although, temperatures as high as 35°C have been observed (35). In this region, the annual rainfall levels are relatively low (26,36). According to the INAMHI Meteorological Yearbook, historical records of low rainfall were observed in the Inter-Andean region in the January to June 2016 semester, with the most significant being in the town of Ibarra (2.5mm), (37). These climatic conditions favor salt concentration in the soil (38–40).

The watershed is distinguished by reliefs that range from gentle slopes to 70° steep slopes, with elevations ranging from 1160 meters above sea level in the Mira River to 4214 meters above sea level in the Ñagñaro Lagoon (41). Furthermore, intense seismic activity, which causes fracturing and subsidence, is present in the parish and volcanic activity (26).

CHAPTER 2. Background Information

2.1 Geologic Background

The Cordillera Real, El Valle Inter Andean, and the Cordillera Occidental are the three regional geological and morpho-structural systems known in the Sierra Ecuadorian area, from east to west. The Inter-Andean Valley, also known as the Graben or Inter-Andean Depression, results from the Andes' Quaternary geological evolution (42). The Inter Andean Valley was filled with sediments from mountain range erosion and volcanic materials resulting from the region's intense volcanic activity during this time. The vast number of volcanoes found in Ecuador are evidence of this activity. There are 98 volcanoes between active and inactive status, according to the Geophysical Institute of the National Polytechnic School (43). In the province of Imbabura, eleven of these volcanoes are located. The most crucial ones are (23): Imbabura, Cotacachi, Cuicocha, Chachimbiro, Yanahurco de Piñan, and Culbiche. The Chachimbiro volcano and the Yanahurco de Piñan volcano, both part of the Western Mountain range, are the ones that are nearest to the research area. As a result of subsequent compressional events associated with the Andean Orogeny, tectonic inversion towards the sedimentary basin boundaries occurred. For this reason, the study area has low reliefs in the form of a plateau with some hills and a slight increase in slope to the north and west (Cordillera Occidental), (44).

Salinas' polymictic geological materials are from the Yanahurco Volcanic Formation and are found in undifferentiated terraces (26). Andesitic lavas, volcanic breccias, and pyroclastic products of various sizes make up the Yanahurco volcano. This unit recognizes three different levels. Volcanic breccias make up the lower level, travertines and tobaceous sediments make up the intermediate level, and volcanic breccia formed by pyroclasts make up the upper level (23). The terraces are formed by alluvial deposits formed by the erosion of volcanic materials. Lavas, tuffs, cangahuas and volcanic breccias fragments of various sizes make up these deposits (35). The construction of soils on fine volcanic rocks predominates in the upper portion of these terraces. Sugar cane cultivation and salt extraction are primarily developed on these soils.

2.2 Preparation of the cream

The unique ecology of Las Salinas, which was derived from a critical product for indigenous society such as salt, helped its residents to be the most affluent community in the Otavalo ethnic group in the 16th century. This exploitation's peculiarity was that the salt used was not sea salt or rock salt, but a salt that naturally pervades the valley land and river water (45).

Finally, the use of Salinas salt for medicinal purposes is now even more well-known. The salt manufactured in the canton of Ibarra's Santa Catalina of Salinas contains 7.85 micrograms of iodine/g (ug) (46). For more than a century, iodine has been regarded as one of the most effective antiseptics (47). However, in Santa Catalina de Salinas, a by-product of salt extraction is an anti-inflammatory cream. The process for obtaining this product is then described, which is broken down into five steps (**Figure 3**).

(a) Collection of Raw Materials   (b) Land preparation in the filtration

Cream   Iodine   (d) Removal of the iodine solution   (c) Salt water cooking
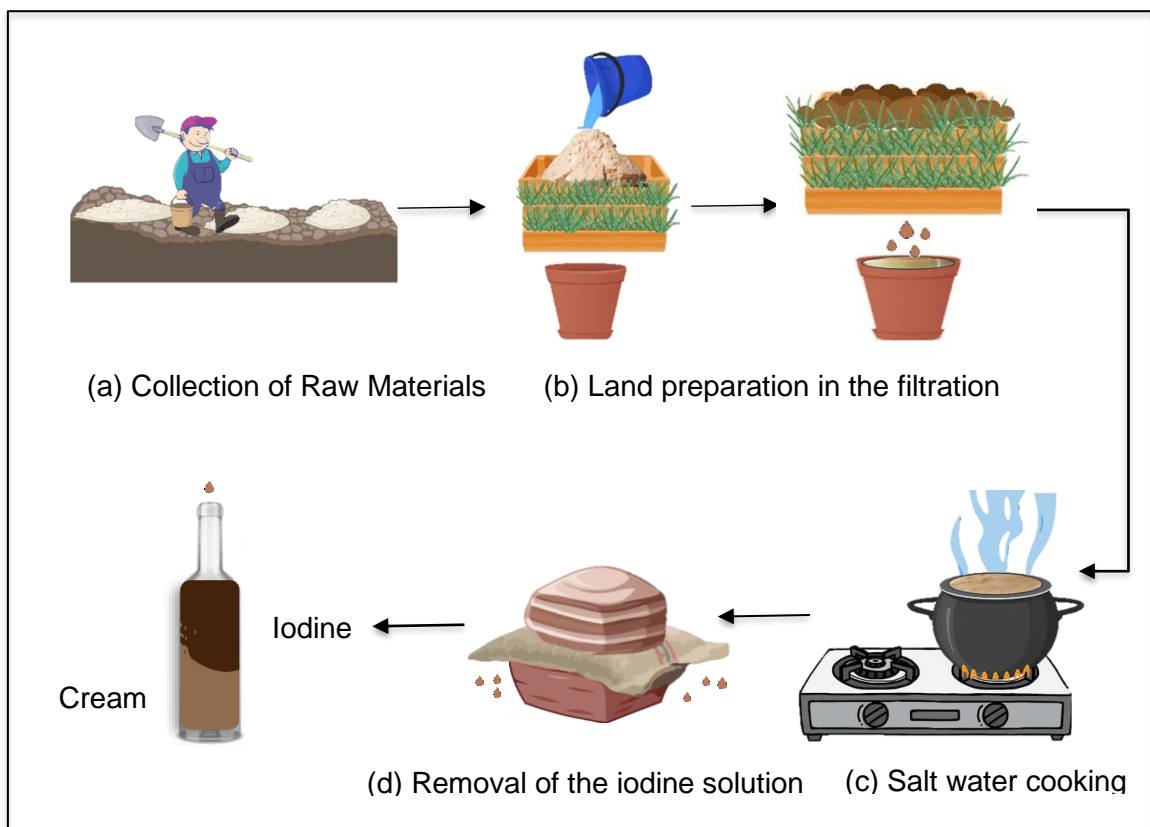
Figure 3. *Workflow of the artisanal salt extraction process in Santa Catalina of Salinas of Ibarra, Imbabura. From collecting the soil to receiving salt and iodine, this diagram depicts the various phases of the process.*

A. Collection of Raw Materials

The preparation of this cream begins with the collection of salty soil. This originates from the parish's salty soil, where the individual gathers only in the superficial part of the soil, so there is a higher salt content there. This is due to the effect called the capillarity phenomenon, which resides at the phreatic zone level. The waters with the most extensive level of salt have a phreatic level of less than one meter, using the terms of Coras et al., 2014, which has allowed the adhesion forces to favor the rising of the salt to the surface (48) (**Figure 2A**)

B. Land preparation in the filtration quadrants

Once the salty soil is obtained, it is placed in a filtration quadrant made from chagualquero (penca) and a base of hawthorn longs. Next, the quadrant was filled with chocoto, which is a mixture of soil, straw, and chamba or grass (49).

The salty soil plus water will be situated in the quadrant and allow the earth's salts to leach. This process occurs within 30 hours after the water has been put. The filtration has a period of 3 to 4 days after this time; the land stops having enough salt, which is why this land is discarded (**Figure 2B**).

C. Saltwater cooking

The water collected from the filtration is cooked until it is mostly evaporated, and the salt is then crystallized. This process will take between 3 and 4 hours, but it all depends on the fire's strength and salty water cooking volume (**Figure 2C**).

D. Removal of the iodine solution

This approach leads to the removal of iodine, the same one that will start our product. The iodine is bottled to obtain a cream. After the iodine has been bottled for approximately seven months, it begins to take on a creamy and oily appearance, in addition to its color becoming more like white (**Figure 2D**).

3.1 Classification Nomenclature

For this research, twenty-five samples were selected for the analyses. The Tolas (base, medium, and top) (**Figure 1B**) and the precipitation phases of the cream were used in this study (**Figure 3**). Information on each sample is included in **Table 1**. The composition of the samples difficulted the observation on each of the analyses. For his reason, some samples were excluded from the studies, the motive is explained in the section of the activity that corresponds to it.

Table 1. Summary of samples analyzed by section

Code of Sample	Sample Description	FTIR		HPLC		XRD	SEM	Antimicrobial Activity
		Non-Polar	Polar	Non-Polar	Polar			
1 (thick consistency state)	Crem phase 4	X	-	-	X	-	-	X
2 (medium-thick consistency state)	Crem phase 3	-	-	-	-	-	-	X
3 (semi- liquid state)	Crem phase 2	-	-	-	-	-	-	X
4 (liquid state)	Crem phase 1	X	X	-	-	-	-	X
M1	Sample 1	X	X	-	X	-	-	-
M2	Sample 2	X	X	-	-	-	-	-
M3T1	Sample 3, Tola 1	X	-	-	X	X	X	-
M4T1	Sample 4, Tola 1	X	X	-	-	X	X	-
M5T1	Sample 5, Tola 1	X	X	X	-	X	X	-
M6T2- BASE	Sample 6 base, Tola 2	X	X	-	-	X	X	-
M7T2-MEDIM	Sample 7 medium, Tola 2	X	X	-	X	X	X	-
M8T2-TOP	Sample 8 top, Tola 2	X	X	-	-	X	X	-
T2M4	Sample 4, Tola 2	X	X	-	-	X	X	-
T2M6	Sample 6, Tola 2	X	X	-	-	X	X	-
T3M7-TOP	Sample 7 top, Tola 3	X	X	X	-	-	-	-
T3M9-BASE	Sample 9 base, Tola 3	X	X	-	-	X	X	-
T3M10-MEDIUM	Sample 10 medium, Tola 3	-	X	X	-	-	-	-
T3M11-TOP	Sample 11 top, Tola 3	X	X	X	-	X	X	-
T4M12	Sample 12, Tola 14	X	X	-	-	-	-	-
T4M13-MEDIUM	Sample 13 medium, Tola 4	X	X	-	-	X	X	-
T4M14-TOP	Sample 14 top, Tola 4	X	X	-	-	X	X	-
T7M19	Sample 19, Tola 7	X	X	-	-	-	-	-
T8M23-MEDIUM	Sample 23 medium, Tola 23	X	X	-	-	-	-	-
T8M24-BASE	Sample 24 base, Tola 8	-	X	-	-	-	-	-
T11M33-BASE	Sample 33 base, Tola 11	X	X	-	-	X	X	-

3.2 Reagents

Methanol (*HPLC grade, >=99.9%*), n-hexane ($CH_3(CH_2)_4CH_3$), ethyl acetate ($C_4H_8O_2$), acetone (*HPLC grade*), dimethyl sulfoxide (($CH_3)_2SO_3$), acetonitrile (CH_3CN), Miller Luria Bertani Agar, ampicillin (*Genamerica*) and *Escherichia coli* TG1 (*E. coli*).

3.3 Materials and Equipment

Materials	
Glass Pasteur pipettes	Spatula
Eppendorf Tube 5.0 mL	Syringes 3mL
Drigalski Spreader	Agar plate
Glass bottles w/blue cap autoclavable 250 ml	Falcon tubes 15 ml

Equipment	Specifications
Micropipettes	Thermo™ Scientific™ Finnpipette F1 Fixed Volume TS1000H Topscien
Vortex	GEMMY
Analytical balance	HR-150A Cobos precision
Centrifuge	"Mixtasel-BL" with maintenance-free induction motor
FTIR spectrometer	Agilent Cary 630
X-Ray Diffraction	MiniFlex benchtop X-ray diffractometer
SEM	Phenom ProX Desktop SEM
HPLC apparatus	UltiMate 3000
C-18 column for HPLC	Hypersil GOLD™ (150 mm× 4.6 mm, 5µ particle size)
Autoclave	Presoclave II
Digital shaker with incubation	Thermo™ Scientific™ SHKE4450
Vertical Laminar Flow Bench	Telstar AV-100
Hybridization Oven	

3.4 Characterization and Methods

3.4.1 Organic composition determination

Santa Catalina de Salinas, salty soil samples were carried out according to a previously reported method described in Suárez et al. (2011). The preparation of non-polar and polar samples were carried out following the methodology described in the inorganic and organic characterization of Santa Lucía salt mine peloid for quality evaluations (50). In the analysis of the non-polar and polar fraction, the sample obtained (~ 0.76g) contains 1mL of each solvent.

For non-polar compounds, each sample was washed three times with methanol for 20 min to get rid of the sulfur in the samples and to avoid polar compounds. Then, the extracted methanol was separated by centrifugation and decantation, and the solid phase was macerated with hexane, two washes for 1 hour. The resultant hexane fraction (2mL) was later concentrated by evaporation down to 0.5µL (**Figure 3.1**). The final sample was analyzed by FTIR spectroscopy.

For the polar fraction analysis, the powder (1 g) of each recollected sample was extracted for 20 min using hexane to avoid the loss of other polar compounds, contrary to the procedure used for the non-polar fraction, where methanol was used. The hexane extract was separated by centrifugation, and the solid phase was macerated with 3mL of ethyl acetate, acetone, and methanol for 20 min. The resultant fractions were later concentrated by evaporation up to 0.5 µL (**Figure 3.2**). Continuation, this concentrated extract was analyzed by FTIR spectrometry.
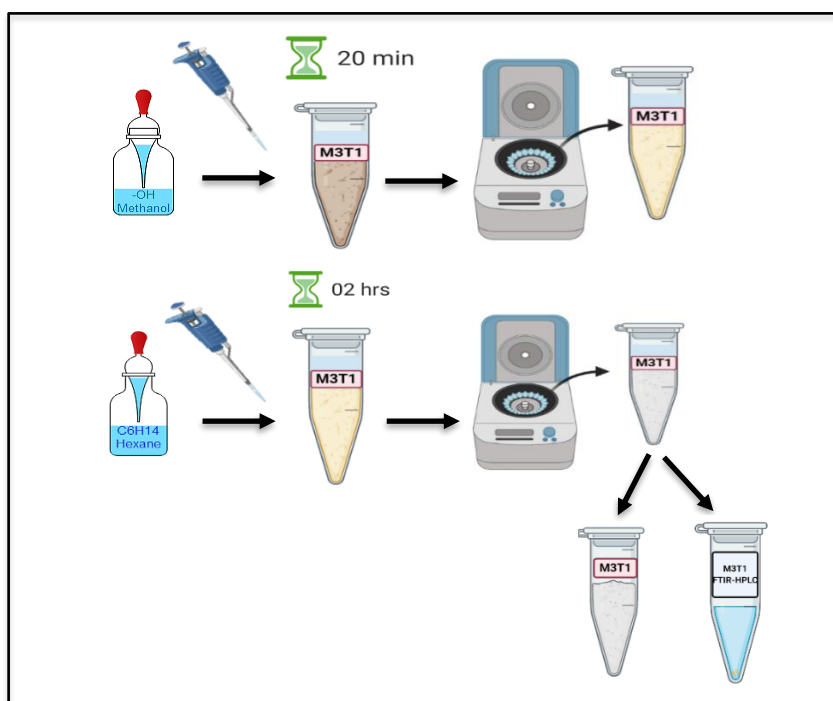
Figure 4.1 Extraction of the Non-polar Fraction
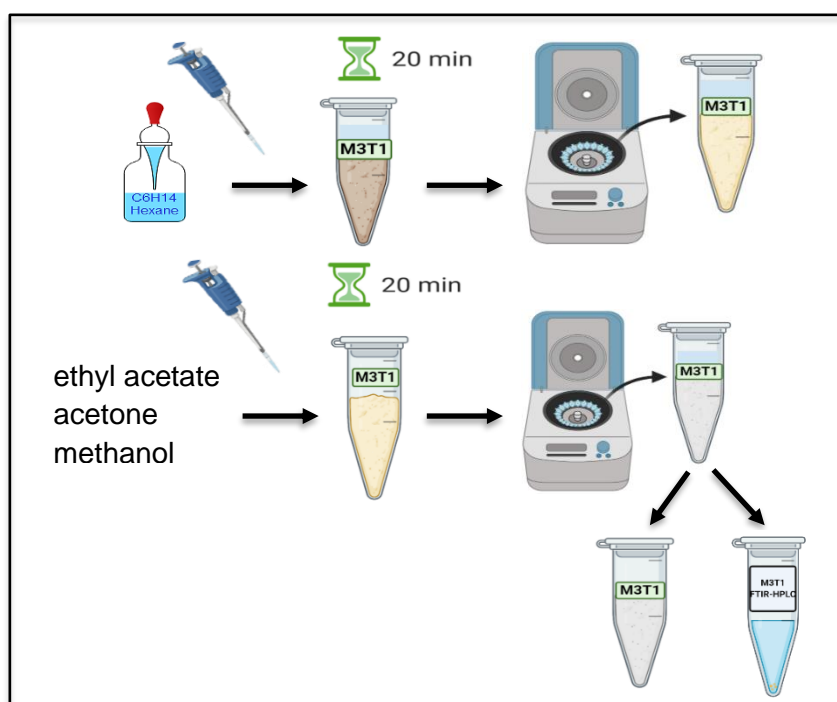
Figure 4.2 *Extraction of the Polar Fraction*

3.4.2 ATR-FTIR spectroscopy

Saline sample characterization was examined by ATR-FTIR spectroscopy. Measurements were carried out for liquid samples obtained from Section 3.4.1. Previously the non-polar fraction samples were dissolved on $10\mu l$ hexane and polar fraction samples on $10\mu l$ methanol.

Infrared spectral analyses were carried out in the mid-infrared region (from 4000 to 400 cm−1) and spectral data obtained presented as transmittance values.

3.4.3 High Pressure Liquid Chromatography (HPLC)

A HPLC apparatus equipped with an autosampler, a quaternary pump, and a column compartment. The analysis was carried out using a reverse-phase C-18 column. The mobile phase were water and acetonitrile. The final mixture was purified into Titan 47 mm Membrane Disc filters after the samples were dissolved in ACN and DMSO. The mobile phase's flow rate was 1.0 mL/min, and the injection volume was 500 µL. The column temperature was kept at 30 ∘C, and detection was carried out at 254 nm.

3.4.4 X-Ray Diffraction

X-ray diffraction (XRD) is a robust tool used to differentiate the crystalline phases found in materials. Significantly, to measures the basic properties (grain size, the shape of imperfection, diffraction angle, purity, and composition) of these phases (51).

Due to their hygroscopic properties, only 14 of the 23 samples were analyzed in this section (**Table 1.**). The samples were preheated to 80° C before analysis so that samples with high relative humidity could be differentiated. The samples were then ground in an agate mortar, and powdered samples were packed into a standard back-fill powder diffraction sample holder. As the powder is dispersed over a small area, it has the benefit that the area reached by the X-ray beam during the entire scan remains relatively stable. This is important to achieve the right proportions of the peak relative intensities (**Figure 5**).
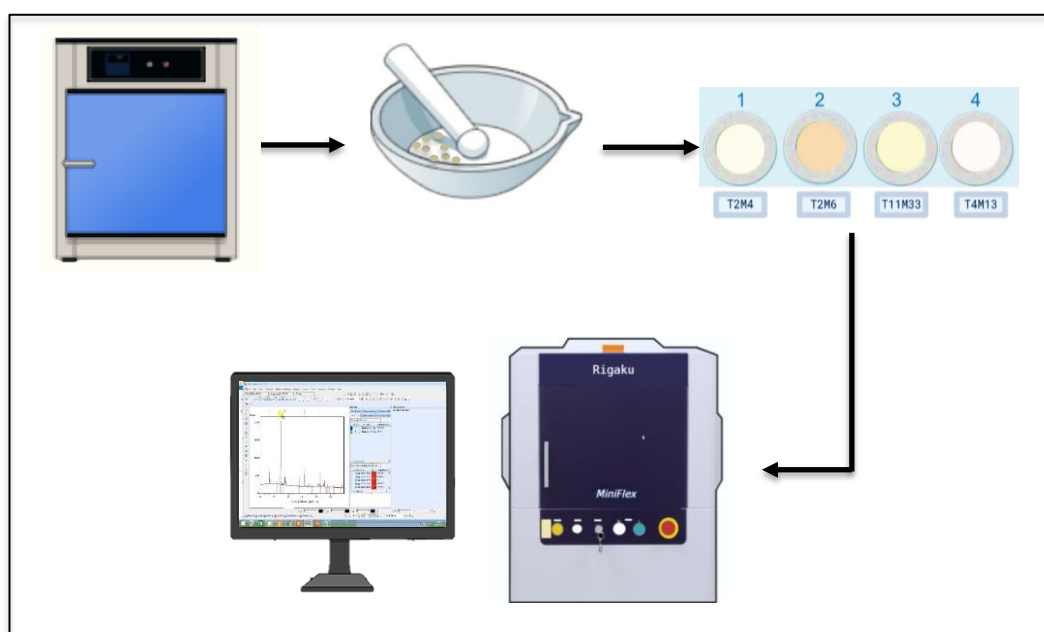
Figure 5. Treatment and Analysis of Samples in XRD Diffractometer

MiniFlex benchtop X-ray diffractometer using Cu Kα radiation (λ =1.5418740 Å). Intensities were measured at step size 2θ= 0.02° steps with counting times of 5° per minute, at a speed of 20°/min. Phase identification (i.e., pattern matching) of the XRD data was carried out using COD-Inorg REV218120 2019.09.10 (52).

3.4.5 Scanning electron microscopy (SEM)

The salty soil microstructure was characterized by scanning electron microscopy from Phenom model ProX-SEM-EDS equipment operated at 10 kV with an electron-optical

magnification range 20000x and a resolution of 8 nm BSD. One of the samples' conditions to be analyzed by the SEM is that they are dry (53). However, only 14 meet (**Table 1.**) this criterion, the same ones that are analyzed in the following appendix.

The analysis was carried out on a 47.9 um area because the samples began to calcine when attempting a complete mapping. Each measurement was repeated in at least two areas to obtain up to 2 spot measurements by each soil sample.

3.4.6 Biological activity

The culture media was prepared for solid and liquid media. Solid media was prepared using 12 g of Luria Bertani (LB) Agar, Miller from TM MEDIA placed in a clean 1-liter flask, and 300 mL of distilled water. Liquid media was prepared using 6 g of Luria Bertani (LB) Broth Base from Invitrogen placed in a clean 1-liter flask and add 300 mL of distilled water. It is relevant to note that containers used for media might have vented tops and should be capable of holding 20% more than the medium's intended volume, allowing for expansion during sterilization. Swirl the flask to mix the powder mixture into the water as homogeneously as possible. Cover the flask with aluminum foil and put it in the autoclave for 30 minutes at 1 atm and 120 °C. Once the sterilization is finished, take the liquid media flask out and let it cool down at room temperature for 50 to 60 minutes. The solid media flask was distributed in the necessary Petri dishes in a Laminar Flow Hood until the place's whole area is filled. Allow the plates to cool and the LB-Agar to completely solidifies.

The Bacteria strain *E. coli* TG1 has been selected as a representative type of bacteria because it has a significant influence on humans, causing serious disease. This variation can be used to determine if a raw material has antimicrobial activity as a first estimate. The bacterial stock cultures were incubated for 24 hours at 37°C and 124 rpm on Luria Bertani (LB) broth base, following by refrigeration storage at 4°C.

Chapter 4. Result and Discussion

4.1 ATR-FTIR Studies

Table 2 shows the FTIR spectra of the Santa Catalina de Salinas-Ibarra samples. The samples that were not used in these studies were omitted because the signal/noise ratio was so poor that the sensitivity was severely diminished, resulting in shallow resolution spectra. However, the findings are unaffected since it was determined that the samples contained the same functional groups, such as, O-H stretch, C-O stretch, C=C stretch, and from methylenes (C-H$_2$)/and from methyls (C-H$_3$). The samples selected for review followed the criterion of getting the most significant number of functional groups studied; for more information, check **Appendix A.**

Table 2. Assignment of the principal descriptive IR absorption bands in saline samples

Code of Sample	Sample Description	Non-Polar Fraction			Polar Fraction	
		O-H Stretch	C-O stretch	C=C stretch	C-H$_2$/C-H$_3$ bending	C=C stretch
1 (thick consistency state)	Crem phase 4	X	X	X	X	X
4 (liquid state)	Crem phase 1	X	X	X	-	X
M1	Sample 1	X	X	-	X	X
M2	Sample 2	X	X	X	X	X
M3T1	Sample 3, Tola 1	-	-	-	-	-
M4T1	Sample 4, Tola 1	X	X	X	-	-
M5T1	Sample 5, Tola 1	X	X	X	X	-
M6T2- BASE	Sample 6 base, Tola 2	X	X	X	-	-
M7T2-MEDIM	Sample 7 medium, Tola 2	X	X	X	X	X
M8T2-TOP	Sample 8 top, Tola 2	X	X	X	X	-
T2M4	Sample 4, Tola 2	X	X	X	X	-
T2M6	Sample 6, Tola 2	X	X	X	-	-
T3M7-TOP	Sample 7 top, Tola 3	X	X	X	X	-
T3M9-BASE	Sample 9 base, Tola 3	X	X	X	X	-
T3M10-MEDIUM	Sample 10 medium, Tola 3	X	X	-	-	-
T3M11-TOP	Sample 11 top, Tola 3	X	X	-	X	-
T4M12	Sample 12, Tola 14	X	X	X	-	-
T4M13-MEDIUM	Sample 13 medium, Tola 4	X	X	X	X	-
T4M14-TOP	Sample 14 top, Tola 4	X	X	X	X	-
T7M19	Sample 19, Tola 7	X	X	X	X	X
T8M23-MEDIUM	Sample 23 medium, Tola 23	X	X	-	X	-
T8M24-BASE	Sample 24 base, Tola 8	X	X	X	-	-
T11M33-BASE	Sample 33 base, Tola 11	X	X	X	-	-

In the FTIR spectrum of the non-polar samples (**Figure 6**), the characteristic peaks for hexane of sp3 C-H stretching at 3000 -2840cm-1, methylene groups can be observed bending at 1470 cm-1, and methyl groups bending at approximately 1375 cm-1 (**Figure 6A** (54)). These peaks correspond to the solvent used for the dilution of samples, and these peaks are not

considered for the analysis of the peaks of the non-polar samples. Moreover, it is necessary to consider some of the hexane peaks decrease as it volatilizes, and it can be seen that they still contain hexane in the samples. However, hexane is present on the samples, and according to the colors, the peaks correspond to the hexane and non-polar samples. The samples 1, M1, and M7T2 shown peaks at 3400 cm-1, 1640 cm-1, 1150-1000 cm-1 corresponding to the functional group of hydroxyls, unsaturation, and C-O stretch, respectively (**Figure 6B, 6C, 6D**). While the sample T7M19 does not exhibit the peaks in the previous samples.
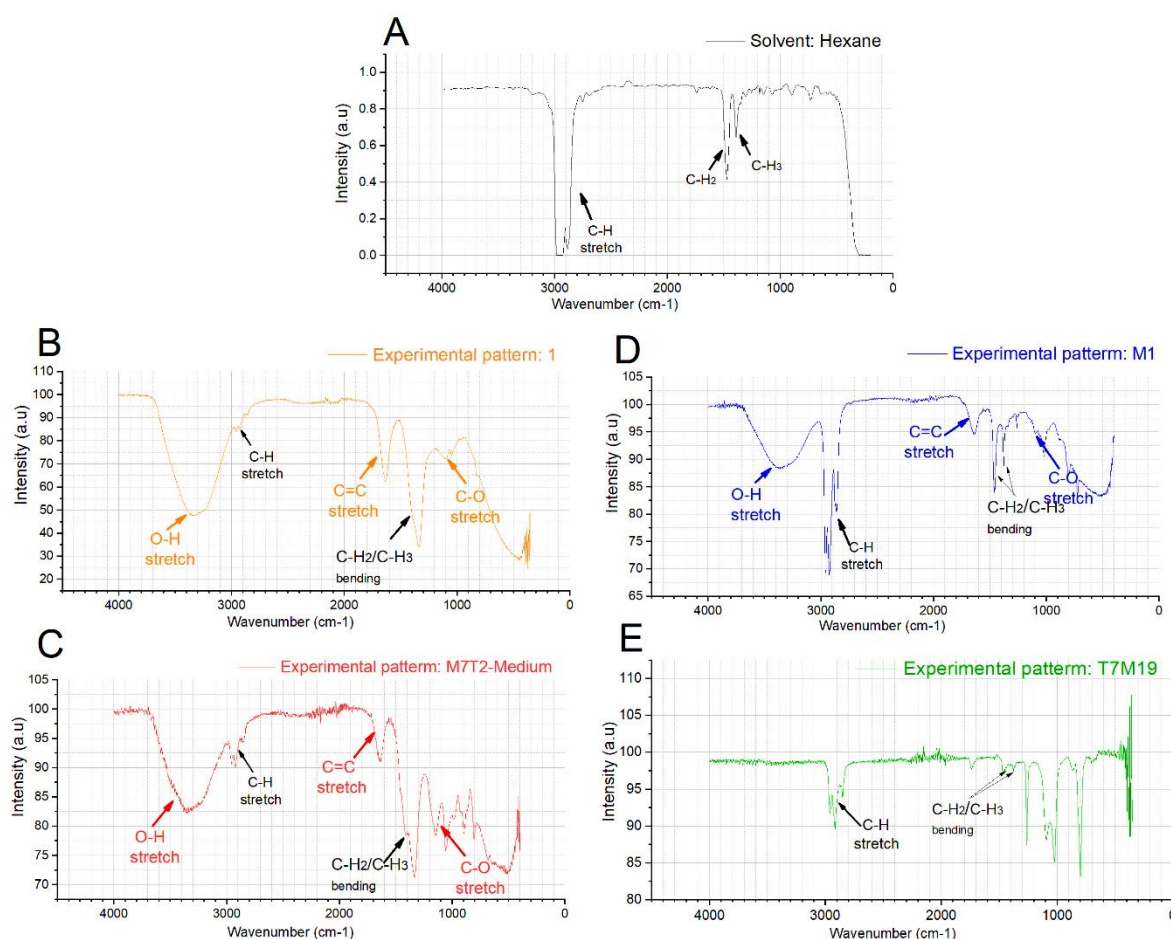
Figure 6. *FTIR spectra of saline samples and its major components: O-H stretch, C=C stretch, and C-O stretch. (Note: The assignments of the numbered bands in the figure are described in Table 2).*

On the other side, in the FTIR spectrum of the polar samples (**Figure 7**), it can be observed the characteristic peaks for methanol of sp3 C-H stretching at 3000 -2840cm-1, methyl groups bending at approximately at 1375 cm-1, C-O-H bending at 1440-1220 cm-1, and C-O stretching at 1100-1000 cm-1(**Figure 7A** (55)). Also, in this case, it appears that the solvent is present in the polar samples. Thus, samples M2 and M5T1 shown peaks at 1650 cm-

1 and 1450 cm-1 corresponding to unsaturation, and CH3/CH2 bending respectively (**Figure 7B and 7C**).

Thus, the FTIR spectrum allows us to know the functional groups present in nonpolar and polar samples but it is not possible to determine the compounds' structures.
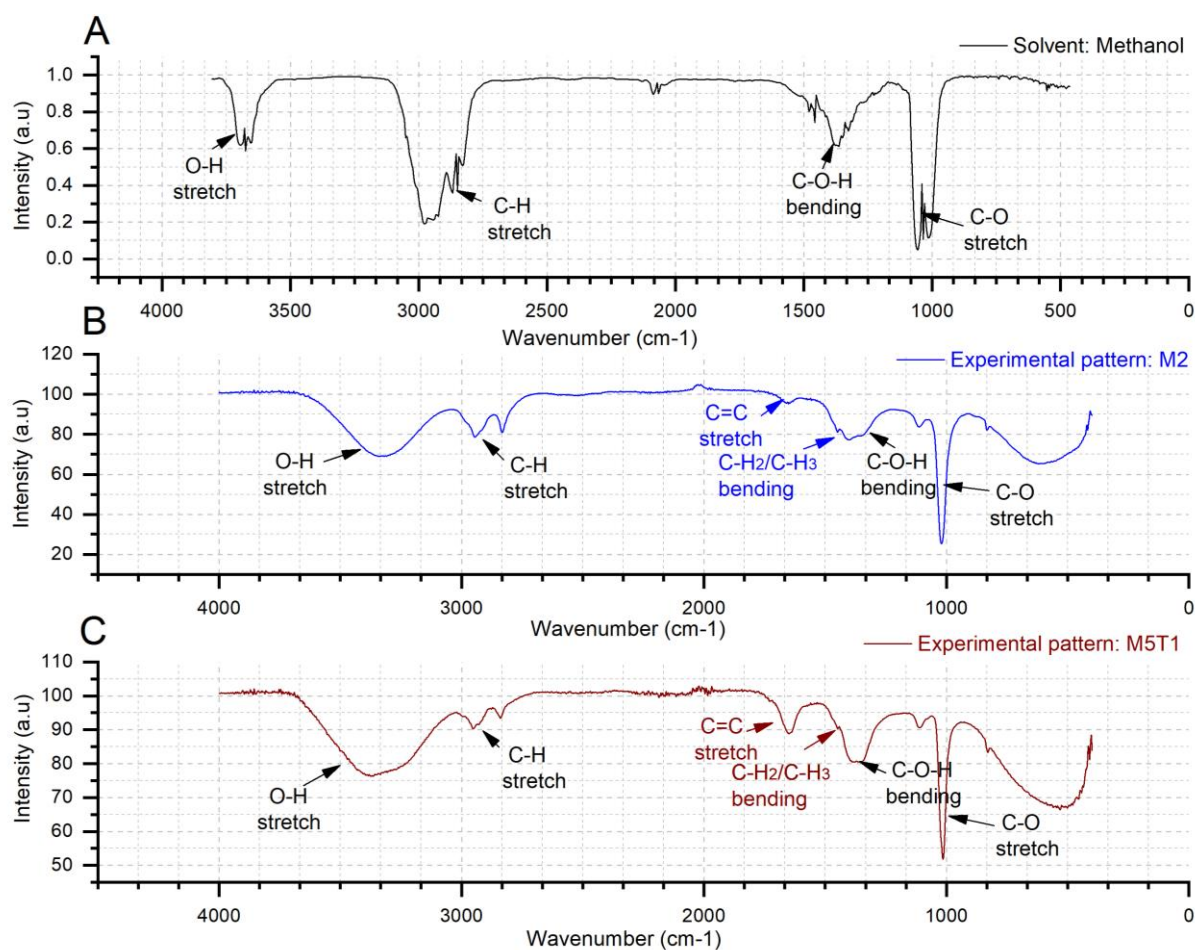
Figure 7. *FTIR spectra of saline samples and its major components: C-H2/C-H3 bending, and C=C stretch (Note: The assignments of the numbered bands in the figure are described in Table 2).*

4.2 HPLC Analysis

HPLC is capable of separating and identifying substances in any sample that can be dissolved in a solvent at trace concentrations as low as parts per trillion. In this case, nonpolar and polar sample fractions were characterized using HPLC spectrometry. Some of the samples showed similar results, despite some exhibit additional peaks. A comparison of HPLC profiles at 254 nm of the samples showed expected differences and similarities of peaks. It was performed a blank of ACN to discard the peaks which own to the solvent (**Table 3**). Samples 1P, M3T1P, M5T1A, and M7T2P share similar principal peaks with retention times at 1.85

minutes, 8.34 minutes, and 8.41 minutes with purities of 12-29%, 10-54%, and 16-11%, respectively. However, samples M5T1P and M7T2P showed additional peaks with retention times at 2.30 minutes (27.47% purity) and 8.14 minutes (14.26% purity) (**Figure 8. A, B, C, and D**). On the other hand, sample M1P show two principal peaks with retention times at 1.97minutes and 2.483 minutes with purities of 56.19 and 17.91%, respectively (**Figure 9A**). Furthermore, samples T3M7A and T3M10A share similar principal peaks with retention times at 1.4 minutes, 2.3 minutes, and 3.5 minutes with purities of 12-14%, 25%, and 12-18%, respectively. Also, they differ in additional peak with retention times at 0.03 minutes (12.54% purity) and 2.61 minutes (11.18% purity), and 0.05 minutes (11.05% purity), and 3.36 minutes (12.42% purity), respectively (**Figure 9 B and C**). Finally, the sample T3M11A exhibits only one principal peak with a retention time of 6.03 minutes with a purity of 11.74% (**Figure 9D**).

In conclusion, the HPLC profiles of all studied samples revealed the presence of several chemical entities in each sample, with some of them being the majority.

Table 3. Retention time, width (50%), type, resolution, asymmetry, and plates of ACN sample

No.	Retention Time (min)	Width (50%) (min)	Type	Resolution (EP)	Asymmetry (EP)	Plates (EP)
1	2.277	n.a.	BM	n.a.	n.a.	
2	2.323	0.025	MB	n.a.	1.01	n.a.
3	2.397	n.a.	BM	n.a.	n.a.	47518
4	2.473	n.a.	MB	n.a.	n.a.	n.a.
5	3.653	0.042	BM	n.a.	8.03	n.a.
6	3.773	n.a.	Rd	n.a.	n.a.	41998
7	3.980	n.a.	Rd	n.a.	n.a.	n.a.
8	4.310	n.a.	M	n.a.	n.a.	n.a.
9	5.253	n.a.	Ru	n.a.	n.a.	n.a.
10	5.410	n.a.	Ru	n.a.	n.a.	n.a.
11	5.773	1.004	M	n.a.	n.a.	n.a.
12	5.967	n.a.	Rd	n.a.	n.a.	183
13	6.113	n.a.	Rd	n.a.	n.a.	n.a.
14	7.033	n.a.	M	n.a.	n.a.	n.a.
15	7.147	n.a.	M	n.a.	n.a.	n.a.
16	7.470	0.147	M	2.22	n.a.	n.a.
17	8.377	0.335	MB	n.a.	0.57	14295
18	8.757	n.a.	BM	n.a.	n.a.	3465
19	8.837	n.a.	M	n.a.	n.a.	n.a.
20	9.260	0.069	M	1.09	n.a.	n.a.
21	9.417	0.100	MB	1.11	n.a.	98763
22	9.573	0.067	BMB	1.52	0.69	48882
23	9.817	0.122	BMB	n.a.	1.09	113666
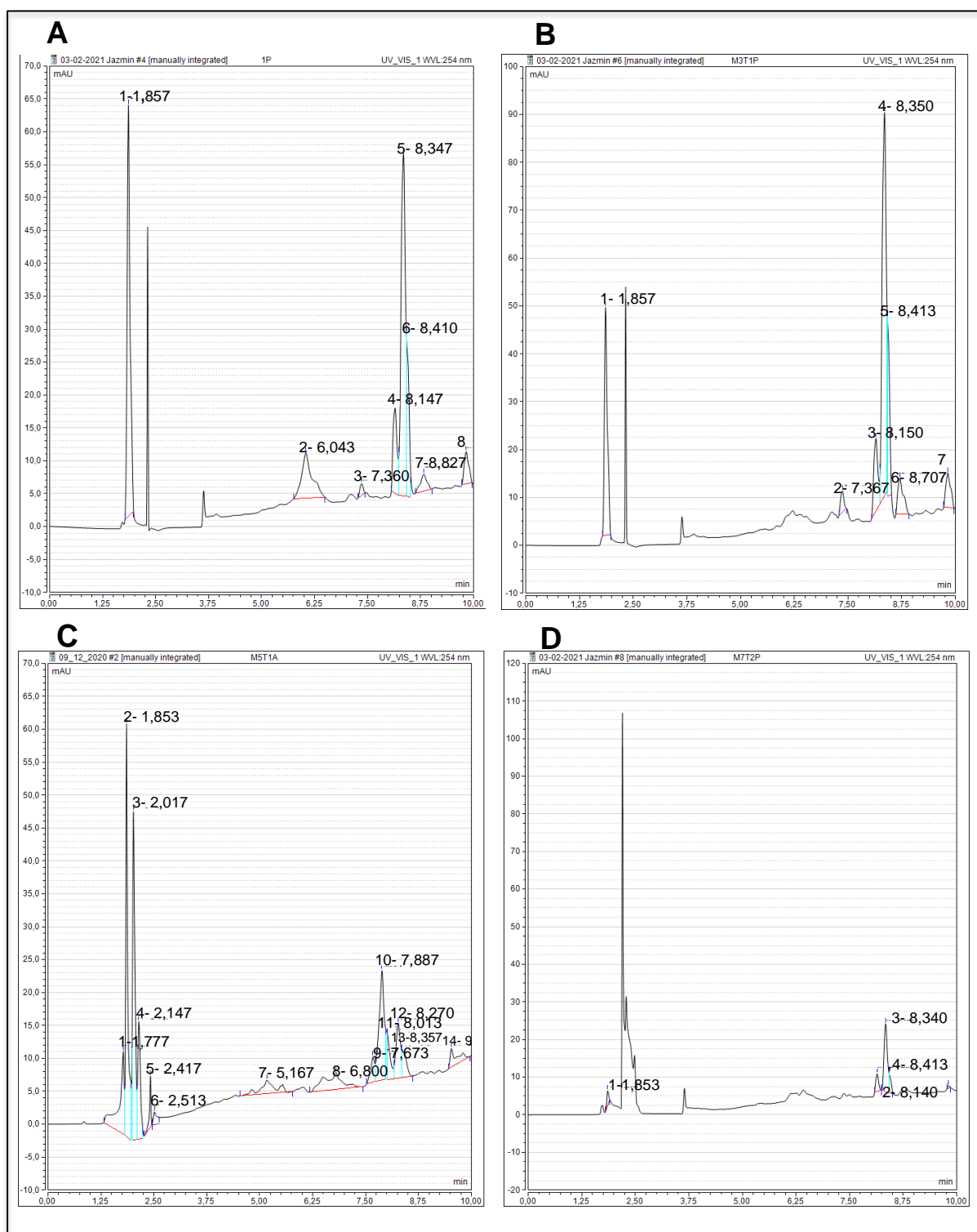
Figure 8. *HPLC analytical chromatograms of saline samples. A) Analytical HPLC chromatogram of polar sample 1; B) Analytical HPLC chromatogram of polar sample M3T1; C) Analytical HPLC chromatogram of non-polar sample M5T1 and D) Analytical HPLC chromatogram of polar sample M7T2.*
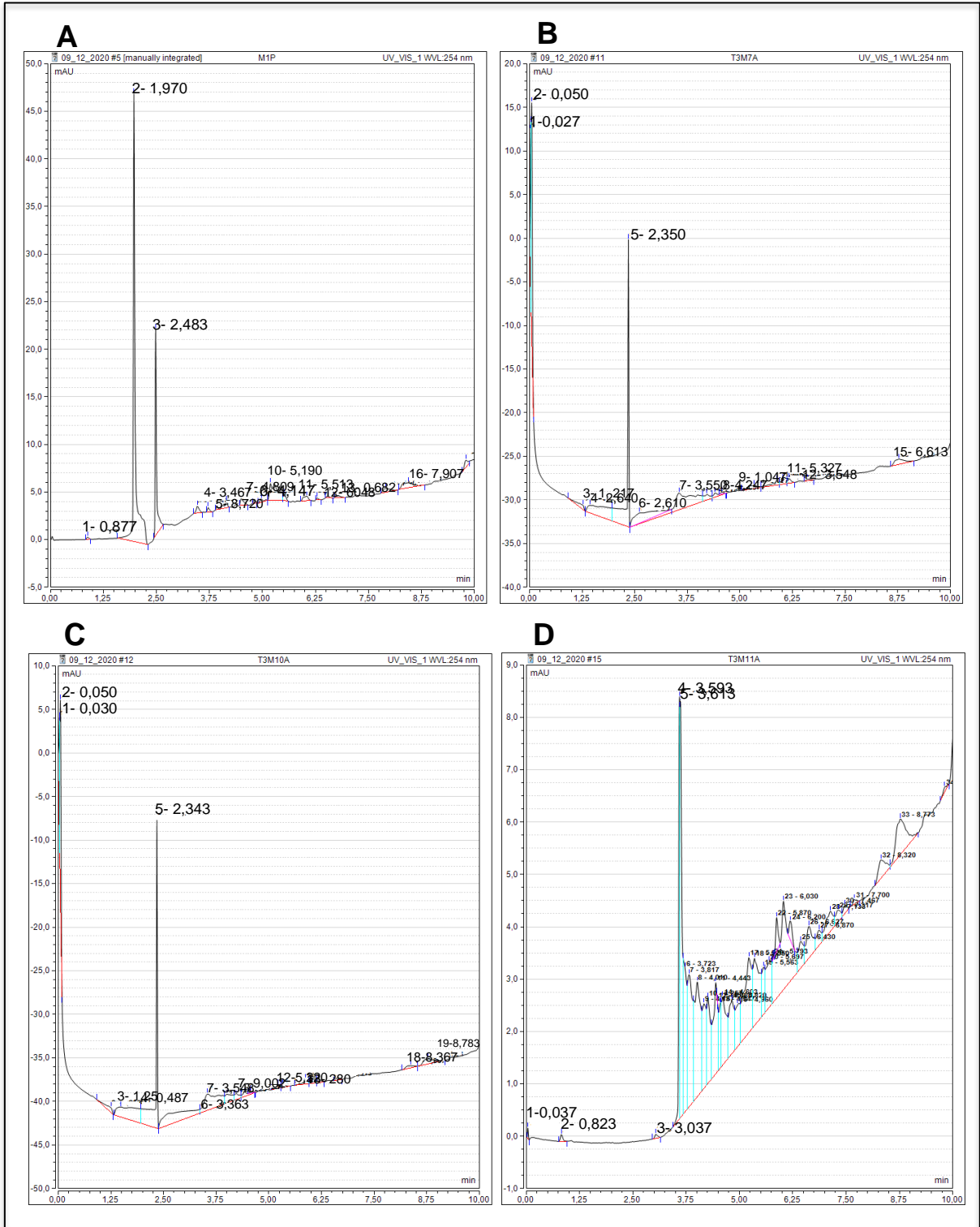
Figure 9. *HPLC analytical chromatograms of saline samples. A) Analytical HPLC chromatogram of polar sample M1; B) Analytical HPLC chromatogram of non-polar sample T3M7; C) Analytical HPLC chromatogram of non-polar sample T3M10 and D) Analytical HPLC chromatogram of non-polar sample T3M11.*

4.3 X- Ray Diffraction Analysis

Diffractograms showing the effects of X-ray diffraction are provided based on examining the powder assemblies of the Santa Catalina de Salinas-Ibarra samples. According to Bragg's law (56), the diffractograms represent the intensities of each diffracted peak on the abscissa and the angle 2theta in the ordinate. Semi-quantitative estimation of the mineral content was carried out using the reference intensity ratio (RIR) method (57). The majority and minority phases from higher-intensity peaks were also used to decide whether the minerals should be approved or rejected (58).

Diffractograms of the samples listed in **Table 4.** were obtained in dry. In this study, only three samples (M4T1, M6T2, T4M14) were selected from the 14 diffractograms analyzed; the others are in the **Appendix B**. It can be seen that the samples have a crystalline structure due to the existence of sharp narrow diffraction peaks. In the following, each of the four XRD measurements is discussed individually.

Table 4. Samples used and their composition

Code of Sample	Sample Description	Mineral Composition[a], (%)					
		H	N	G	C	S	A
M3T1	Sample 3, Tola 1	63.70	36.30	U.M	U.M	U.M	U.M
M4T1	Sample 4, Tola 1	45.60	18.70	12.60	23.10	U.M	U.M
M5T1	Sample 5, Tola 1	41.40	34.20	UM	24.50	U.M	U.M
M6T2-BASE	Sample 6 base, Tola 2	41.70	26.00	U.M	U.M	32.30	U.M
M7T2-MEDIUM	Sample 7 medium, Tola 2	32.90	44.60	U.M	22.40	U.M	U.M
M8T2-TOP	Sample 8 top, Tola 2	71.20	28.8	U.M	U.M	U.M	U.M
T2M4	Sample 4, Tola 2	88.70	11.30	U.M	U.M	U.M	U.M
T2M6	Sample 6, Tola 2	100.0	UM	U.M	U.M	U.M	U.M
T3M9-BASE	Sample 9 base, Tola 3	100.0	U.M	UM	U.M	U.M	UM
T3M11-TOP	Sample 11 top, Tola 3	44.60	38.40	U.M	16.90	U.M	U.M
T4M13-MEDIUM	Sample 13 medium, Tola 4	43.70	56.30	U.M	U.M	U.M	U.M
T4M14-TOP	Sample 14 top, Tola 4	30.20	25.50	U.M	30.60	U.M	13.70
T8M24-BASE	Sample 24 base, Tola 8	52.70	U.M	15.1	32.20	U.M	U.M
T11M33-BASE	Sample 33 base, Tola 11	30.20	35.50	U.M	34.20	U.M	U.M

[a] H Halite, N Nitratine, G Gypsum, C Calcite, S Syngenite, A Anhydrite, U.M Unidentified Mineral

M4T1 Sample

Figure 10 shows the XRD diffractogram for M4T1. The most intense peak in the exact figure is located at $2\theta = 31.70°$, $45.45°$, and $56.48°$ and corresponds to the halite's 111 plane, which refers to the interplanar spacing between its layers. Besides, peaks representing nitratine were also observed at $2\theta = 29.38°$, $38.96°$, and $47.93°$. A peak was also observed at $2\theta = 29.46°$, and this represented calcite. Another peak was observed at $2\theta = 29.20°$, and this represented gypsum.

The composition of the semi-quantitative analysis is given by the following percentages halite (45.60%), nitratine (18.70%), calcite (23.10%), and gypsum (12.60%). It's also worth noting that the majority phase has a calcite content of around 7%, which is the lowest in this sample's semi-quantitative analysis. These minerals' crystalline structure is gypsum monoclinic structure (59), whereas calcite and nitratine have a trigonal structure (60,61). Finally, halite, which has a cubic structure(62).
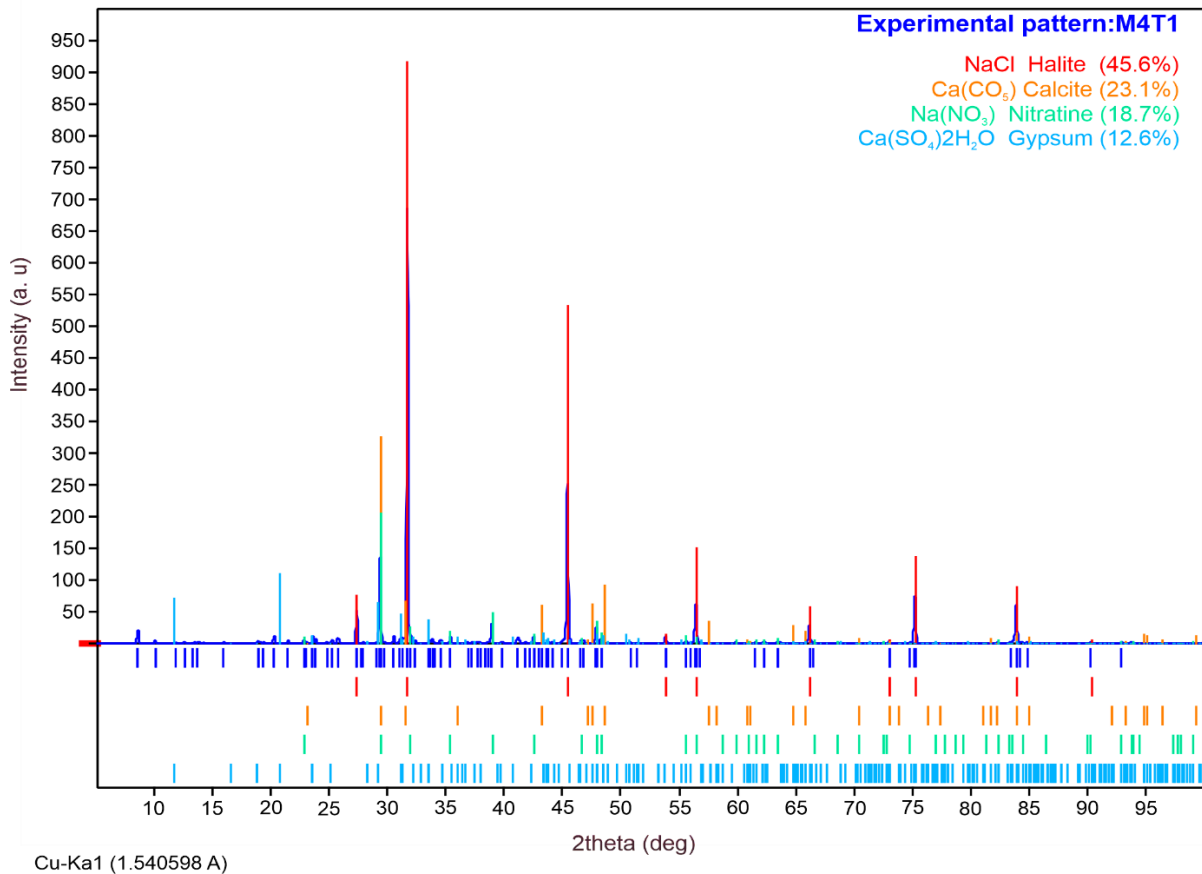
Figure 10. *XRD patterns of the M4T1 sample, which contains the most minerals contained in this analysis. See location in Figure 1.*

M6T2- Base Sample

Figure 11 shows the XRD diffractogram for M6T2, shows that the peak with the highest intensity is still the halite ($2\theta = 31.70°$). A peak representing nitratine was observed at $2\theta = 29.38°$. However, the syngenite mineral was identified in this image at $2\theta = 28.21°$, and $2\theta = 9.32°$. This mineral has crystal system is monoclinic with lattice parameters a= 9.7700 Å b= 7.1500 Å c= 6.2500 Å β= 104.000 ° (63). The composition of the semi-quantitative analysis is given by the following percentages halite (41.7%), nitratine (26%), and syngenite (32.3%).

The majority phase concerning the syngenite is 11% of the semi-quantitative analysis of the M6T2 sample.
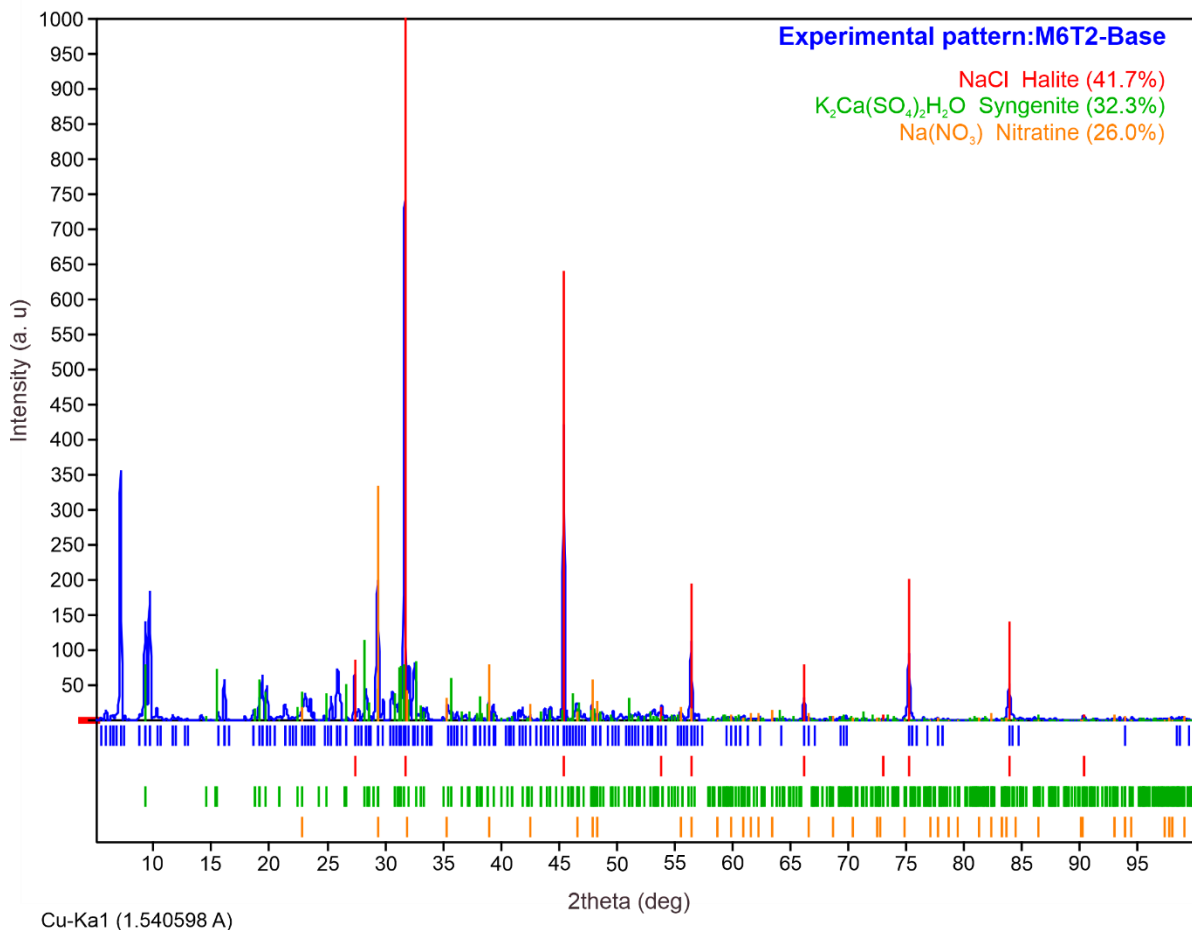
Figure 11. XRD pattern of sample T2M6- Base can be seen the presence of the syngenite mineral.

T4M14-Top Sample

Figure 12 shows the XRD diffractogram for T4M14-Top, peak $2\theta = 31.70°$ keeps a greater intensity than the other minerals**.** Peaks representing nitratine was observed at $2\theta = 29.38°$. The mineral anhydrite can be seen in this sample at $2\theta = 25.44°$. The crystalline structural system of anhydrite is orthorhombic, formed by lattice parameters a = 6.9910 Å, b = 6.9960 Å, c = 6.2380 Å (64). According to the XRD pattern, the T4M14-Top sample semi-quantitative analysis is composed of the following minerals halite (47.20%), anhydrite (22.90%), calcite (18.30%), and nitratine (11.60%). The majority phase for the syenite is 13.10% of the semi-quantitative analysis of the T4M14-Top sample.
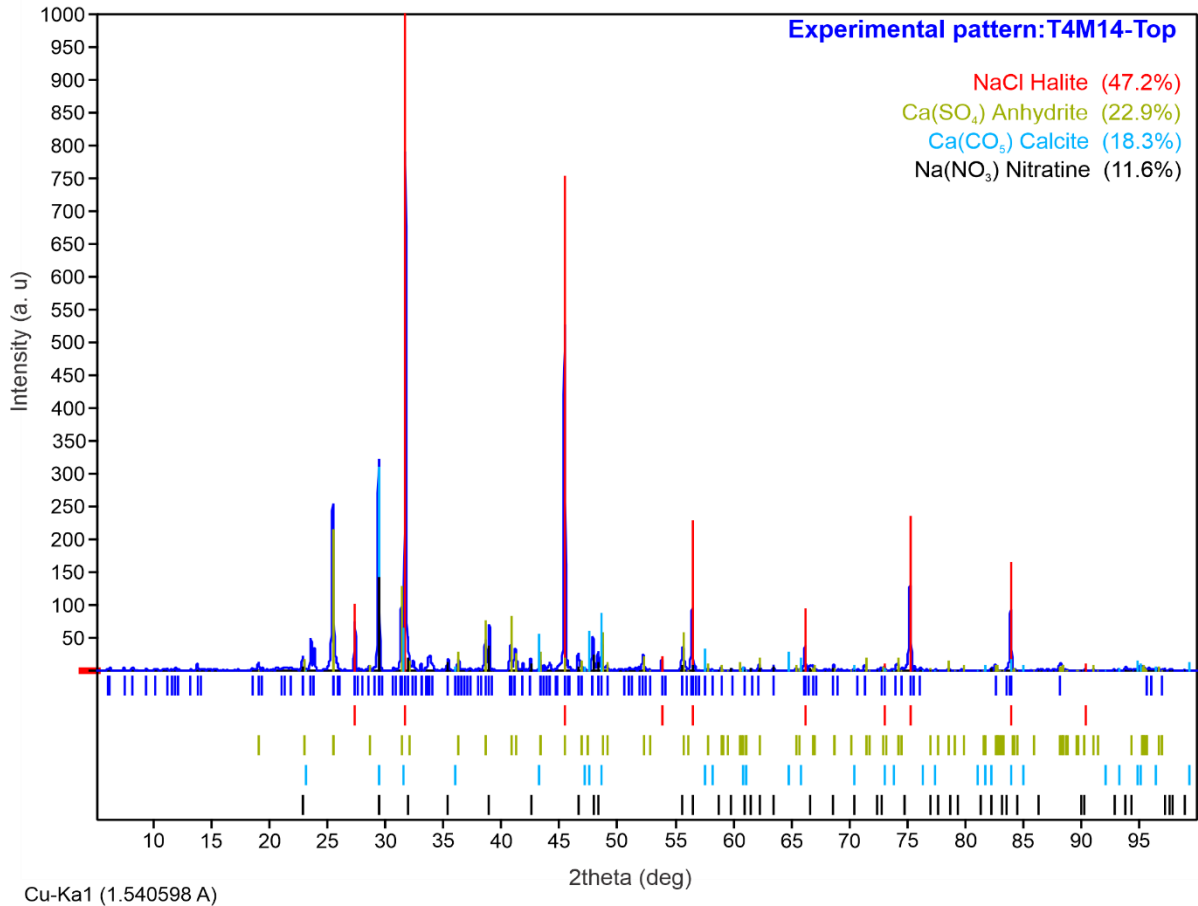
Figure 12. *XRD pattern of sample T4m14- Top can be seen the presence of the anhydrite mineral. See location in Figure 1.*

The use of XRD permitted identifying the significant constituents of compounds present in the saline samples of Santa Catalina of Salinas- Ibarra. Further, samples of M4T1, M6T2- Base, and T4M14-Tops were selected to showcase the various minerals on display in the table. The results of this study showed that in fact, the halite mineral (diagnostic peaks at d (200) = 2.8203 A˚, d (202) = 1.9942 A˚ and d (222) = 1,6283 A˚, is present in all samples, with a higher intensity peak. The crystal structure of NaCl halite is cubic with lattice parameters a= 5.6406 Å. All XRD patterns reflect the existence of pure NaCl peaks. Along with halite, the X-ray diffractograms showed the reflections of nitratine d (104) =3.0387 A˚, calcite d (211) = 3.0289 A˚, syngenite d (121) = 2.8287 A˚, and anhydrite d (210) = 3.4955 A˚. Using XRD is observed sharp peaks at 2θ= 31.7˚ and multiple peaks at 2θ =45.44˚ and 29.38˚ (**Figure 13**). The results of the present study for M4T1, M6T2- Base, and T4M14-Tops corroborated these findings. Identifying the significant constituents of a natural product is essential as it will improve its application and use.
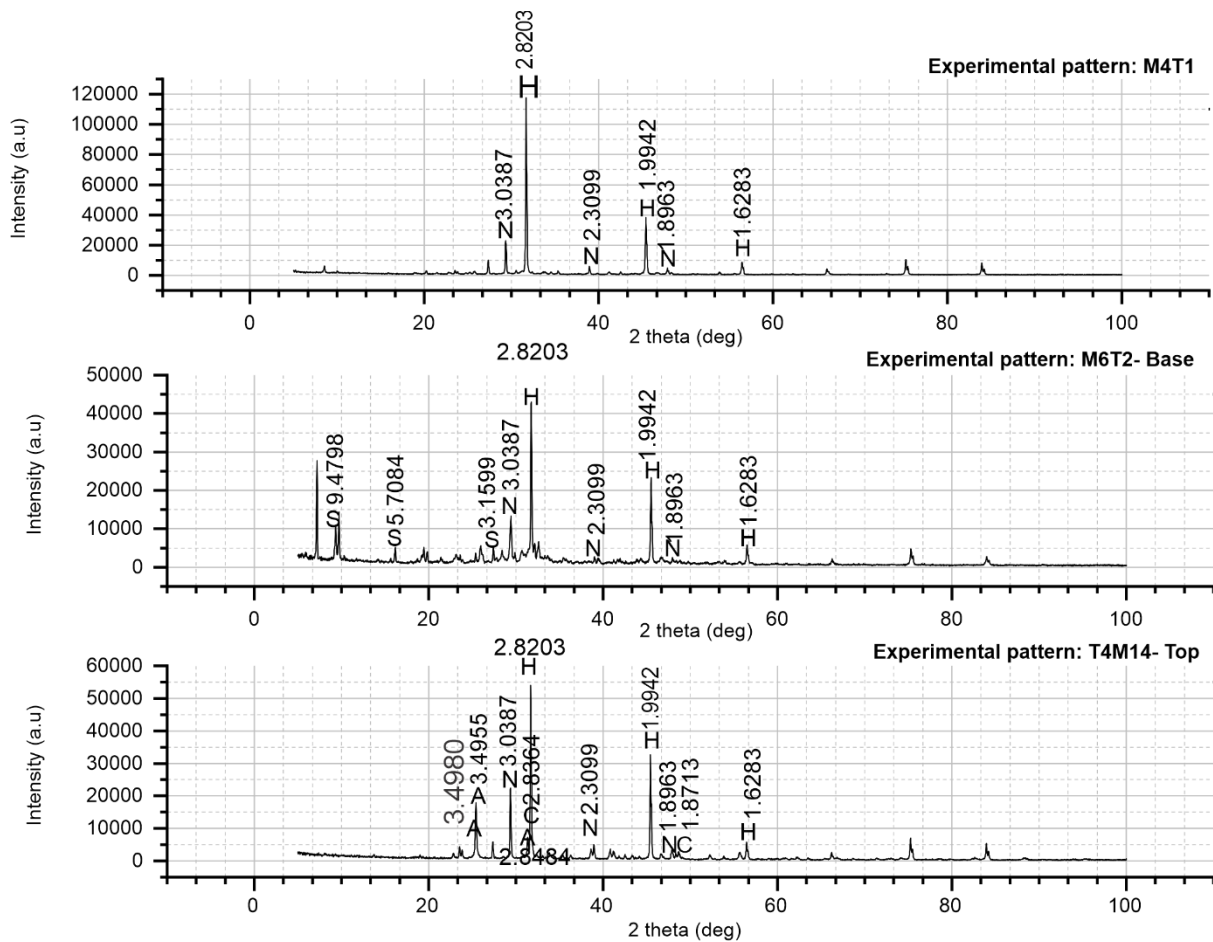
Figure 13. *X-ray diffraction patterns (CoKα radiation) of saline samples (M4T1, M6T2- Base and T4M14- Top). H, halite; N, nitratine; C, calcite; S, syngenite; A anhydrite.*

4.4 Scanning Electron Microscopy Analysis (SEM)

The complementary SEM data are considered essential for confirming the nature of the elemental chemical composition observed by the XRD**.** The chemical elements contained in the tolas samples are quantified using descriptive statistics from scanning electron microscopy, such elements are; oxygen, carbon, sodium, chlorine, nitrogen, sulfur, calcium, and potassium are shown in **Figure 14.** These data are obtained based on **Tables 5,6,7** where the percentage of atomic concentration of each chemical element in the saline samples is mentioned. **Figure 14** indicates that oxygen and carbon are found at higher concentrations than the other elements. However, it is essential to note that the carbon element results could be skewed due to the use of carbon conductive adhesive tabs used by SEM. Following that can be seen sodium and chlorine, and a lower proportion the sulfur, calcium, and potassium. **Table 4** lists the samples that will be analyzed in this study; however, the samples to be reported (M4T1, M6T2-Base, and T4M14-Top) were chosen based on the XRD results.
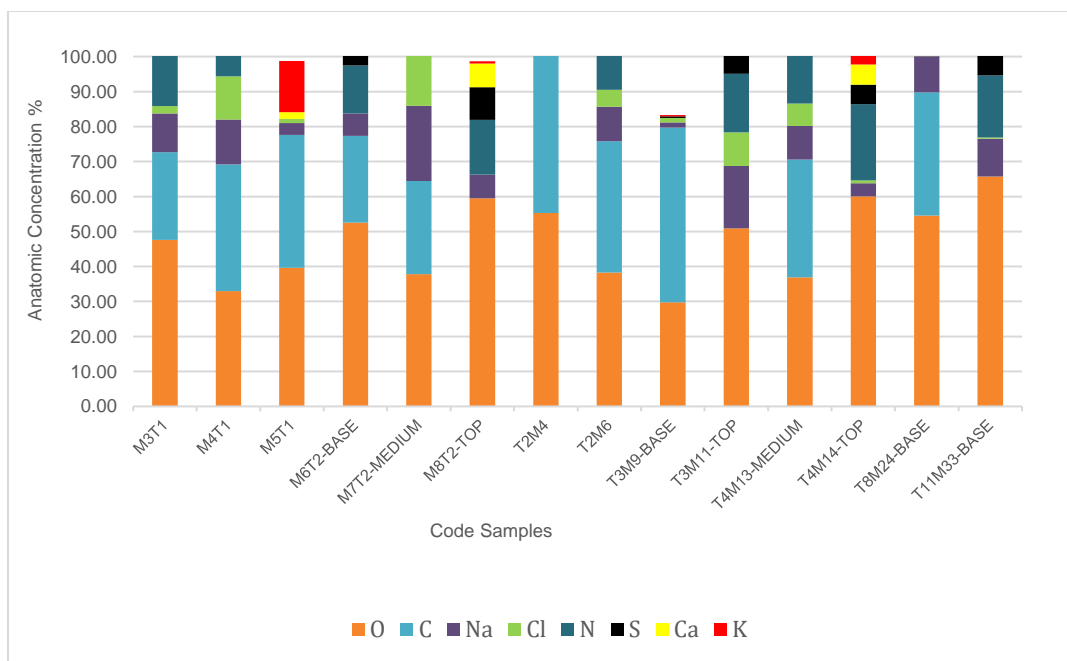
Figure 14. *SEM Average of the spots of the elemental composition of 14 samples of the saline soil.*

Table 5. SEM analysis of spot 1 of the Santa Catalina de Salinas-Ibarra saline samples

Code Sample	Spot 1: Atomic Concentration %							
	O	C	Na	Cl	N	S	Ca	K
M3T1	45.83	31.41	13.60	2.16	-	5.33	2.30	-
M4T1	17.77	52.25	-	15.97	-	-		-
M5T1	37.01	53.85	3.71	1.42	-	-	2.07	1.55
M6T2-BASE	51.46	23.85	6.65	-	12.47	3.75	1.51	-
M7T2-MEDIUM	18.87	39.00	23.21	17.02	-	-	0.99	-
M8T2-TOP	69.68	-	2.70	-	12.81	6.68	6.80	0.39
T2M4	39.15	54.18	2.47	1.41		0.47	0.99	1.33
T2M6	11.24	55.26	19.90	13.60	-	-	-	-
T3M9-BASE	32.44	32	-	1.32	-	-	-	-
T3M11-TOP	30.56	-	29.98	25.64	13.61	-	-	0.21
T4M13-MEDIUM	16.32	52.99	15.42	14.56	--	0.43	0.27	-
T4M14-TOP	56.37	-	1.53	0.76	21.89	6.94	6.33	5.11
T8M24-BASE	46.69	35.19	8.14	2.46	-	1.70		5.82
T11M33-BASE	69.28	-	13.37	-	-	11.45	5.62	-

Table 6. SEM analysis of spot 2 of the Santa Catalina de Salinas-Ibarra saline samples

Code Sample	Spot 2: Atomic Concentration %							
	O	C	Na	Cl	N	S	Ca	K
M3T1	41.02	30.47	5.25	-	17.23	2.29	1.11	0.67
M4T1	51.29	22.52	11.57	-	11.62	2.84	-	-
M5T1	43.76	25.25	2.51	0.39	-	-	-	27.68
M6T2-BASE	56.22	-	8.34		17.04	10.66	5.82	1.54
M7T2-MEDIUM	25.56	-	39.31	32.68		1.27	0.86	0.33
M8T2-TOP	59.95	-	10.25		11.88	11.19	6.47	0.25
T2M4	61.06	-	6.83	4.07	22.80	1.31	1.13	1.77
T2M6	51.67	24.64	3.02	0.49	13.26	0.83	1.12	2.98
T3M9-BASE	27.11	67.89	1.47	1.23	-	0.87	-	0.70
T3M11-TOP	57.99	_	12.96	1.84	25.27	-	-	1.36
T4M13-MEDIUM	43.45	28.49	6.10	3.63	16.88	1.23	0.21	-
T4M14-TOP	57.52	-	6.61	0.98	25.92	3.30	4.58	0.63
T8M24-BASE	66.04	-	15.70	-	-	12.33	5.93	-
T11M33-BASE	61.73	-	9.97	-	19.73	4.81	2.72	0.38

Table 7. SEM analysis of spot 3 of the Santa Catalina de Salinas-Ibarra saline samples

Code Sample	Spot 3: Atomic Concentration %							
	O	C	Na	Cl	N	S	Ca	K
M3T1	55.95	13.28	14.35	-	13.01	-	-	-
M4T1	29.75	33.97	14.09	8.71	13.12	0.36	-	-
M5T1	38.05	34.88	4.10	1.62	-	-	1.80	-
M6T2-BASE	49.96	25.67	4.43	-	11.68	3.77	1.97	1.49
M7T2-MEDIUM	69.03	14.32	1.78	1.01	9.76	0.73	0.45	-
M8T2-TOP	48.95	-	7.25	-	22.22	10.21	7.09	1.25
T2M4	65.58	-	6.19	3.55	21.04	-	1.44	2.20
T2M6	51.88	32.77	6.58	0.49	-	4.52	2.59	-
T3M9-BASE	-	-	-	-	-	-	-	-
T3M11-TOP	64.02	-	10.61	1.34	11.54	7.46	3.91	0.71
T4M13-MEDIUM	50.93	19.59	7.18	1.13	17.71	2.25	1.22	-
T4M14-TOP	66.33	-	3.01	-	17.30	6.56	6.51	-
T8M24-BASE	50.93	-	7.18	-	-	2.25	-	19.59
T11M33-BASE	66.10	-	9.19	0.32	15.84	4.31	2.34	1.00

M4T1 Sample

The spots that were made in the M4T1 sample are shown in Figure 13a. The sample's elemental analysis was derived from the X-ray spectra of the spots of the micrograph created by the SEM (**Figure 15b**). This elemental analysis is shown in **Tables 7, 8, 9**, **10, and 11**. The presence of the compounds NaCl (halite), Na (NO$_3$) (nitratine), Ca (SO$_4$), 2H$_2$O (gypsum), and Ca (CO$_3$) (calcite) is confirmed by SEM analysis performed on the M4T1 sample.

Table 7. SEM analysis of the sample M4T1, spot 1

Atomic number	Element symbol	Element name	Atomic concentration percentage	Weight concentration percentage	Oxide	Stoichiometric percentage
6	C	Carbon	52.25	34.86	C	63.54
8	O	Oxygen	17.77	15.80		
17	Cl	Chlorine	15.97	31.46	Cl	19.42
11	Na	Sodium	14.00	17.89	Na	17.03

Table 8. SEM analysis of the sample M4T1, spot 2

Atomic number	Element symbol	Element name	Atomic concentration percentage	Weight concentration percentage	Oxide	Stoichiometric percentage
8	O	Oxygen	51.29	50.80		
6	C	Carbon	22.52	16.75	C	46.23
7	N	Nitrogen	11.62	10.08	N	23.86
11	Na	Sodium	11.57	16.47	Na	23.76
16	S	Sulfur	2.84	5.63	S	5.83
14	Si	Silicon	0.16	0.27	Si	0.32

Table 9. SEM analysis of the sample M4T1, spot 3

Atomic number	Element symbol	Element name	Atomic concentration percentage	Weight concentration percentage	Oxide	Stoichiometric percentage
6	C	Carbon	33.97	23.83	C	48.36
8	O	Oxygen	29.75	27.80		
11	Na	Sodium	14.09	18.92	Na	20.05
7	N	Nitrogen	13.12	10.73	N	18.68
17	Cl	Chlorine	8.71	18.04	Cl	12.40
16	S	Sulfur	0.36	0.67	S	0.51

Table 10. SEM analysis of the sample M4T1, spot 4

Atomic number	Element symbol	Element name	Atomic concentration percentage	Weight concentration percentage	Oxide	Stoichiometric percentage
8	O	Oxygen	34.56	31.39		
6	C	Carbon	26.94	18.37	C	41.17
11	Na	Sodium	17.61	22.98	Na	26.90
7	N	Nitrogen	12.15	9.66	N	18.57
17	Cl	Chlorine	8.74	17.59	Cl	13.36

Table 11. SEM analysis of the sample M4T1, spot 5

Atomic number	Element symbol	Element name	Atomic concentration percentage	Weight concentration percentage	Oxide	Stoichiometric percentage
8	O	Oxygen	44.17	46.45		
6	C	Carbon	31.34	24.74	C	56.13
7	N	Nitrogen	15.27	14.06	N	27.35
11	Na	Sodium	7.86	11.88	Na	14.08
16	S	Sulfur	1.36	2.87	S	2.44

Figure 15. *a) SEM image of the spots of M4T1 sample surface; b) spectrum of the sample whose elements are given in Table 6,7,8,9 and 10.*

M6T2- Base Sample

The spots that were made in the M6T2- Base sample is shown in Figure 14a. The sample's elemental analysis was derived from the X-ray spectra of the spots of the micrograph created by the SEM (**Figure 16b**). This elemental analysis is shown in **Tables 12 and 13**. The

presence of the compounds NaCl (halite), $K_2Ca (SO4)_2 \cdot H_2O$ (syngenite) and Na (NO_3) (nitratine) is confirmed by SEM analysis performed on the M6T2- Base sample.

Table 12. SEM analysis of the sample M6T2-Base, spot 1

Atomic number	Element symbol	Element name	Atomic concentration percentage	Weight concentration percentage	Oxide	Stoichiometric percentage
6	C	Carbon	44.28	33.79	C	68.35
8	O	Oxygen	35.22	35.80		
7	N	Nitrogen	9.56	8.50	N	14.75
16	S	Sulfur	4.81	9.79	S	7.42
11	Na	Sodium	3.24	4.74	Na	5.01
20	Ca	Calcium	2.90	7.38	Ca	4.47

Table 13. SEM analysis of the sample M6T2-Base, spot 2

Atomic number	Element symbol	Element name	Atomic concentration percentage	Weight concentration percentage	Oxide	Stoichiometric percentage
8	O	Oxygen	69.00	54.28		
11	Na	Sodium	12.83	14.50	Na	41.37
16	S	Sulfur	11.65	18.38	S	37.59
20	Ca	Calcium	6.09	11.99	Ca	19.63
19	K	Potassium	0.44	0.84	K	1.42

Figure 16. *a) SEM image of the spots of M6T2- Base sample surface; b) spectrum of the sample whose elements are given in Table 11 and 12.*

T4M14-Top Sample

The spots that were made in the T4M14-Top sample are shown in Figure 14a. The sample's elemental analysis was derived from the X-ray spectra of the spots of the micrograph created by the SEM **(Figure 17b)**. This elemental analysis is shown in **Tables 14, 15, 16, and**

17. The presence of the compounds NaCl (halite), and Na (NO_3) (nitratine), Ca (CO_3) (calcite) and $CaSO_4$ (anhydrite) is confirmed by SEM analysis performed on the T4M4- Top sample.

Table 14. SEM analysis of the sample T4M14-Top, spot 1

Atomic number	Element symbol	Element name	Atomic concentration percentage	Weight concentration percentage	Oxide	Stoichiometric percentage
8	O	Oxygen	56.37	45.72		
7	N	Nitrogen	21.89	15.55	N	50.18
16	S	Sulfur	6.94	11.28	S	15.90
20	Ca	Calcium	6.33	12.86	Ca	14.51
19	K	Potassium	5.11	10.13	K	11.71
11	Na	Sodium	1.53	1.78	Na	3.51
12	Mg	Magnesium	1.07	1.32	Mg	2.46
17	Cl	Chlorine	0.76	1.37	Cl	1.74

Table 15. SEM analysis of the sample   T4M14-Top, spot 2

Atomic number	Element symbol	Element name	Atomic concentration percentage	Weight concentration percentage	Oxide	Stoichiometric percentage
8	O	Oxygen	57.52	51.27		
7	N	Nitrogen	25.92	20.23	N	61.03
11	Na	Sodium	6.61	8.47	Na	15.57
20	Ca	Calcium	4.58	10.22	Ca	10.78
16	S	Sulfur	3.30	5.90	S	7.78
17	Cl	Chlorine	0.98	1.93	Cl	2.30
19	K	Potassium	0.63	1.38	K	1.49
12	Mg	Magnesium	0.45	0.61	Mg	1.06

Table 16. SEM analysis of the sample T4M14-Top, spot 3

Atomic number	Element symbol	Element name	Atomic concentration percentage	Weight concentration percentage	Oxide	Stoichiometric percentage
8	O	Oxygen	66.33	56.30		
7	N	Nitrogen	17.30	12.86	N	51.38
16	S	Sulfur	6.56	11.15	S	19.47
20	Ca	Calcium	6.51	13.84	Ca	19.33
11	Na	Sodium	3.01	3.67	Na	8.94

Table 17. SEM analysis of the sample T4M14-Top, spot 4

Atomic number	Element symbol	Element name	Atomic concentration percentage	Weight concentration percentage	Oxide	Stoichiometric percentage
8	O	Oxygen	68.52	62.02		
7	N	Nitrogen	17.24	13.66	N	54.75
11	Na	Sodium	4.58	5.96	Na	14.56
16	S	Sulfur	2.81	5.10	S	8.94
12	Mg	Magnesium	2.28	3.14	Mg	7.24
20	Ca	Calcium	2.26	5.12	Ca	7.17
19	K	Potassium	1.77	3.92	K	5.63
17	Cl	Chlorine	0.53	1.07	Cl	1.70

Figure 17. a) SEM image of the spots of T4M14-Top sample surface; b) spectrum of the sample whose elements are given in Table 13,14,15 and 16.

The elemental analysis of Santa Catalina de Salinas-Ibarra reveals a heterogeneous distribution of O, C, Na, Cl, N, S, Ca, and K in general. These are the main cations that

contribute to the composition of sediments. A detailed quantitative analysis could not be carried out because powder samples were used instead of flat samples. Furthermore, it was also not calibrated with a standard sample for each element (65). However, the semi-quantitative elemental analysis allows us to see a more significant amount of halite and nitratine. This is understandable given the presence of Na, Ca, CI, and SO4 components in the saltier source waters, derived from evaporite dissolution by volcanic deposits (66,67).

According to Pueyo et al. (1999), halite-nitratine's presence as an interaction proves the nature of pre-existing mineral redissolution processes and precipitation of new solutes in residual porosity (68). As water evaporates, it concentrates, allowing a series of salts to precipitate in the order of increasing solubilities. Calcite ($CaCO_3$) is the first mineral that nearly always precipitates due to its poor solubility (69). Additionally, gypsum is often associated with rock salt and sulfur deposits (70,71). The most abundant sulfate mineral in nature is calcium sulfate, which is found in anhydrite and gypsum (58). According to Freyer and Voigt (2003), evaporitic deposits also contain varying concentrations of double or triple salt minerals, such as syngenite, $K_2Ca (SO_4)_2 H_2O$ (72). Syngenite forms the upper part of a salt crust on sandstone, is believed. This is due to that is to have formed from solutions that ascended through the lower part of the crust, which is made up of gypsum (73). The crystals of syngenite, which are followed by gypsum crystals, have been found in soil conditions. This behavior is caused by the contact of some minerals with potassium-rich brines (74). However, the potassium element is poor in the M6T2- BASE sample (**Figure 16**). It is believed to be because of a lack of complete mapping of the sample.

4.5 Antibacterial activity

The liniment is made from the iodine solution residue left over after the salt has been extracted. Residents of the Santa Cautalina de Salinas area have had a positive experience with this product. Nevertheless, any product that is applied to the skin directly must be sanitary, both chemical and microbiological. However, no research on this therapeutic liniment has been identified so far. As a result, it was critical to include this study in the research.

The samples were examined for antibacterial activity (1, 2,3, and 4). This was accomplished through the use of the agar diffusion method. Labels 1a, 1b, and 1c refer to the phase 1 dilutions (1000 g/ ml, 100 g/ ml, and 10 g/ ml, respectively) for this test. Similarly, labels 2a, 2b, and 2c refer to the same dilutions of phase 2, 3a, 3b, and 3c refer to the respective dilutions of phase 3, and 4a, 4b, and 4c refer to the dilutions of phase 4.
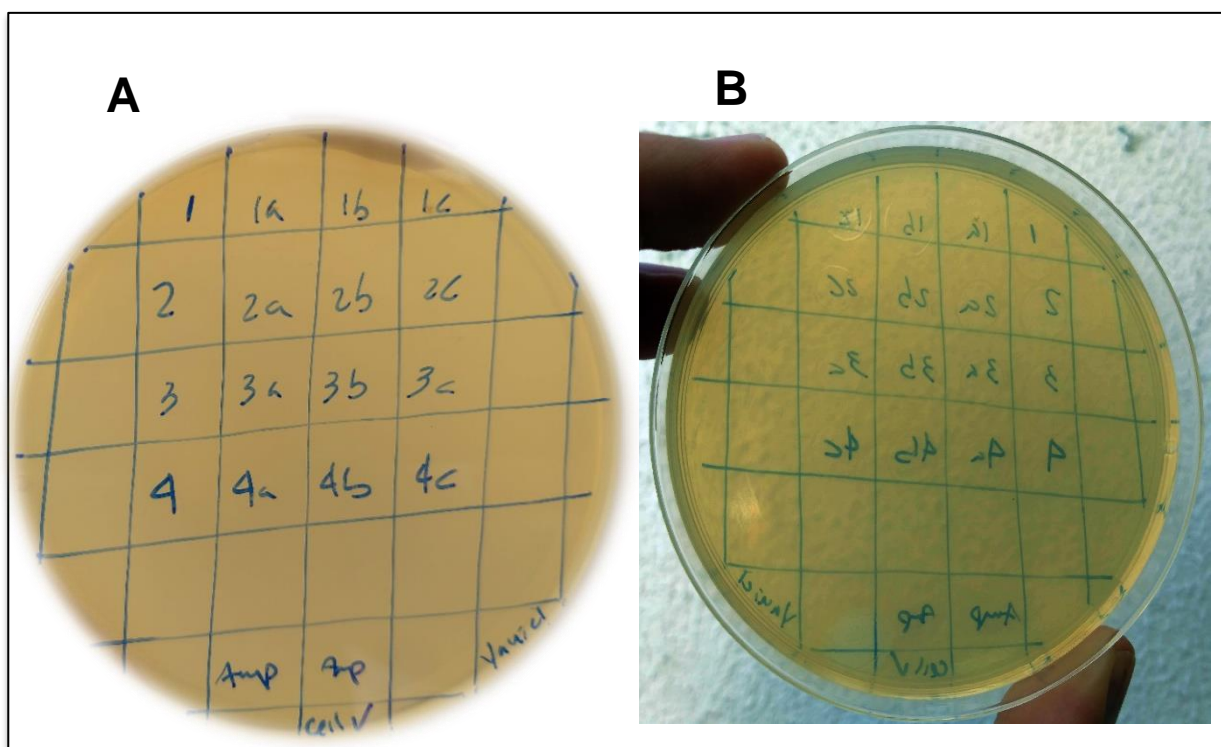
Figure 18. *Antibacterial activity carried out with the E. coli* TG1 strain. *The samples were drawn from an anti-inflammatory liniment used by residents of Santa Catalina de Salinas parish. A) labeling on the agar plate, B) result of antibacterial activity*

The antibacterial activity test on agar revealed that samples 1,2,3,4, and its dilutions do not inhibit bacteria. The study "Bacteriostatic and bactericidal clays" found that these did not present antibacterial properties because they did not contain reduced metals in their composition. However, It was also possible to establish that if a reducing agent, natural or synthetic, is applied to the clay, it will develop bacteriostatic or bactericidal properties (75). On the other hand, the samples analyzed from Santa Catalina de Salinas presented a pH of 6, and according to Philip et al., 2018, the investigations carried out by this bacterium's optimum pH range is between 6.5 and 7.5, based on temperature (76).

Conclusions

The analytical procedure developed in this work allowed us to realize a preliminary characterization, for the first time, of the total organic composition (polar and non-polar fractions) of the Tolas and liniment originating from salt extraction of Santa Catalina of Salinas del canton Ibarra. Results obtained from extraction and chromatogram analyses of the non-polar and polar fraction of the Santa Catalina de Salinas- Ibarra saline samples are not conclusive. For this reason, different test methods for determining the chemical composition of materials are required. However, using an XRD-diffractometer and a scanning electron microscope (SEM), it was possible to ascertain that the samples taken from the Tolas included more halite, nitratine, calcite, syngenite, and anhydrite. On the other hand, antibacterial activity analysis of the saline samples of Santa Catalina de Salinas- Ibarra do not show any antibacterial inhibition *E. coli* TG1 strains, which could be directly related to the scarcity of reduced metals in its composition.

FUTURE WORKS

1 Work is needed into the physicochemical and elemental determination of saline samples for understand potential element mobility.
2 Test different methods for determining the chemical composition of the samples.
3 Deepen the anti-inflammatory activity study to potentiate the bioactive compounds of this liniment in the pharmaceutical sectors

References

1. Pomeroy C. The Salt of Highland Ecuador: Precious Product of a Female Domain. Ethnohistory. **2014;**35(2):131–60.

2. Jaramillo H. The Otavaleño Institute of Anthropology: Its Publications 1966-2007. Cordero S, Frances E, editors. Vol. 4. Quito; **2007**. 66–68 p.

3. Mannar MGV, Dunn JT. Salt Iodization for the Elimination of Iodine Deficiency. **1995**. 1–101 p.

4. Salazar E. History of salt in Pre-Columbian and Colonial Ecuador. Antropol Cuad Investig. **2010**;(10):14–29.

5. Pomeroy C. Salt in Andean Cultures. ABYA- YALA Fund. **1986**;53(9):4–69.

6. Hassaurek F. Four years among spanish - americans. H. 0 . HOU. Hurd and Ho2323hton, 459 Broome Street. **1868**. 334–345 p.

7. Salomon F. The Ethnic Lords of Quito In The Time of The Incas Etnoltistoria Series. Gallocapitan. **1980**;144–5.

8. Estupiñán Viteri T. Los Sigchos, the last refuge of the Incas from Quito. A preliminary proposal. Bull l'Institut français d'études Andin. **2011**;40(1):192.

9. Wörrle B. From cooking to witchcraft. Abya-Yala. **1999**. 9–233 p.

10. Kinoshita Y, Cloutier AK, Rozak DA, Khan MSR, Niwa H, Uchida-Fujii E, et al. A novel selective medium for the isolation of Burkholderia mallei from equine specimens. BMC Vet Res. **2019**;15(1):1–7.

11. Bidart C. Epidemiology, Control and Prevention of Equine Death. Univ Repub Fac Vet. **2016**;147:6–40.

12. Corrie FE. Iodine and livestock. Fertil J. **1929**;1:2–32.

13. Páez DA. Considerations for an epidemiology of food and eating: A genealogy of nutritional studies in Ecuador. Salud Colect. **2018**;14(3):607–22.

14. Martos-Martínez JM. Study of incidence and determination of predictive factors of occult thyroid carcinoma in patients with multinodular goiter. Dialnet. Universidad de Sevilla; **2014**.

15. Fierro R, Recalde F. Previous Studies and Planning of Research Work on Endemic Goiter in The Andean Region. J Fac Med Sci. **2017**;9(1):56–66.

16. Benítez F. Notes on the prophylaxis of endemic goiter. Rev Fac Cien Med Hered since **1992**. 2017;3(1):73–80.

17. Peris Roig B, Atienzar Herráez N, Merchante Alfaro AA, Calvo Rigual F, Tenías Burillo JM, Selfa Moreno S, et al. Endemic goiter and iodine deficiency: Is it still a reality in Spain? An Pediatr. **2006**;65(3):234–40.

18. Delgado S. Establishing the Microbiological Quality in Natural Products for Medicinal use, Category C, that are used in Anti-Inflammatory Affections Period 2012-2013. Revista Brasileira de Ergonomia. **2016.**

19. Moron F, Levy M. General pharmacology. Cheping, N. García M, editor. La Habana; **2002**. 3–4 p.

20. Flores LE, López JI, Arelis DT, Medina L de los Á. Preliminary phytochemical analysis of the bark of Schoepfia schreberi used for the treatment of blows and wounds in the municipality of La Venta. Sci Portal. **2014**;6:37–43.

21. Corrales IE, Reyes JJR, Piña R. Medicinal Plants of Stomatological Interests. Ramanujan J. **2014**;53(256):79–98.

22. OMS. WHO strategy on traditional medicine 2002-2005. World Heal. World Health Organization. **2002**. 1–63 p.

23. Jean M, Robertson H. UNESCO Dossier for the Aspiring Geopark Project of Imbabura , Ecuador focusing on responsible participatory community tourism development based on singular geological identity. ResearchGate. **2014**;42–9.

24. Arellano S, Arroyo D, Carrión E, Merizalde C. UNESCO ' s Global Geoparks and its importance on communities'. **2019**;6(1):93–108.

25. Opinion. The Blacks of Chota. Opinion. 2017 Jul 5;20–1.

26. Cevallos M. Development Plan and Territorial Organization of the Rural Parish "Santa Catalina de Salinas." Igarss 2014. **2015**;(1):1–89.

27. Echeverria J, Uribe M. Northern andean northern area: archeology and ethnohistory. **1995.** 10–451 p.

28. Yamberla N. The Rehabilitation of the Railway in the Section Including Ibarra-Salinas and its Impact on the Socio-Economic Development of the Canton Ibarra. **2016**.

29. Wolf T. The region between the Mojanda y Cajas junction and the border of Colombia. In: Geography and geology of Ecuador. **1892**. p. 104.

30. Suárez E. Geological and Geochemical Characterization of Soils in the South and Northwest Sector of the Blanca Nieves Mining Project, "Jijón y Caamaño" Parish, Carchi Province. **2020**;23.

31. Smith AP, Young TP. Tropical Alpine Plant Ecology. Annu Rev Ecol Syst. **1987**;18(1):137–58.

32. Crespo P, Célleri R, Buytaert W, Ochoa B. Impacts of land use change on the hydrology of the Andean humid páramos. ResearchGate. **2014**;(July):287–304.

33. Hofstede R, Calles J, López V, Polanco R, Torres F, Ulloa J, et al. The Andean Páramos. Tiempos de Crisis sistémica. **2014**. 7–110 p.

34. Winckell A, Marocco R, Winter T, Huttel C, Pourrut P, Zebrowski C, et al. The Natural Landscapes of Ecuador. Vol. 1, Geografía básica del Ecuador: Geografía física. **1997**. 3–145 p.

35. National Institute of Meteorology and Hydrology. Hydrological study Mira. Hydrological Studies and Research. Quito; **2005** Oct.

36. Donoso E. Analysis of the environmental system according to the senplades methodology, as a contribution to the territorial planning and management of the ibarra canton. Pontifical Catholic University of Ecuador; **2012**.

37. INAMHI. Six-monthly weather bulletin **2016**.

38. Molina J. Evaluation of Soil Salinity in The Calera Hacienda - Iancem to Determine Management and Conservation Measures. Pontifical Catholic University of Ecuador; **2018**.

39. Madrigal LP. Climate change, soil salinity and crop production in irrigation areas. Terra Latinoam. **2016**;34(2):207–18.

40. Benet A, Canton Y. Saline Soil Improvement and Erosion Control. **2005**;1.

41. Andrade G, Carranco A, Pachacama F, Rodriguez O. Contributions to the Ibarra Geological Sheet Project: Salinas - LA Merced Scale 1: 50,000. Central University of ECuador; **2012**.

42. Winter T, Marocco R. Sketch of the Geodynamic Evolution of Ecuador. 1988;(1).

43. Geophysical Institute National Polytechnic School. Classification of Volcanoes in Ecuador. **2020**.

44. Garces G. Irrigation profile. **1996**. p. 1–35.

45. Caillavet C. I.3. The salt of Otavalo. Indigenous continuities and colonial ruptures. In: Northern Ethnic Groups. Lima: Institut français d'études andines; **2000**. p. 59–83.

46. Fierro B, Penafiel W, De Groot L, Ramirez I. Endemic Goiter and Endemic Cretinism in the Andean Region. In: New England Journal of Medicine. The New England Journal of Medicine; **1969**. p. 302.

47. Abraham G. The history of iodine in medicine. Part I: From discovery to essentiality. Orig Internist. **2006**;13(1):29–36.

48. Coras M, Ontiveros R, Diakite L. Groundwater flow and concentration of salts in

agricultural soils Resumen Introducción. **2014**;5:537–48.

49. Ibarra Y. Bombodromo Palenque and Salt Museum in Salinas Ecuador- YouTube. Ecuador; **2018**.

50. Suárez M, González P, Domínguez R, Bravo A, Melián C, Pérez M, et al. Identification of organic compounds in San Diego de los Baños peloid (Pinar del Río, Cuba). J Altern Complement Med. **2011**;17(2):155–65.

51. Kohli R, Mittal KL. Methods for Assessing Surface Cleanliness. Vol. 12, Developments in Surface Contamination and Cleaning, Volume 12. **2019**. 97 p.

52. Crystal Impact GbR. Match! Download Area. **2020**.

53. Hanako G. Scanning electron microscopy and microanalysis of elements of the BioMimic Scientific and Technological Cluster. INECOL. **2017**.

54. Book NCW. n-Hexane. **2018**.

55. Book NCW. Methyl Alcohol. **2018**.

56. Le Pevelen DD. X-ray crystallography of small molecules: Theory and workflow. Encycl Spectrosc Spectrom. **2016**;624–39.

57. Toraya H. A new method for quantitative phase analysis: direct derivation of weight fractions from observed intensities and chemical composition data of individual crystalline phases. Rigaku. **2018**;34(1):3–8.

58. Morales J, Astilleros J, Díaz L, Jiménez A. Study of the crystallization of calcium sulfate at 80ºC: implications in the crystallization of anhydrite. Macla. **2012**;(16):170–1.

59. Boeyens JCA, Ichharam VVH. Redetermination of the crystal structure of calcium sulphate dihydrate, CaSO4 • 2H2O. Zeitschrift fur Krist - New Cryst Struct. **2002**;217(JG):9–10.

60. Norman E. A Redetermination of the Carbon-Oxygen Distance in Calcite and the Nitrogen-Oxygen Distance in Sodium Nitrate. **1932**;(6011):1–3.

61. Ahtee M, Nurmela M, Suortti P, Järvinen M. Correction for preferred orientation in Rietveld refinement. J Appl Crystallogr. **1989**;22(3):261–8.

62. Jürgens B, Irran E, Schneider J, Schnick W. Trimerization of NaC2N3 to Na3C6N9 in the solid: Ab initio crystal structure determination of two polymorphs of NaC2N3 and of Na3C6N9 from x-ray powder diffractometry. Inorg Chem. **2000**;39(4):665–70.

63. Corazza E, Sabelli C. The crystal structure of pirssonite, CaNa 2 (CO 3) 2 .2H 2 O . Acta Crystallogr. **1967**;23(5):763–6.

64. Cheng G C H ZJ. The crystal structure of anhydrite (CaSO4). **1963**;2:767–9.

65. Kuisma-Kursula P. Accuracy, Precision and Detection Limits of SEM-WDS, SEM-EDS

and PIXE in the Multi-Elemental Analysis of Medieval Glass. X-Ray Spectrom. **2000**;29(1):111–8.

66. Risacher F, Alonso H. Geochemistry of the Salar de Atacama, part 2: Evolution of the waters. Rev Geol Chile. **1996**;23(2):123–34.

67. Smoot JP, Lowenstein TK. Chapter 3 Depositional Environments of Non-Marine Evaporites. Dev Sedimentol. **1991**;50(C):189–347.

68. Pueyo JJ, Chong G, Vega M. Mineralogy and evolution of mother brines in the Pedro de Valdivia nitrate deposit, Antofagasta, Chile. SciELO. **1998** Jul;25(1):3–15.

69. Aquilano D, Otálora F, Pastero L, García-Ruiz JM. Three study cases of growth morphology in minerals: Halite, calcite and gypsum. Vol. 62, Progress in Crystal Growth and Characterization of Materials. Elsevier Ltd; **2016**. p. 227–51.

70. López PL, Auqué LF, Garcés I, Chong G. Chemical characteristics and evolutionary patterns of the surface brines of the Salar de Llamara, Chile. Rev Geol Chile. **1999**;26(1):89–108.

71. Grimsley G. Origin of Gypsum , with Special Reference to the Origin of the Michigan Deposits, Vol . 19 (1903 - 1904), pp . 110- Published by : Kansa. **1903**;19:110–7.

72. Freyer D, Voigt W. Crystallization and Phase Stability of CaSO4 and CaSO 4 - Based Salts. Monatshefte fur Chemie. **2003**;134(5):693–719.

73. Schweigstillová JSV&. HD. New investigations on the salt weathering of Cretaceous sandstones, Czech Republik. Sandstone Landscapes Eur Past, Presence Futur. **2005**;44:177–9.

74. Mees F, Tursina T V. Salt Minerals in Saline Soils and Salt Crusts [Internet]. Interpretation of Micromorphological Features of Soils and Regoliths. Elsevier B.V.; **2018**. 289–321 p. Available from: http://dx.doi.org/10.1016/B978-0-444-63522-8.00011-5

75. Gomes CF, Gomes JH, da Silva EF. Bacteriostatic and bactericidal clays: an overview. Environ Geochem Health [Internet]. **2020**;42(11):3507–27. Available from: https://doi.org/10.1007/s10653-020-00628-w

76. Philip P, Kern D, Goldmanns J, Seiler F, Schulte A, Habicher T, et al. Parallel substrate supply and pH stabilization for optimal screening of E. coli with the membrane-based fed-batch shake flask. Microb Cell Fact [Internet]. **2018**;17(1):1–17. Available from: https://doi.org/10.1186/s12934-018-0917-8

Appendix a. FTIR spectroscopy Sample

This section contains descriptions of all the samples studied
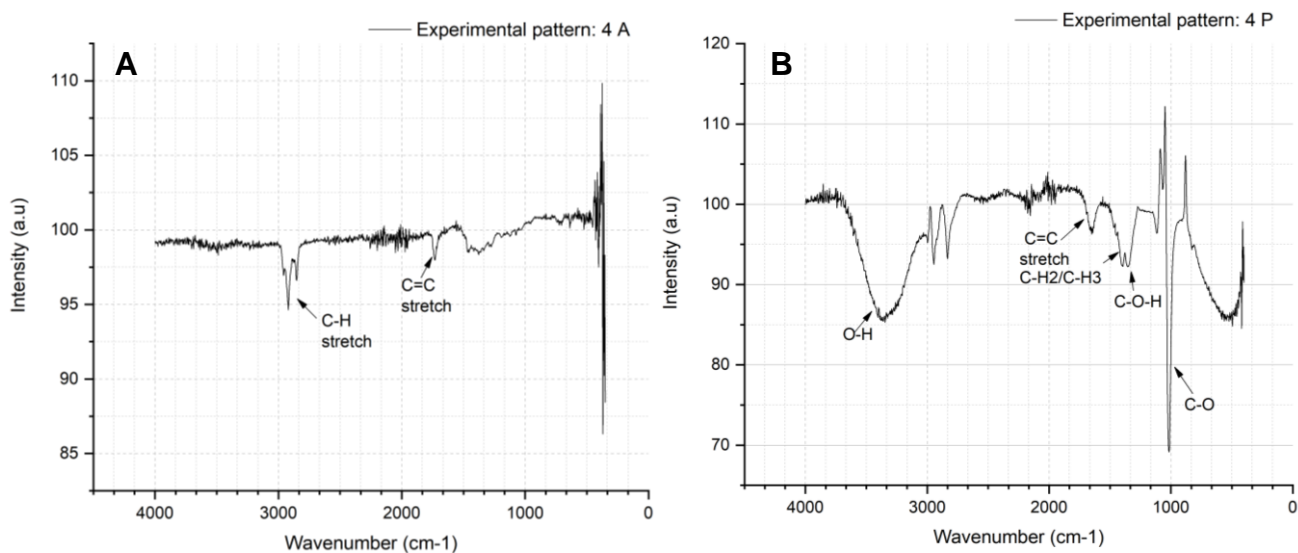
SA 1. FTIR spectroscopy. A) sample 4 nonpolar, B) sample 4 polar
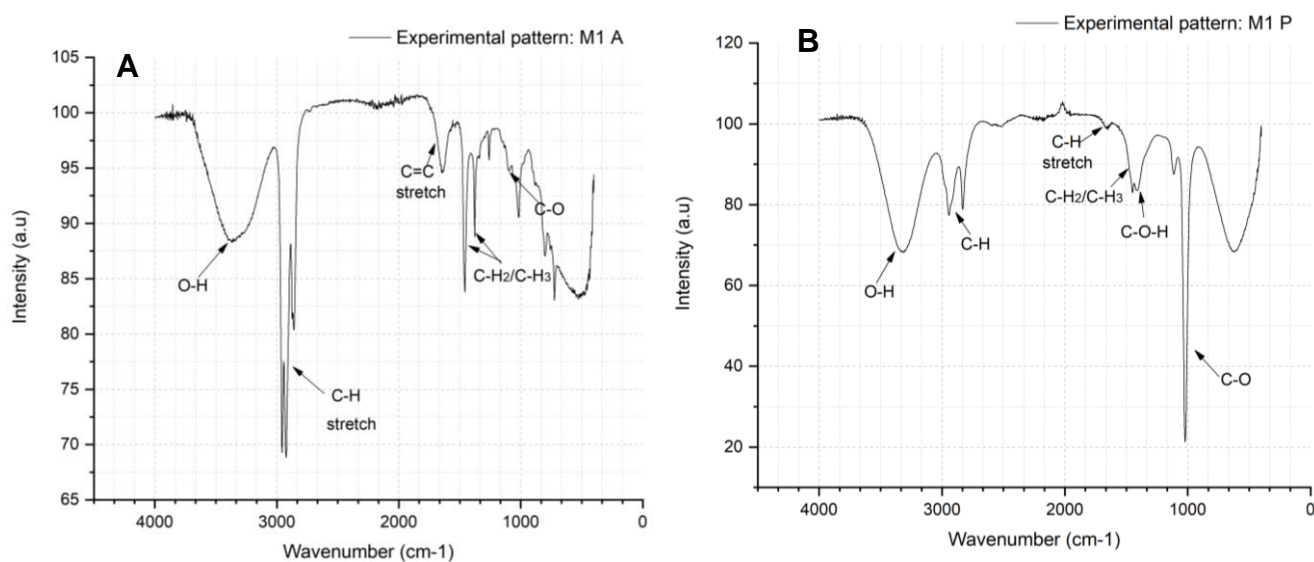
SA 2. FTIR spectroscopy. A) sample M1 nonpolar, B) sample M1 polar
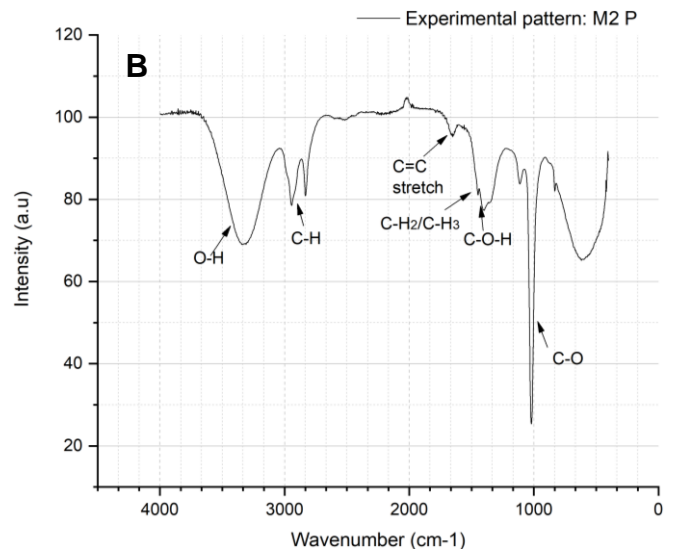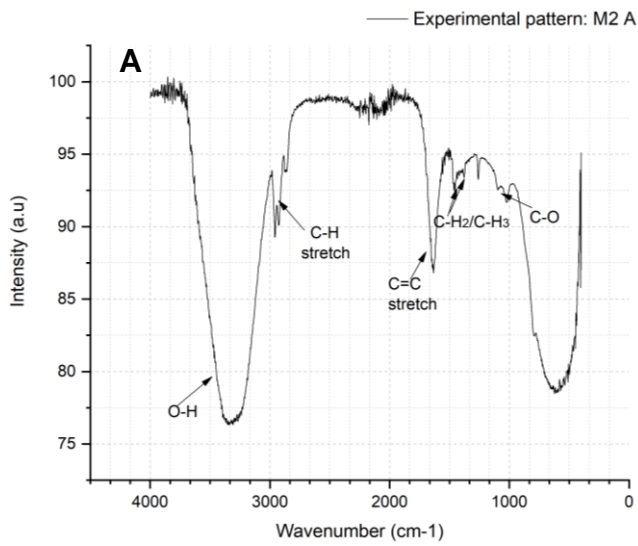
SA 3. FTIR spectroscopy. A) sample M2 nonpolar, B) sample M2 polar
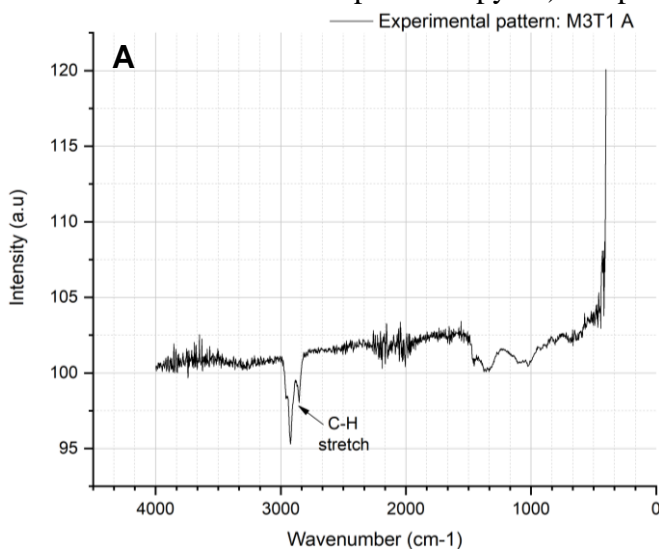
SA 4. FTIR spectroscopy. A) sample M3T1 nonpolar
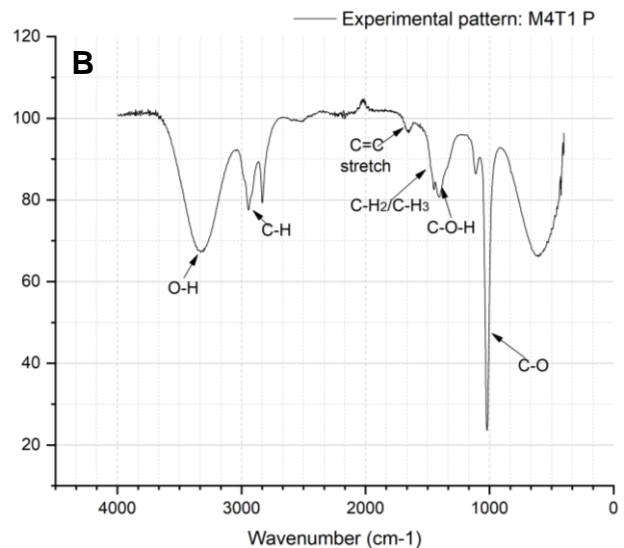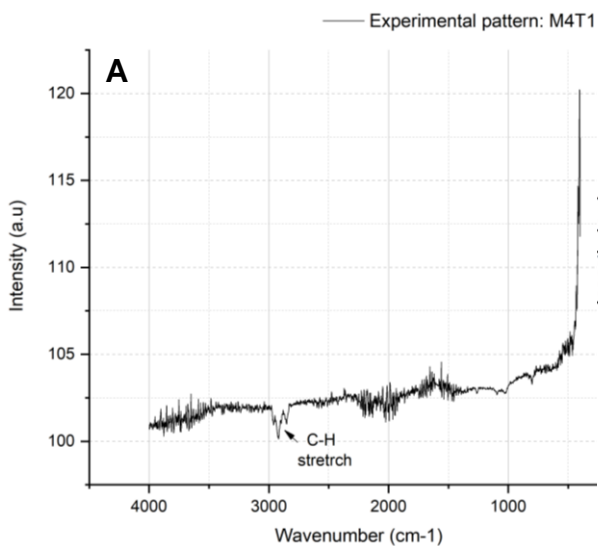
SA 5. FTIR spectroscopy. A) sample M4T1 nonpolar, B) sample M4T1 polar
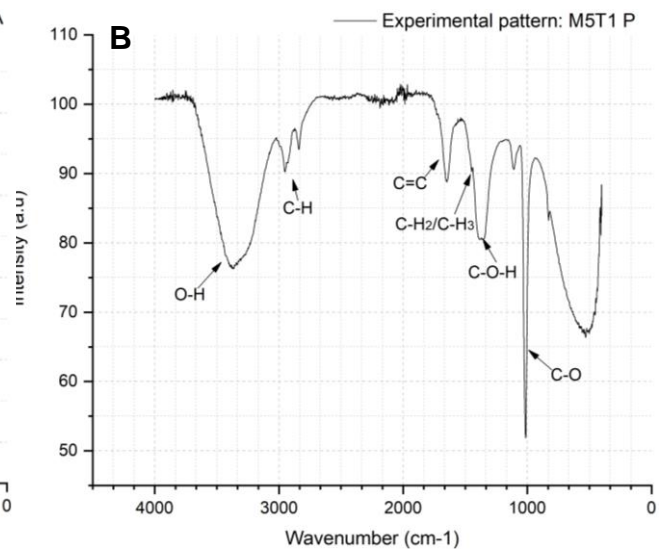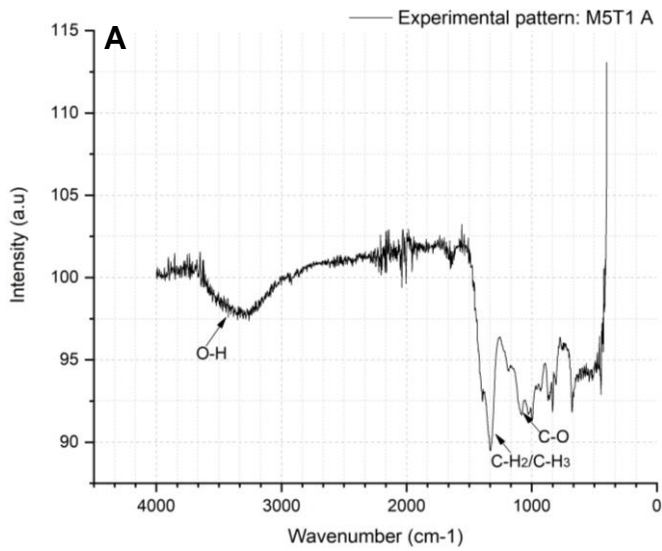
SA 6. FTIR spectroscopy. A) sample M5T1 nonpolar, B) sample M5T1 polar
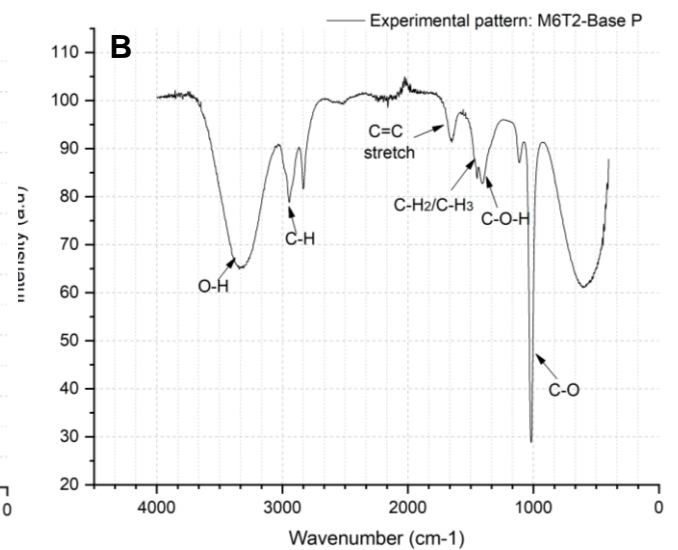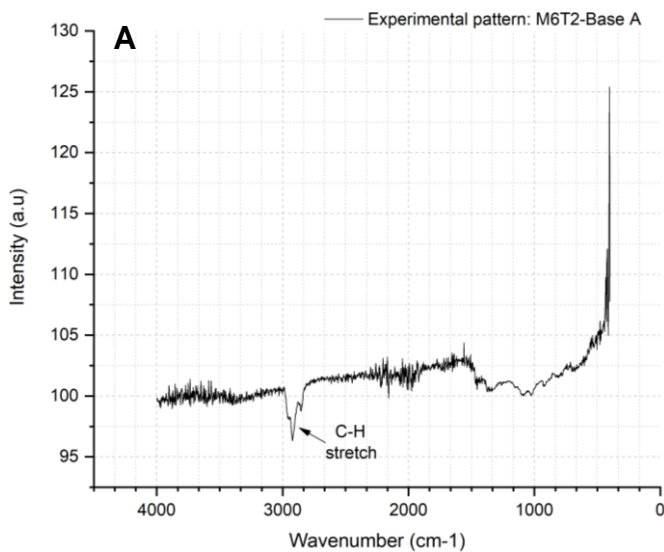
SA 7. FTIR spectroscopy. A) sample M6T2-Base nonpolar, B) sample M6T2-Base polar
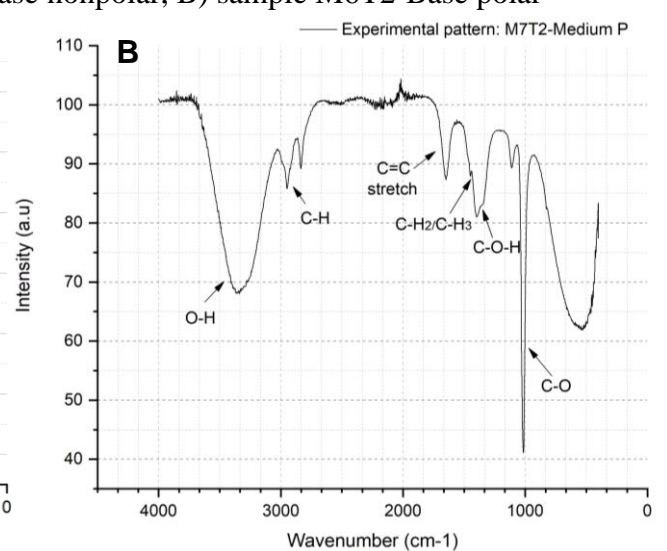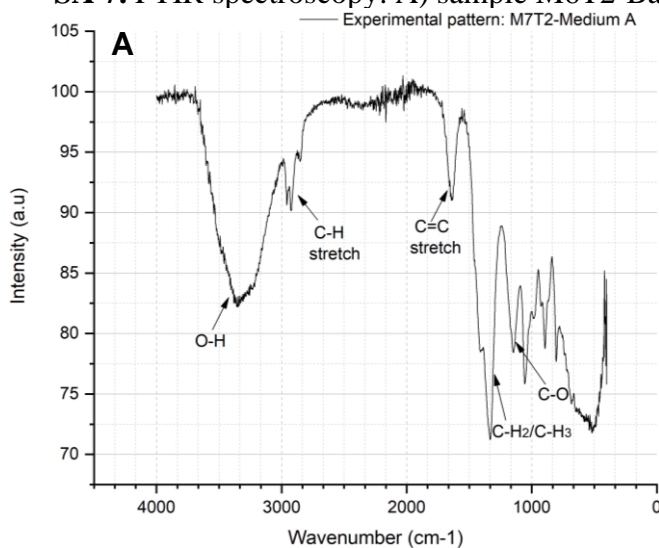
SA 8. FTIR spectroscopy. A) sample M7T2-Medium nonpolar, B) sample M7T2-Medium polar
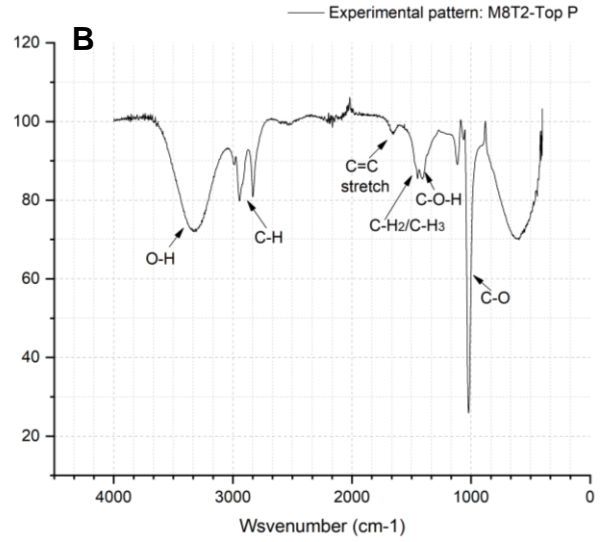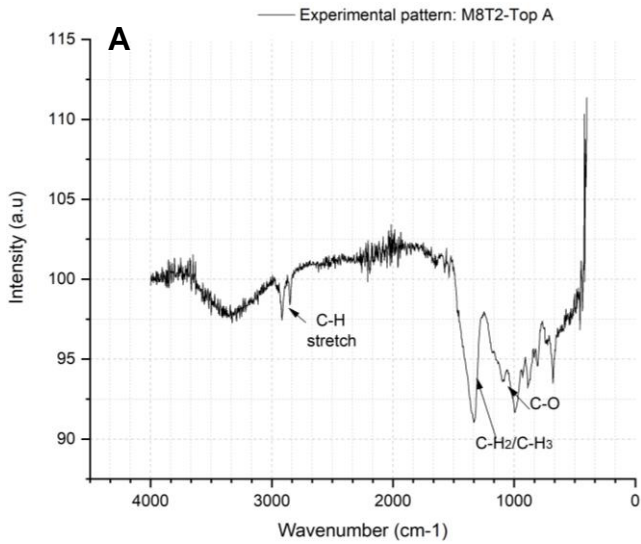
SA 9. FTIR spectroscopy. A) sample M8T2-Top nonpolar, B) sample M8T2-Top polar
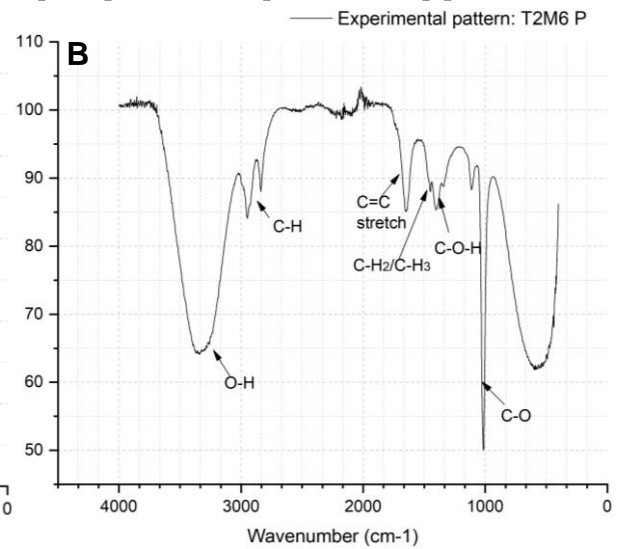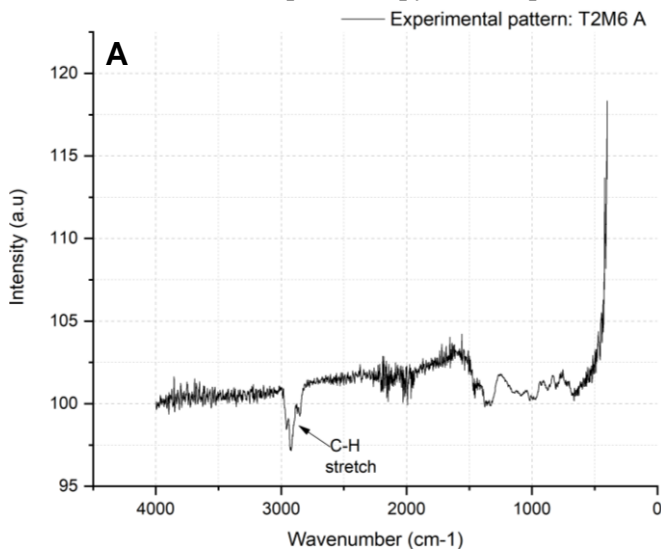
SA 10. FTIR spectroscopy. A) sample T2M6 nonpolar, B) sample T2M6-Top polar
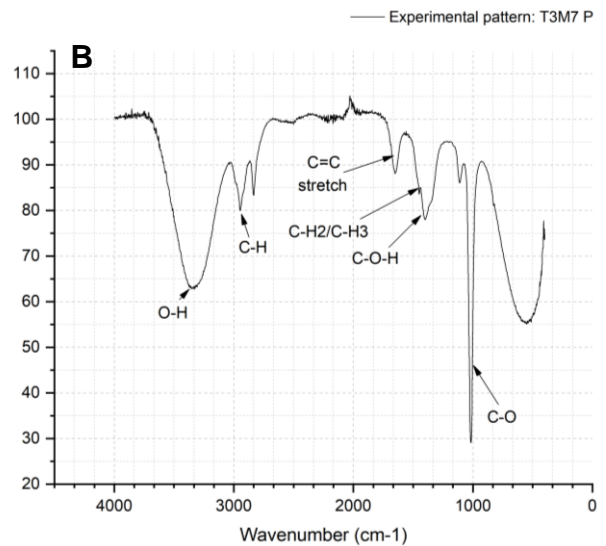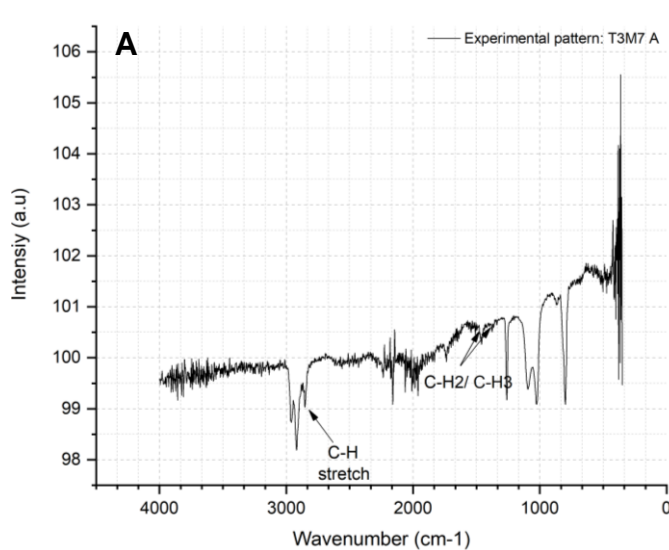
SA 11. FTIR spectroscopy. A) sample T3M7-Top nonpolar, B) sample T3M7-Top polar
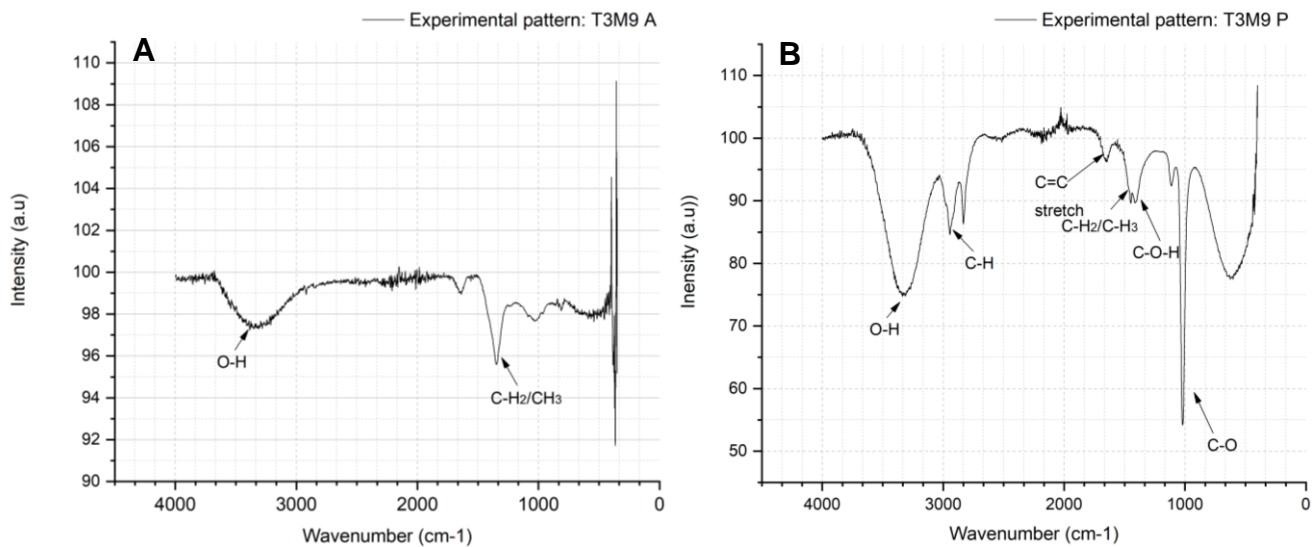
SA 12. FTIR spectroscopy. A) sample T3M9-Base nonpolar, B) sample T3M7-Base polar
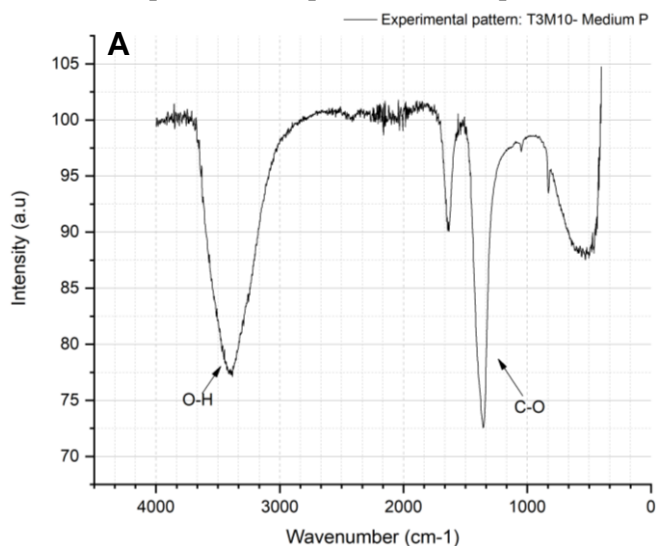
SA 13. FTIR spectroscopy. A) sample T3M10-Medium polar.
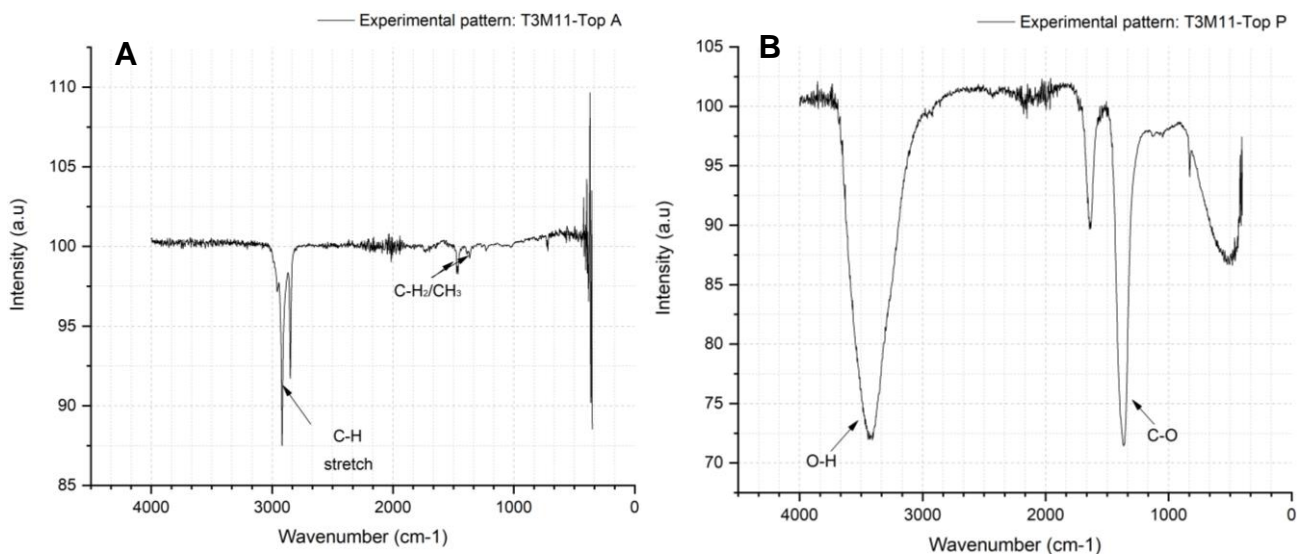
SA 14. FTIR spectroscopy. A) sample T3M11-Top nonpolar, B) sample T3M11-Top polar
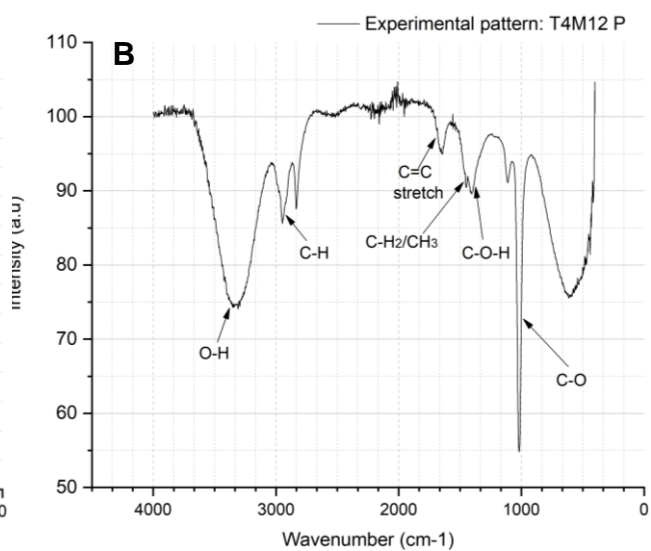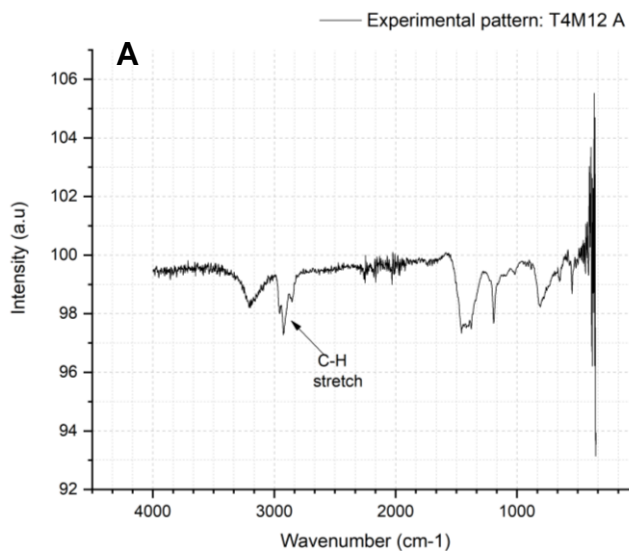
SA 15. FTIR spectroscopy. A) sample T4M12 nonpolar, B) sample T4M12 polar
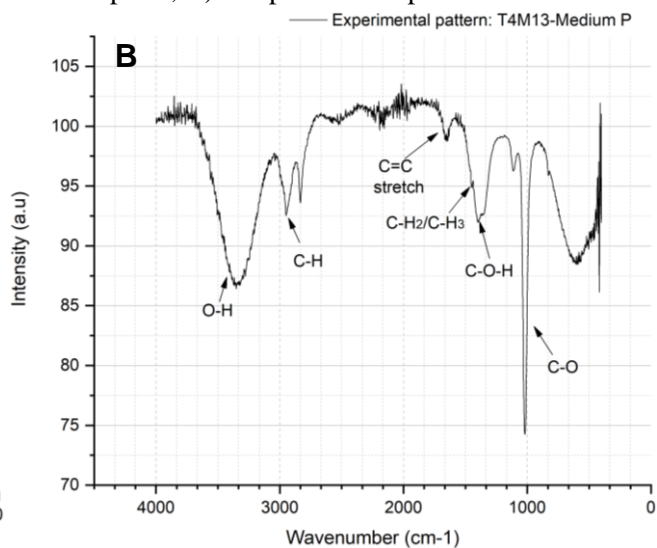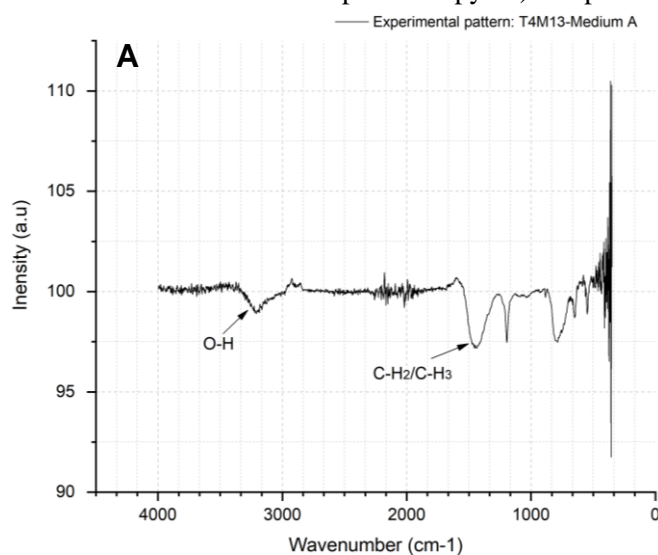
SA 16. FTIR spectroscopy. A) sample T4M13-Medium nonpolar, B) sample T4M13-Medium polar
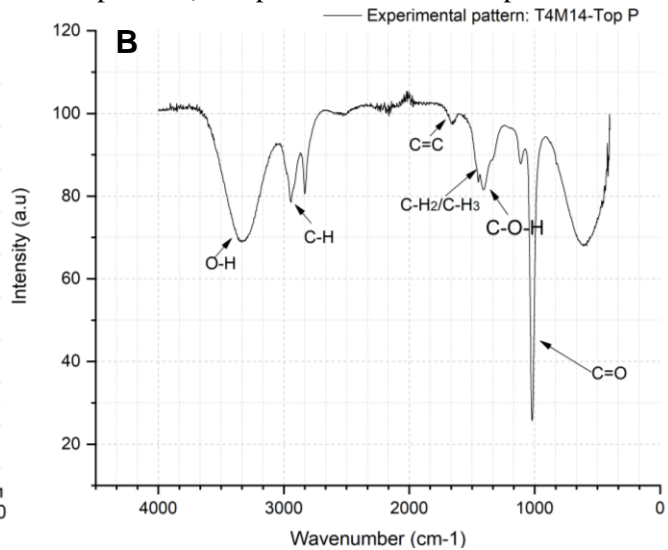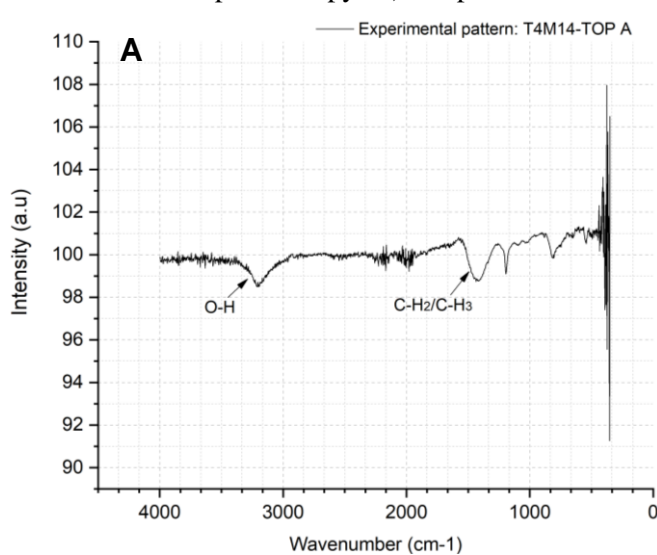
SA 17. FTIR spectroscopy. A) sample T4M14-Top nonpolar, B) sample T4M14-Top polar
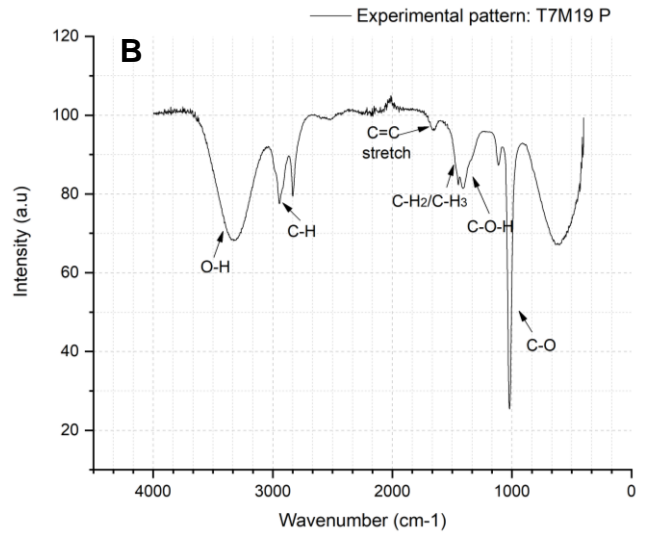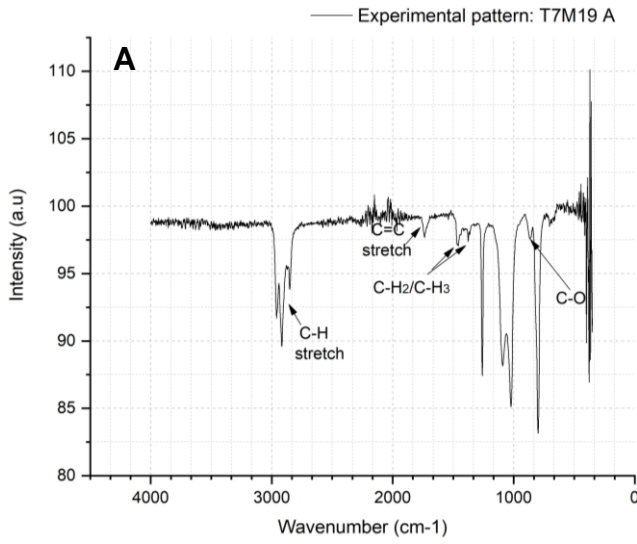
SA 18. FTIR spectroscopy. A) sample T7M19 nonpolar, B) sample T7M19 polar
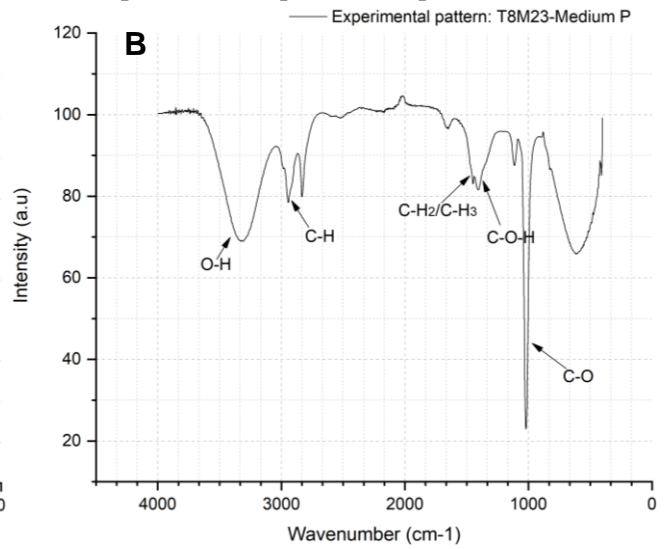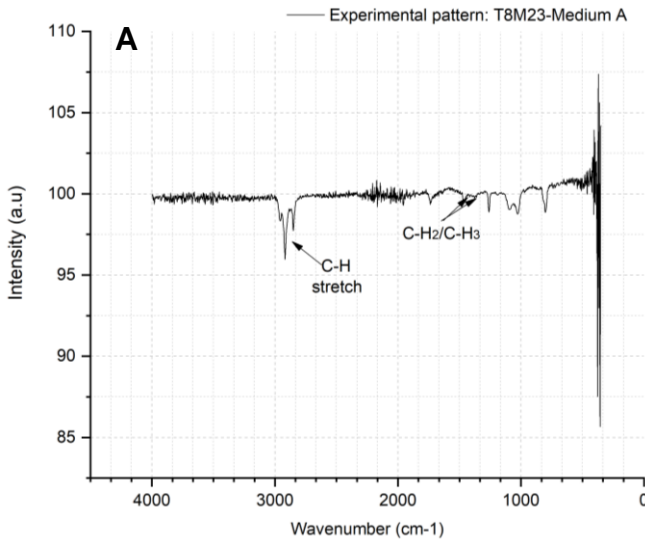
SA 19. FTIR spectroscopy. A) sample T8M23-Medium nonpolar, B) sample T8M23-Medium polar
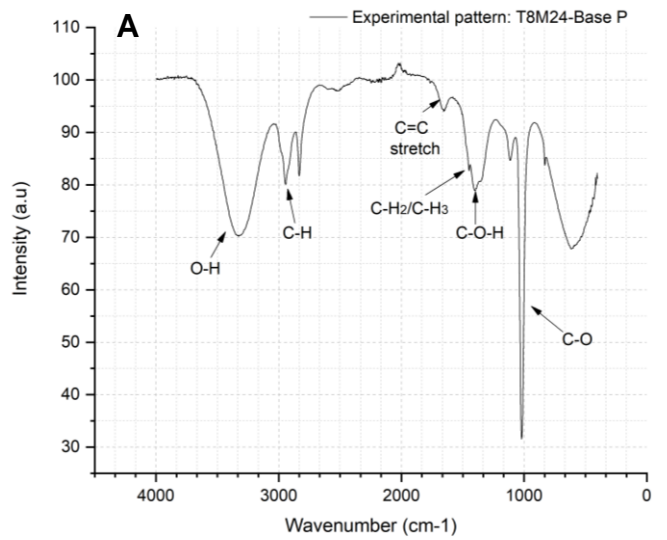
SA 20. FTIR spectroscopy. A) sample T8M24-Base polar
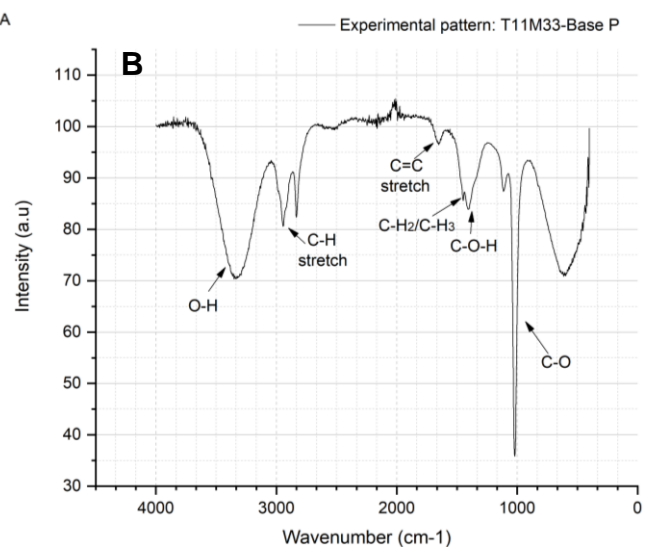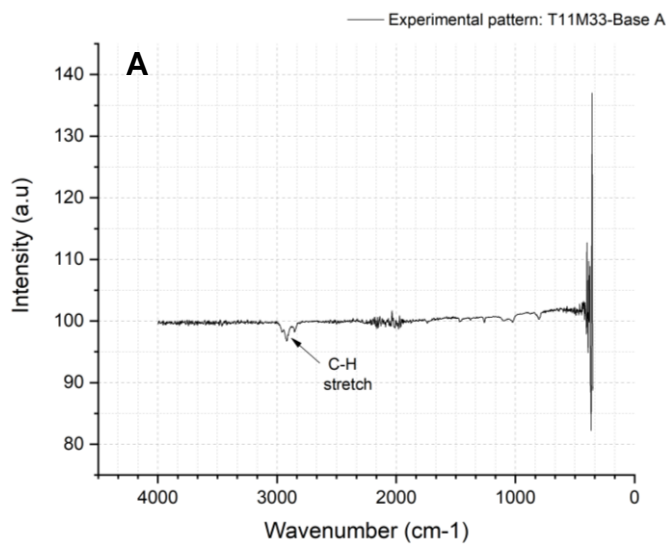
SA 21. FTIR spectroscopy. A) sample T11M33- Base nonpolar, B) sample T11M33- Base polar

Appendix b. XRD diffractometer Sample

This section contains descriptions of the samples studied
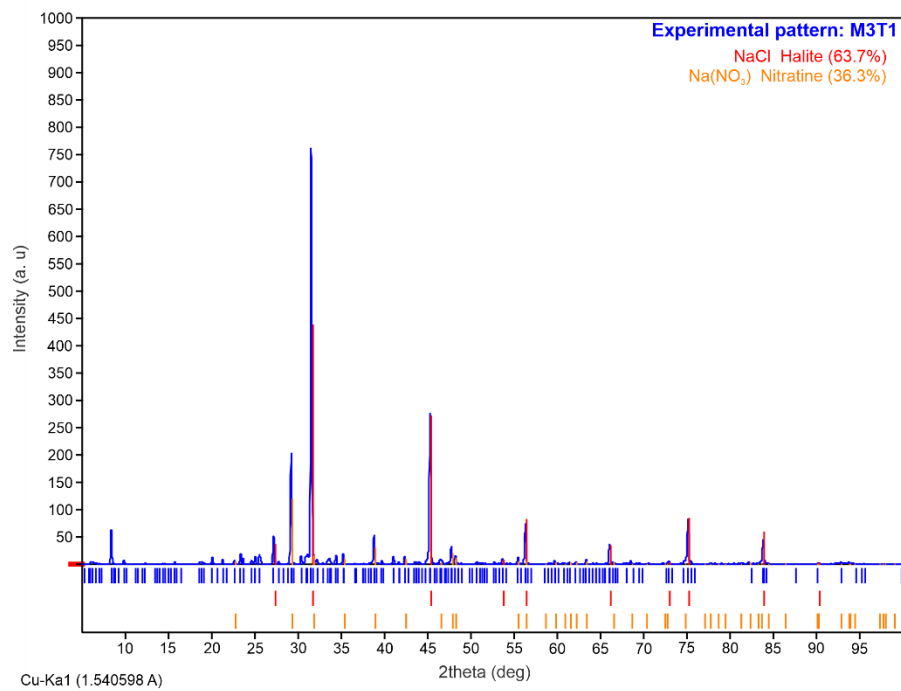
SB 1. XRD patterns of M3T1 sample
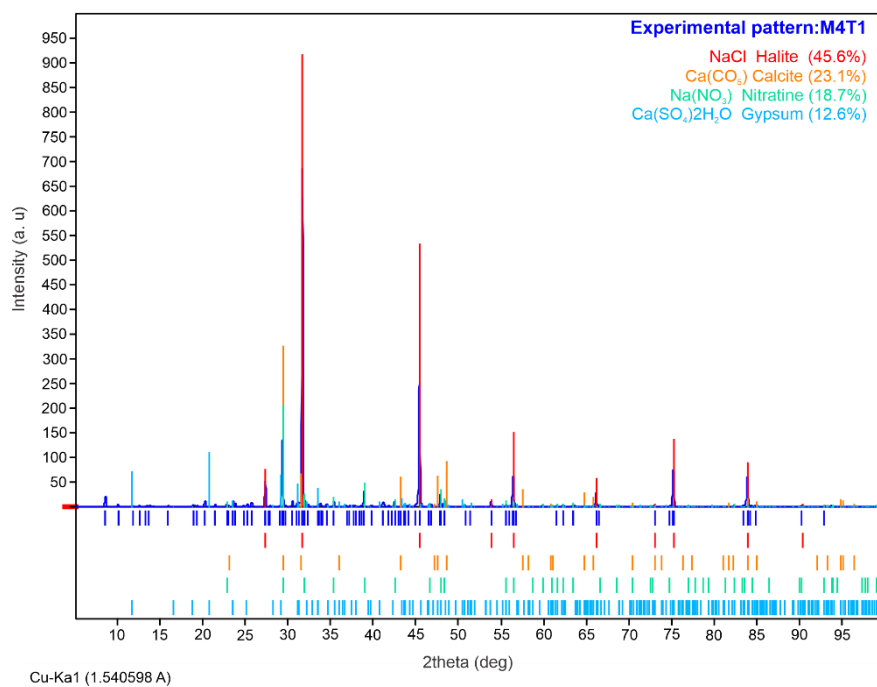
SB. XRD patterns of M4T1 sample
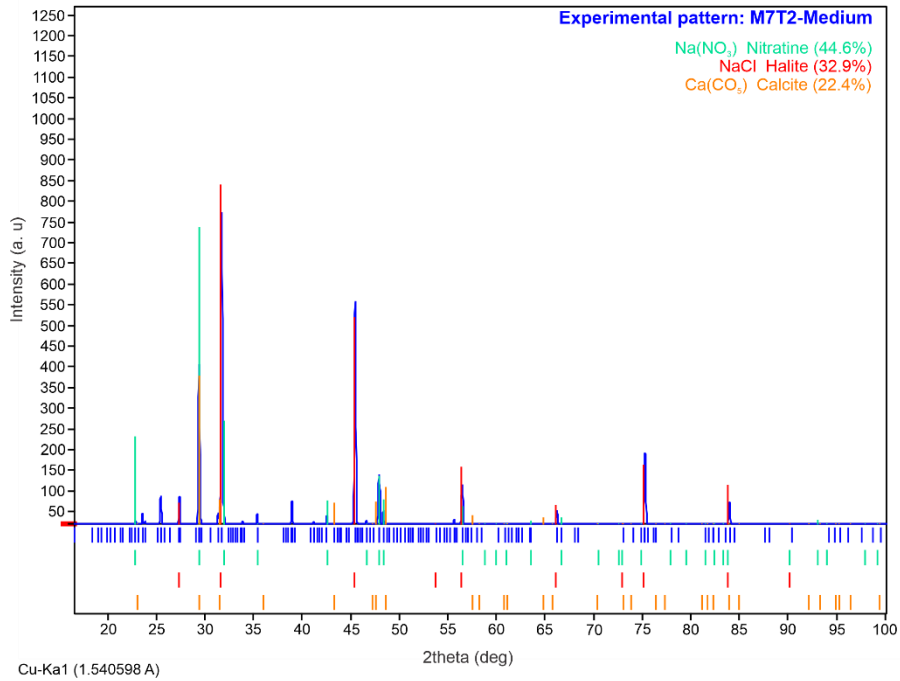
SB 3. XRD patterns of M7T2- Medium sample
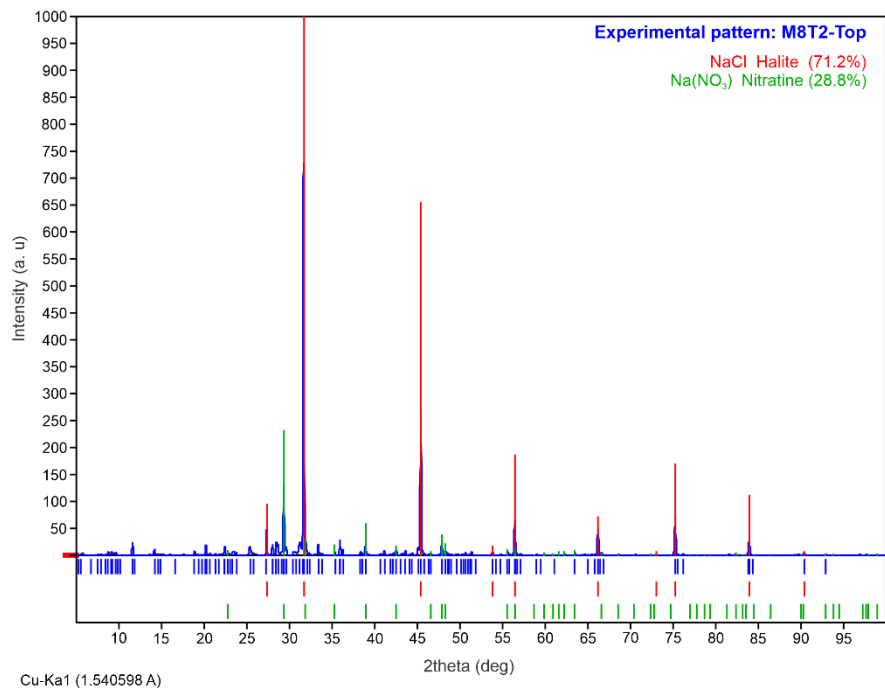
SB 4. XRD patterns of M8T2- Top sample
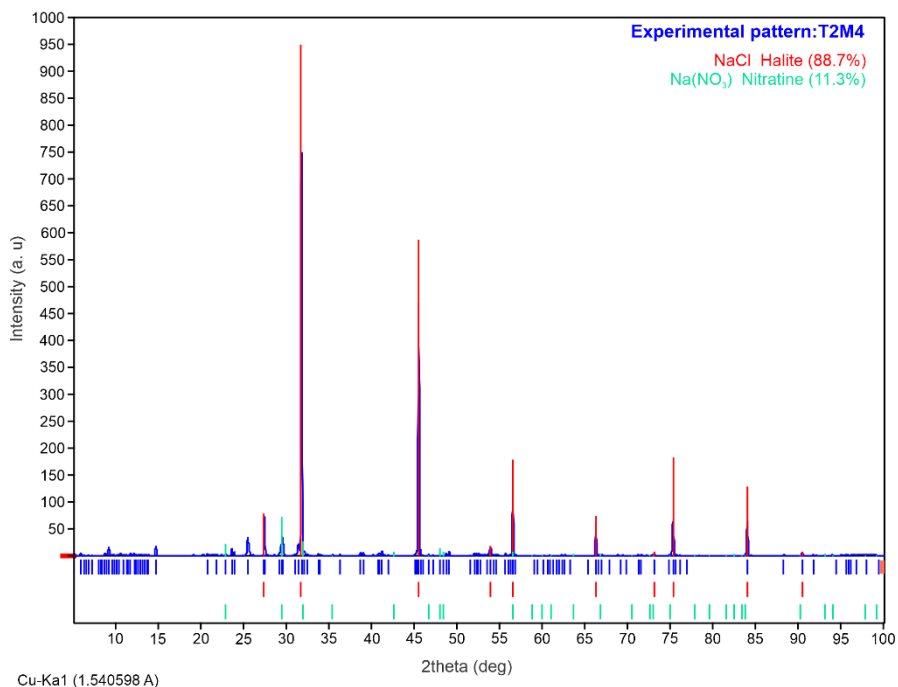
SB 5. XRD patterns of T2M4 sample
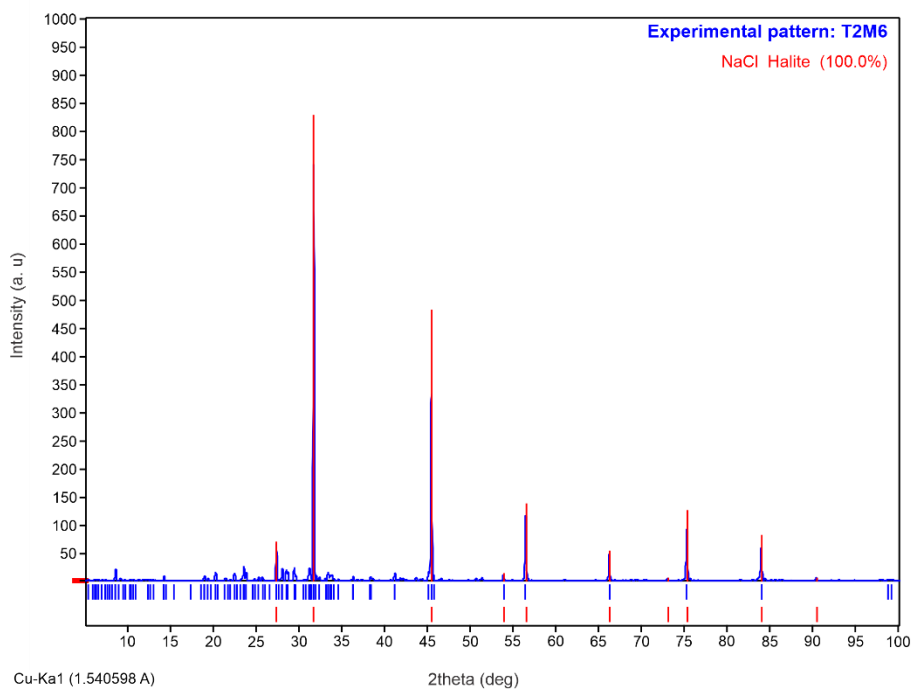
SB 6. XRD patterns of T2M6 sample
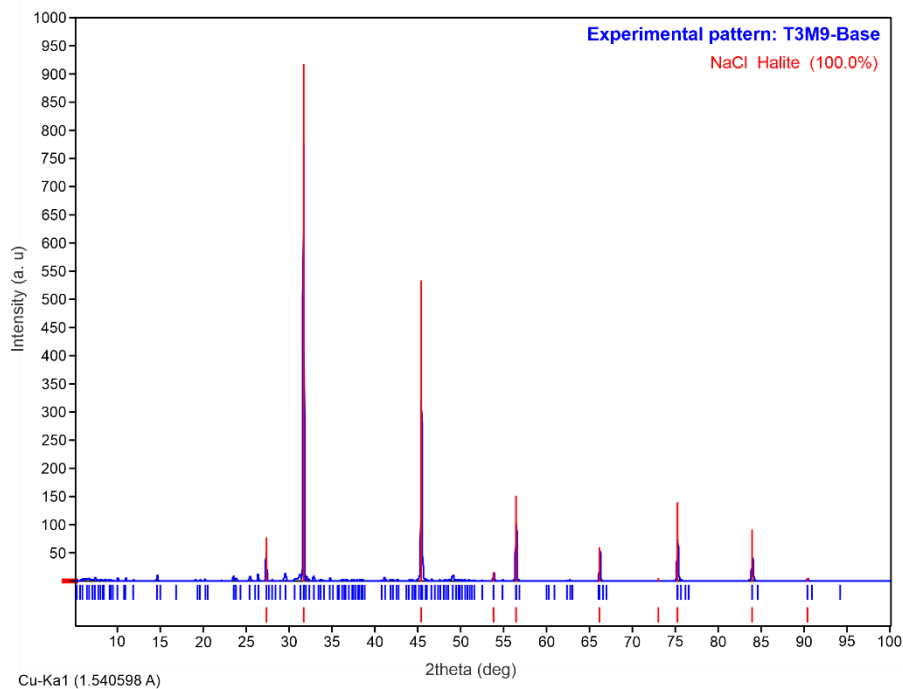
SB 7. XRD patterns of T3M9- Base sample
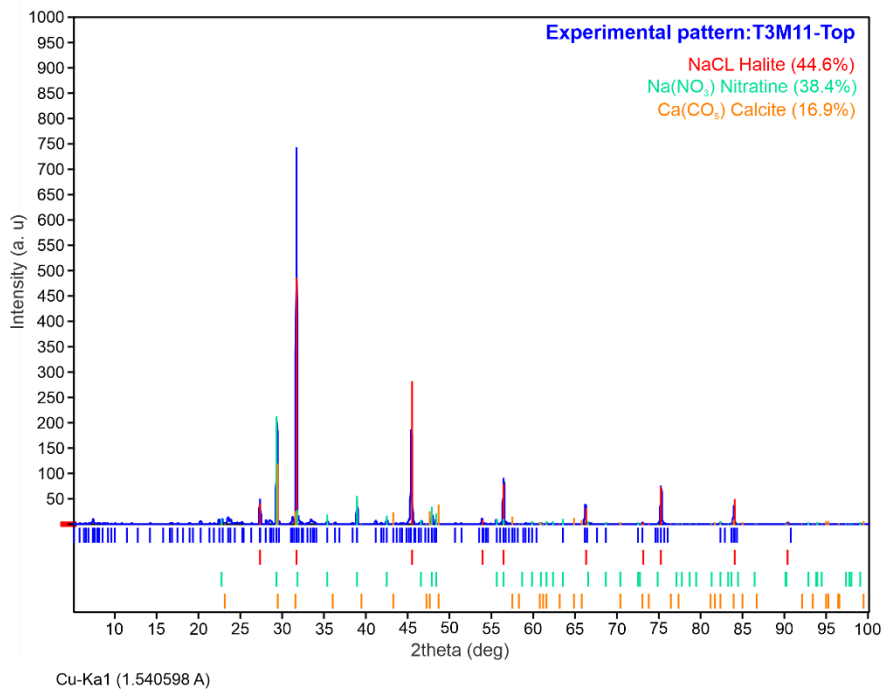
SB 8. XRD patterns of T3M11- Top sample
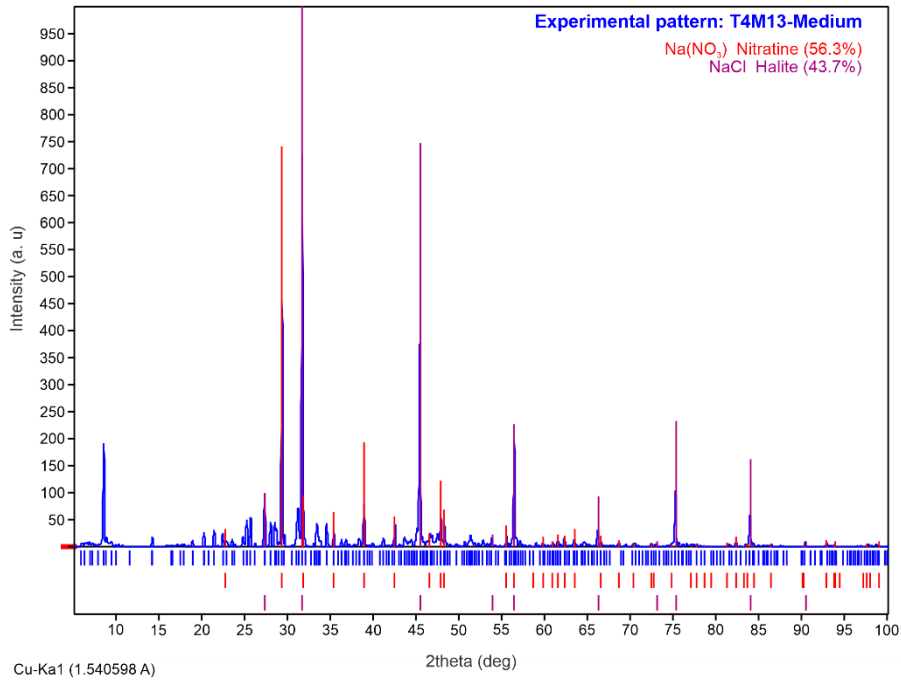
SB 9. XRD patterns of T4M13- Medium sample
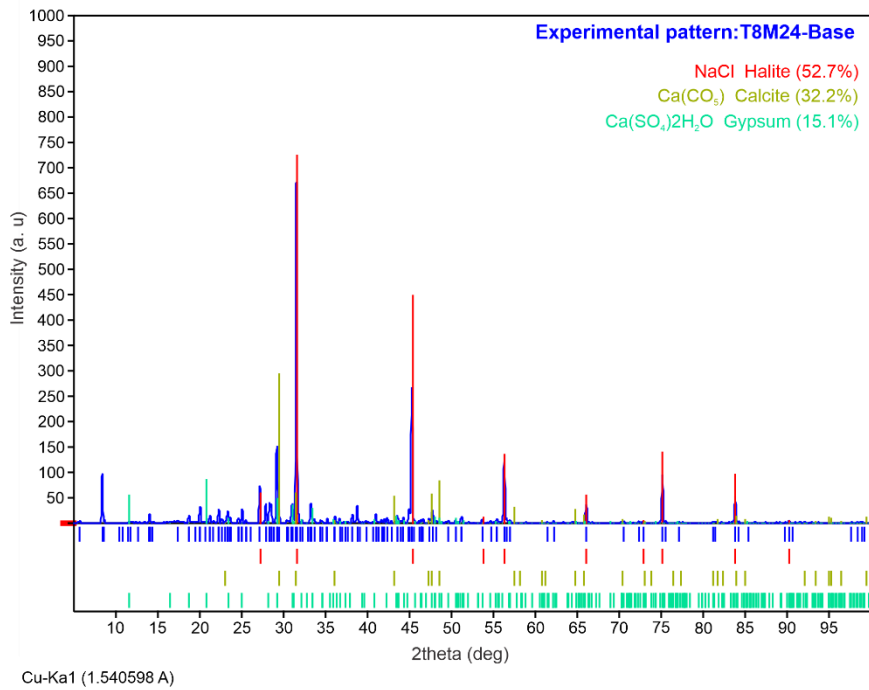
SB 10. XRD patterns of T8M24- Base sample
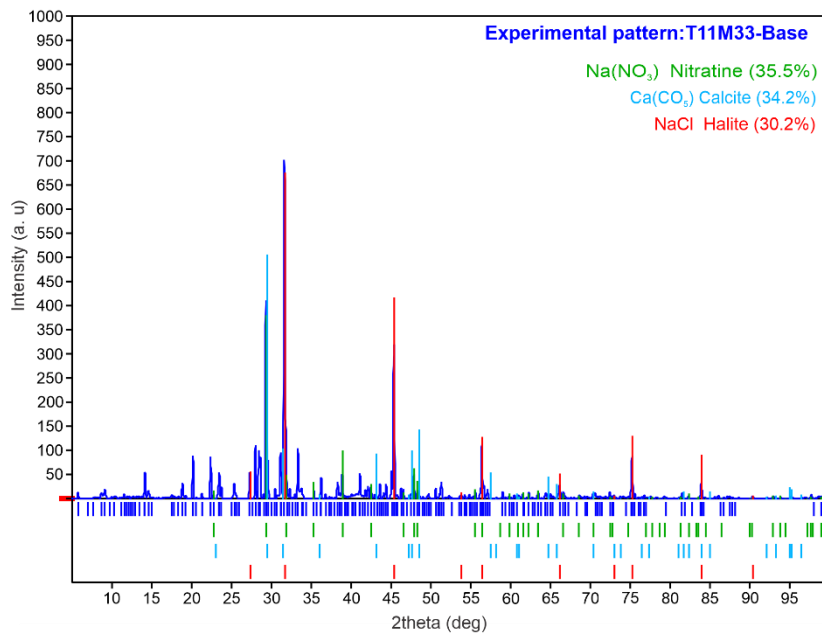
Cu-Ka1 (1.540598 A)

SB 11. XRD patterns of T11M33- Base sample

Appendix C. SEM Sample Description

This section contains descriptions of the samples studied

Table a. SEM analysis of the sample M3T1, spot 1

Atomic number	Element symbol	Element name	Atomic concentration percentage	Weight concentration percentage	Oxide	Stoichiometric percentage
8	O	Oxygen	62.28	47.08		
11	Na	Sodium	14.33	15.57	Na	37.99
16	S	Sulfur	6.04	9.15	S	16.02
14	Si	Silicon	5.48	7.27	Si	14.52
20	Ca	Calcium	4.51	8.55	Ca	11.97
17	Cl	Chlorine	2.16	3.62	Cl	5.73
19	K	Potassium	2.08	3.84	K	5.51
13	Al	Aluminium	1.20	1.53	Al	3.19
12	Mg	Magnesium	1.11	1.28	Mg	2.95
26	Fe	Iron	0.80	2.11	Fe	2.12

Table b. SEM analysis of the sample M3T1, spot 2

Atomic number	Element symbol	Element name	Atomic concentration percentage	Weight concentration percentage	Oxide	Stoichiometric percentage
8	O	Oxygen	41.02	40.94		
6	C	Carbon	30.47	22.83	C	51.67
7	N	Nitrogen	17.23	15.05	N	29.22
11	Na	Sodium	5.25	7.54	Na	8.91
16	S	Sulfur	2.29	4.58	S	3.88
20	Ca	Calcium	1.11	2.77	Ca	1.88
17	Cl	Chlorine	1.03	2.28	Cl	1.75
19	K	Potassium	0.67	1.63	K	1.13

Table c. SEM analysis of the sample M3T1, spot 3

Atomic number	Element symbol	Element name	Atomic concentration percentage	Weight concentration percentage	Oxide	Stoichiometric percentage
8	O	Oxygen	55.95	53.46		
11	Na	Sodium	14.35	19.70	Na	32.57
6	C	Carbon	13.28	9.53	C	30.15
7	N	Nitrogen	13.01	10.89	N	29.54
16	S	Sulfur	3.00	5.74	S	6.81

Table d. SEM analysis of the sample M3T1, spot 4

Atomic number	Element symbol	Element name	Atomic concentration percentage	Weight concentration percentage	Oxide	Stoichiometric percentage
8	O	Oxygen	62.07	55.67		
11	Na	Sodium	16.72	21.55	Na	44.09
7	N	Nitrogen	15.55	12.21	N	41.00
16	S	Sulfur	3.45	6.20	S	9.10
17	Cl	Chlorine	0.66	1.31	Cl	1.74
14	Si	Silicon	0.58	0.91	Si	1.52
20	Ca	Calcium	0.54	1.22	Ca	1.43
26	Fe	Iron	0.00	0.00	Fe	0.00

SC 1. a) SEM image of the spots of M3T1 sample surface; b) spectrum of the sample whose elements are given in Table a,b,c, and d

Table e. SEM analysis of the sample M5T1, spot 1

Atomic number	Element symbol	Element name	Atomic concentration percentage	Weight concentration percentage	Oxide	Stoichiometric percentage
6	C	Carbon	53.85	42.34	C	85.48
8	O	Oxygen	37.01	38.76		
11	Na	Sodium	3.71	5.58	Na	5.88
20	Ca	Calcium	2.07	5.42	Ca	3.28
19	K	Potassium	1.55	3.98	K	2.47
17	Cl	Chlorine	1.42	3.29	Cl	2.25
12	Mg	Magnesium	0.4	0.64	Mg	0.64

Table f. SEM analysis of the sample M5T1, spot 2

Atomic number	Element symbol	Element name	Atomic concentration percentage	Weight concentration percentage	Oxide	Stoichiometric percentage
8	O	Oxygen	43.76	32.28		
19	K	Potassium	27.68	49.9	K	49.21
6	C	Carbon	25.25	13.98	C	44.89
11	Na	Sodium	2.51	2.66	Na	4.46
17	Cl	Chlorine	0.39	0.64	Cl	0.69
13	Al	Aluminium	0.29	0.36	Al	0.52
14	Si	Silicon	0.13	0.17	Si	0.23

Table g. SEM analysis of the sample M5T1, spot 3

Atomic number	Element symbol	Element name	Atomic concentration percentage	Weight concentration percentage	Oxide	Stoichiometric percentage
8	O	Oxygen	38.05	30.46		
6	C	Carbon	34.88	20.96	C	56.31
19	K	Potassium	17.69	34.6	K	28.56
11	Na	Sodium	4.1	4.71	Na	6.61
20	Ca	Calcium	1.8	3.62	Ca	2.91
17	Cl	Chlorine	1.62	2.87	Cl	2.61
16	S	Sulfur	1.33	2.14	S	2.15
7	N	Nitrogen	12.15	9.66	N	18.57

SC 2. a) SEM image of the spots of M5T1 sample surface; b) spectrum of the sample whose elements are given in Table e,f, and g.

Table h. SEM analysis of the sample M7T2, spot 1

Atomic number	Element symbol	Element name	Atomic concentration percentage	Weight concentration percentage	Oxide	Stoichiometric percentage
6	C	Carbon	39.00	23.12	C	48.07
11	Na	Sodium	23.21	26.34	Na	28.60
8	O	Oxygen	18.87	14.90		
17	Cl	Chlorine	17.02	29.80	Cl	20.98
20	Ca	Calcium	0.99	1.97	Ca	1.23
42	Mo	Molybdenum	0.78	3.68	Mo	0.96
14	Si	Silicon	0.13	0.19	Si	0.17

Table i. SEM analysis of the sample M7T2, spot 2

Atomic number	Element symbol	Element name	Atomic concentration percentage	Weight concentration percentage	Oxide	Stoichiometric percentage
11	Na	Sodium	39.31	35.32	Na	52.81
17	Cl	Chlorine	32.68	45.27	Cl	43.90
8	O	Oxygen	25.56	15.98		
16	S	Sulfur	1.27	1.59	S	1.70
20	Ca	Calcium	0.86	1.34	Ca	1.15
19	K	Potassium	0.33	0.50	K	0.44

Table j. SEM analysis of the sample M7T2, spot 3

Atomic number	Element symbol	Element name	Atomic concentration percentage	Weight concentration percentage	Oxide	Stoichiometric percentage
8	O	Oxygen	69.03	68.92		
6	C	Carbon	14.32	10.73	C	46.24
7	N	Nitrogen	9.76	8.53	N	31.51
12	Mg	Magnesium	2.85	4.32	Mg	9.20
11	Na	Sodium	1.78	2.56	Na	5.76
17	Cl	Chlorine	1.01	2.24	Cl	3.28
16	S	Sulfur	0.73	1.45	S	2.34
20	Ca	Calcium	0.45	1.13	Ca	1.46
13	Al	Aluminium	0.07	0.11	Al	0.21

Table k. SEM analysis of the sample M7T2, spot 4

Atomic number	Element symbol	Element name	Atomic concentration percentage	Weight concentration percentage	Oxide	Stoichiometric percentage
8	O	Oxygen	39.71	37.03		
6	C	Carbon	26.24	18.37	C	43.51
7	N	Nitrogen	19.93	16.27	N	33.06
19	K	Potassium	6.46	14.72	K	10.71
11	Na	Sodium	2.29	3.07	Na	3.81
17	Cl	Chlorine	1.66	3.43	Cl	2.76
16	S	Sulfur	1.58	2.95	S	2.62
20	Ca	Calcium	1.23	2.88	Ca	2.04
12	Mg	Magnesium	0.90	1.27	Mg	1.49
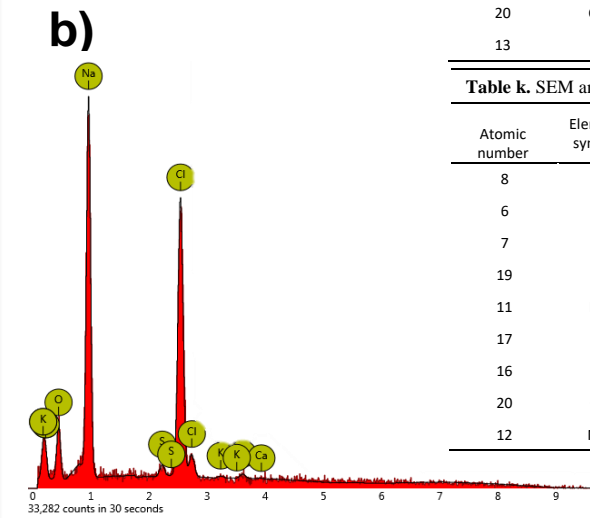
SC 3. *a) SEM image of the spots of M7T2 sample surface; b) spectrum of the sample whose elements are given in Table h,i,j, and k.*

Table l. SEM analysis of the sample M8T2, spot 1

Atomic number	Element symbol	Element name	Atomic concentration percentage	Weight concentration percentage	Oxide	Stoichiometric percentage
8	O	Oxygen	69.68	59.22		
7	N	Nitrogen	12.81	9.53	N	42.27
20	Ca	Calcium	6.80	14.49	Ca	22.44
16	S	Sulfur	6.68	11.39	S	22.05
11	Na	Sodium	2.70	3.30	Na	8.90
12	Mg	Magnesium	0.59	0.76	Mg	1.95
19	K	Potassium	0.39	0.82	K	1.30
14	Si	Silicon	0.33	0.49	Si	1.08

Table m. SEM analysis of the sample M8T2, spot 2

Atomic number	Element symbol	Element name	Atomic concentration percentage	Weight concentration percentage	Oxide	Stoichiometric percentage
8	O	Oxygen	59.95	48.22		
7	N	Nitrogen	11.88	8.37	N	29.67
16	S	Sulfur	11.19	18.04	S	27.95
11	Na	Sodium	10.25	11.85	Na	25.61
20	Ca	Calcium	6.47	13.03	Ca	16.15
19	K	Potassium	0.25	0.49	K	0.62

Table n. SEM analysis of the sample M8T2, spot 3

Atomic number	Element symbol	Element name	Atomic concentration percentage	Weight concentration percentage	Oxide	Stoichiometric percentage
8	O	Oxygen	48.95	39.16		
7	N	Nitrogen	22.22	15.56	N	43.53
16	S	Sulfur	10.21	16.37	S	20.00
11	Na	Sodium	7.25	8.33	Na	14.21
20	Ca	Calcium	7.09	14.21	Ca	13.89
12	Mg	Magnesium	1.69	2.06	Mg	3.32
14	Si	Silicon	1.33	1.86	Si	2.60
19	K	Potassium	1.25	2.45	K	2.45

SC 4. a) SEM image of the spots of M8T2 sample surface; b) spectrum of the sample whose elements are given in Table l,m and n.

Table o. SEM analysis of the sample T2M4, spot 1

Atomic number	Element symbol	Element name	Atomic concentration percentage	Weight concentration percentage	Oxide	Stoichiometric percentage
6	C	Carbon	54.18	43.66	C	89.04
8	O	Oxygen	39.15	42.03		
11	Na	Sodium	2.47	3.81	Na	4.05
17	Cl	Chlorine	1.41	3.35	Cl	2.31
19	K	Potassium	1.33	3.49	K	2.18
20	Ca	Calcium	0.99	2.67	Ca	1.63
16	S	Sulfur	0.47	1.01	S	0.77

Table p. SEM analysis of the sample T2M4, spot 2

Atomic number	Element symbol	Element name	Atomic concentration percentage	Weight concentration percentage	Oxide	Stoichiometric percentage
8	O	Oxygen	61.06	54.89		
7	N	Nitrogen	22.80	17.95	N	58.55
11	Na	Sodium	6.83	8.83	Na	17.55
17	Cl	Chlorine	4.07	8.10	Cl	10.44
19	K	Potassium	1.77	3.90	K	4.55
16	S	Sulfur	1.31	2.36	S	3.37
20	Ca	Calcium	1.13	2.54	Ca	2.89
12	Mg	Magnesium	0.84	1.15	Mg	2.16
14	Si	Silicon	0.19	0.30	Si	0.48

Table q. SEM analysis of the sample T2M4, spot 3

Atomic number	Element symbol	Element name	Atomic concentration percentage	Weight concentration percentage	Oxide	Stoichiometric percentage
8	O	Oxygen	65.58	59.76		
7	N	Nitrogen	21.04	16.79	N	61.14
11	Na	Sodium	6.19	8.11	Na	17.99
17	Cl	Chlorine	3.55	7.17	Cl	10.31
19	K	Potassium	2.20	4.90	K	6.39
20	Ca	Calcium	1.44	3.28	Ca	4.17

Table r. SEM analysis of the sample T2M4, spot 4

Atomic number	Element symbol	Element name	Atomic concentration percentage	Weight concentration percentage	Oxide	Stoichiometric percentage
8	O	Oxygen	61.78	55.69		
7	N	Nitrogen	22.86	18.03	N	59.81
11	Na	Sodium	6.66	8.63	Na	17.43
17	Cl	Chlorine	2.52	5.03	Cl	6.59
19	K	Potassium	2.30	5.06	K	6.01
16	S	Sulfur	1.82	3.29	S	4.76
20	Ca	Calcium	1.49	3.37	Ca	3.91
14	Si	Silicon	0.57	0.90	Si	1.49

SC 5. a) SEM image of the spots of M8T2 sample surface; b) spectrum of the sample whose elements are given in Table o,p,q,and r.

Table s. SEM analysis of the sample T2M6, spot 1

Atomic number	Element symbol	Element name	Atomic concentration percentage	Weight concentration percentage	Oxide	Stoichiometric percentage
6	C	Carbon	55.26	37.22	C	62.26
11	Na	Sodium	19.90	25.66	Na	22.42
17	Cl	Chlorine	13.60	27.03	Cl	15.32
8	O	Oxygen	11.24	10.08		

Table t. SEM analysis of the sample T2M6, spot 2

Atomic number	Element symbol	Element name	Atomic concentration percentage	Weight concentration percentage	Oxide	Stoichiometric percentage
8	O	Oxygen	51.67	50.54		
6	C	Carbon	24.69	18.13	C	51.09
7	N	Nitrogen	13.26	11.36	N	27.43
11	Na	Sodium	3.02	4.24	Na	6.24
19	K	Potassium	2.98	7.13	K	6.17
20	Ca	Calcium	1.12	2.73	Ca	2.31
14	Si	Silicon	1.03	1.76	Si	2.12
16	S	Sulfur	0.83	1.63	S	1.72
12	Mg	Magnesium	0.65	0.97	Mg	1.35
17	Cl	Chlorine	0.49	1.06	Cl	1.01
13	Al	Aluminium	0.27	0.44	Al	0.55

Table u. SEM analysis of the sample T2M6, spot 3

Atomic number	Element symbol	Element name	Atomic concentration percentage	Weight concentration percentage	Oxide	Stoichiometric percentage
8	O	Oxygen	51.88	49.66		
6	C	Carbon	32.77	23.54	C	68.09
11	Na	Sodium	6.85	9.42	Na	14.23
16	S	Sulfur	4.52	8.68	S	9.40
20	Ca	Calcium	2.59	6.20	Ca	5.38
14	Si	Silicon	0.61	1.02	Si	1.26
17	Cl	Chlorine	0.49	1.04	Cl	1.02
12	Mg	Magnesium	0.30	0.44	Mg	0.63

SC 6. a) SEM image of the spots of T2M6 sample surface; b) spectrum of the sample whose elements are given in Table s,t and u..

Table 39. SEM analysis of the sample T3M9, spot 1

Atomic number	Element symbol	Element name	Atomic concentration percentage	Weight concentration percentage	Oxide	Stoichiometric percentage
6	C	Carbon	65.32	55.60	C	96.68
8	O	Oxygen	32.44	36.78		
17	Cl	Chlorine	1.32	3.31	Cl	1.95
30	Zn	Zn	0.93	4.31	Zn	1.38
19	K	Potassium	0.00	0.00	K	0.00

Table 40. SEM analysis of the sample T3M9, spot 2

Atomic number	Element symbol	Element name	Atomic concentration percentage	Weight concentration percentage	Oxide	Stoichiometric percentage
6	C	Carbon	67.89	58.24	C	93.13
8	O	Oxygen	27.11	30.98		
11	Na	Sodium	1.47	2.41	Na	2.02
17	Cl	Chlorine	1.23	3.11	Cl	1.68
16	S	Sulfur	0.87	1.98	S	1.19
19	K	Potassium	0.70	1.96	K	0.97
12	Mg	Magnesium	0.62	1.08	Mg	0.85
14	Si	Silicon	0.12	0.23	Si	0.16

SC 7. *a) SEM image of the spots of T2M6 sample surface; b) spectrum of the sample whose elements are given in Table s,t and u.*

Table v. SEM analysis of the sample T3M11, spot 1

Atomic number	Element symbol	Element name	Atomic concentration percentage	Weight concentration percentage	Oxide	Stoichiometric percentage
8	O	Oxygen	30.56	21.39		
11	Na	Sodium	29.98	30.15	Na	43.17
17	Cl	Chlorine	25.64	39.77	Cl	36.93
7	N	Nitrogen	13.61	8.34	N	19.60
19	K	Potassium	0.21	0.35	K	0.30

Table w. SEM analysis of the sample T3M11, spot 2

Atomic number	Element symbol	Element name	Atomic concentration percentage	Weight concentration percentage	Oxide	Stoichiometric percentage
8	O	Oxygen	57.98	54.18		
7	N	Nitrogen	25.27	20.68	N	60.15
11	Na	Sodium	12.96	17.41	Na	30.85
17	Cl	Chlorine	1.84	3.81	Cl	4.38
19	K	Potassium	1.36	3.09	K	3.23
12	Mg	Magnesium	0.59	0.83	Mg	1.40

Table x. SEM analysis of the sample T3M11, spot 3

Atomic number	Element symbol	Element name	Atomic concentration percentage	Weight concentration percentage	Oxide	Stoichiometric percentage
8	O	Oxygen	64.02	53.75		
7	N	Nitrogen	11.54	8.48	N	32.08
11	Na	Sodium	10.61	12.80	Na	29.50
16	S	Sulfur	7.46	12.56	S	20.74
20	Ca	Calcium	3.91	8.23	Ca	10.88
17	Cl	Chlorine	1.34	2.50	Cl	3.73
12	Mg	Magnesium	0.76	0.97	Mg	2.12
19	K	Potassium	0.34	0.71	K	0.96

SC 8. a) SEM image of the spots of T3M11 sample surface; b) spectrum of the sample whose elements are given in Table v,w and x.

Table y. SEM analysis of the sample T4M13, spot 1

Atomic number	Element symbol	Element name	Atomic concentration percentage	Weight concentration percentage	Oxide	Stoichiometric percentage
6	C	Carbon	52.99	35.50	C	63.33
8	O	Oxygen	16.32	14.57		
11	Na	Sodium	15.42	19.77	Na	18.43
17	Cl	Chlorine	14.56	28.79	Cl	17.40
16	S	Sulfur	0.43	0.76	S	0.51
20	Ca	Calcium	0.27	0.61	Ca	0.33

Table z. SEM analysis of the sample T4M13, spot 2

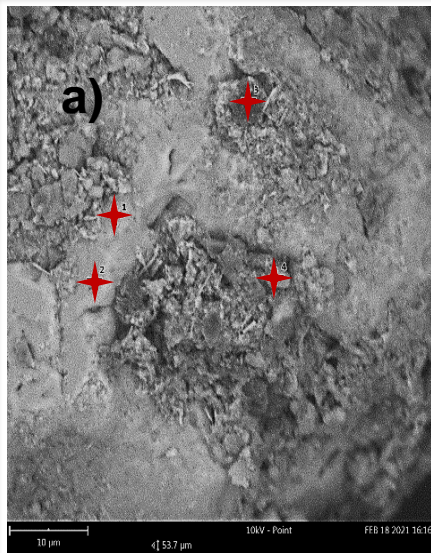| Atomic number	Element symbol	Element name	Atomic concentration percentage	Weight concentration percentage	Oxide	Stoichiometric percentage
8	O	Oxygen	43.45	43.70		
6	C	Carbon	28.49	21.51	C	50.39
7	N	Nitrogen	16.88	14.86	N	29.84
11	Na	Sodium	6.10	8.82	Na	10.79
17	Cl	Chlorine	3.63	8.09	Cl	6.42
16	S	Sulfur	1.23	2.49	S	2.18
20	Ca	Calcium	0.21	0.54	Ca	0.38

Table aa SEM analysis of the sample T4M13, spot 3

Atomic number	Element symbol	Element name	Atomic concentration percentage	Weight concentration percentage	Oxide	Stoichiometric percentage
8	O	Oxygen	50.93	50.17		
6	C	Carbon	19.59	14.49	C	39.92
7	N	Nitrogen	17.71	15.27	N	36.09
11	Na	Sodium	7.18	10.16	Na	14.62
16	S	Sulfur	2.25	4.44	S	4.59
20	Ca	Calcium	1.22	3.01	Ca	2.48
17	Cl	Chlorine	1.13	2.46	Cl	2.30

SC 9. a) SEM image of the spots of T4M13 sample surface; b) spectrum of the sample whose elements are given in Table y,z and aa.

**Table ab.** SEM analysis of the sample T8M24, spot 1

Atomic number	Element symbol	Element name	Atomic concentration percentage	Weight concentration percentage	Oxide	Stoichiometric percentage
8	O	Oxygen	46.69	43.28		
6	C	Carbon	35.19	24.49	C	66.01
11	Na	Sodium	8.14	10.85	Na	15.28
19	K	Potassium	5.82	13.18	K	10.91
17	Cl	Chlorine	2.46	5.06	Cl	4.62
16	S	Sulfur	1.70	3.15	S	3.18

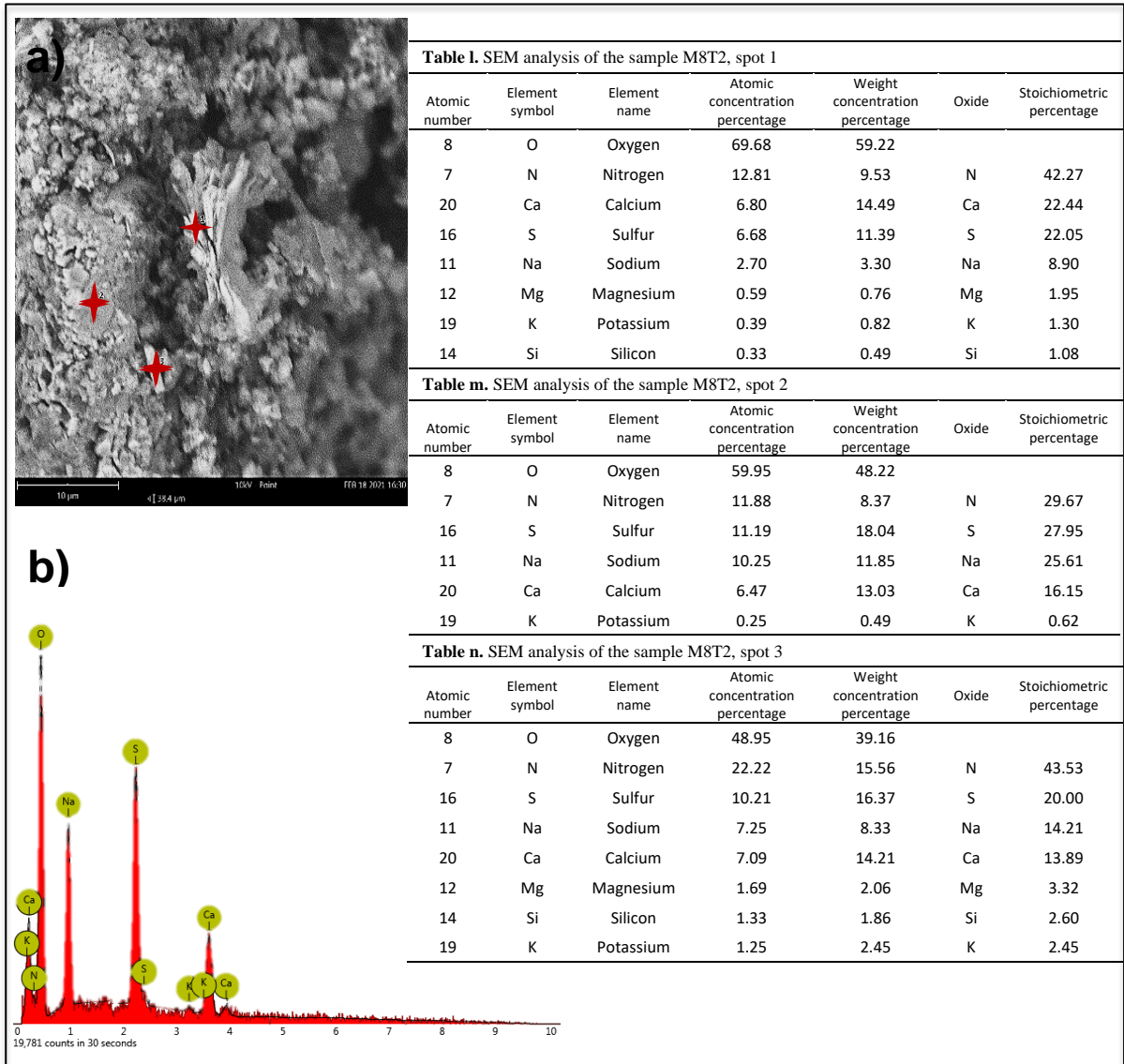**Table ac.** SEM analysis of the sample T8M24, spot 2

Atomic number	Element symbol	Element name	Atomic concentration percentage	Weight concentration percentage	Oxide	Stoichiometric percentage
8	O	Oxygen	66.04	51.53		
11	Na	Sodium	15.70	17.60	Na	46.24
16	S	Sulfur	12.33	19.28	S	36.31
20	Ca	Calcium	5.93	11.58	Ca	17.45

Table ad. SEM analysis of the sample T8M24, spot 3

Atomic number	Element symbol	Element name	Atomic concentration percentage	Weight concentration percentage	Oxide	Stoichiometric percentage
8	O	Oxygen	50.93	50.17		
19	K	Potassium	19.59	14.49	C	39.92
11	Na	Sodium	7.18	10.16	Na	14.62
17	Cl	Chlorine				
16	S	Sulfur	2.25	4.44	S	4.59

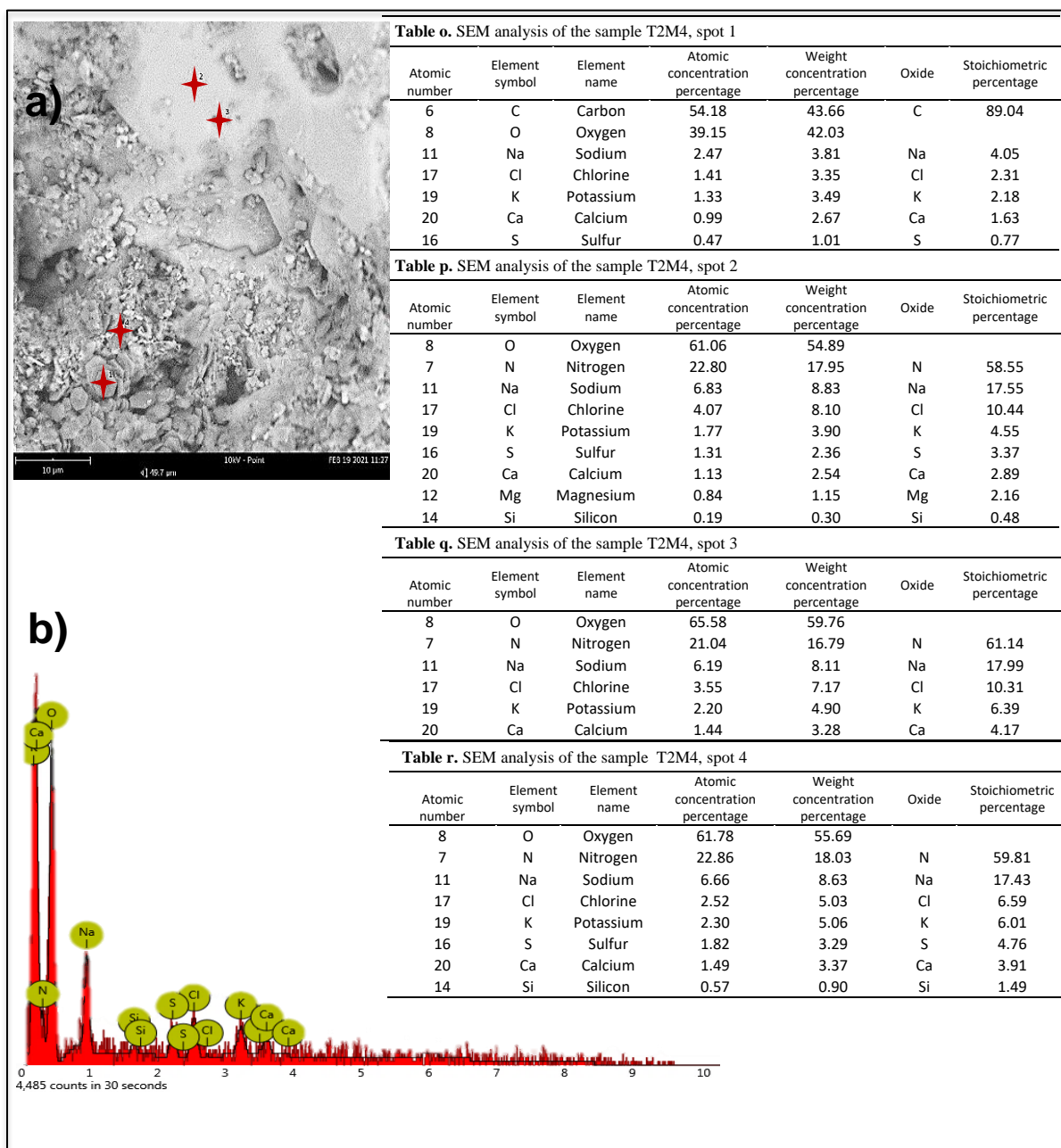**Table ae.** SEM analysis of the sample T8M24, spot 4

Atomic number	Element symbol	Element name	Atomic concentration percentage	Weight concentration percentage	Oxide	Stoichiometric percentage
8	O	Oxygen	50.06	45.49		
7	N	Nitrogen	24.61	19.58	N	49.29
6	C	Carbon	12.59	8.59	C	25.21
19	K	Potassium	10.27	22.79	K	20.56
11	Na	Sodium	2.00	2.61	Na	4.00
17	Cl	Chlorine	0.47	0.95	Cl	0.94

Table af. SEM analysis of the sample T8M24, spot 5

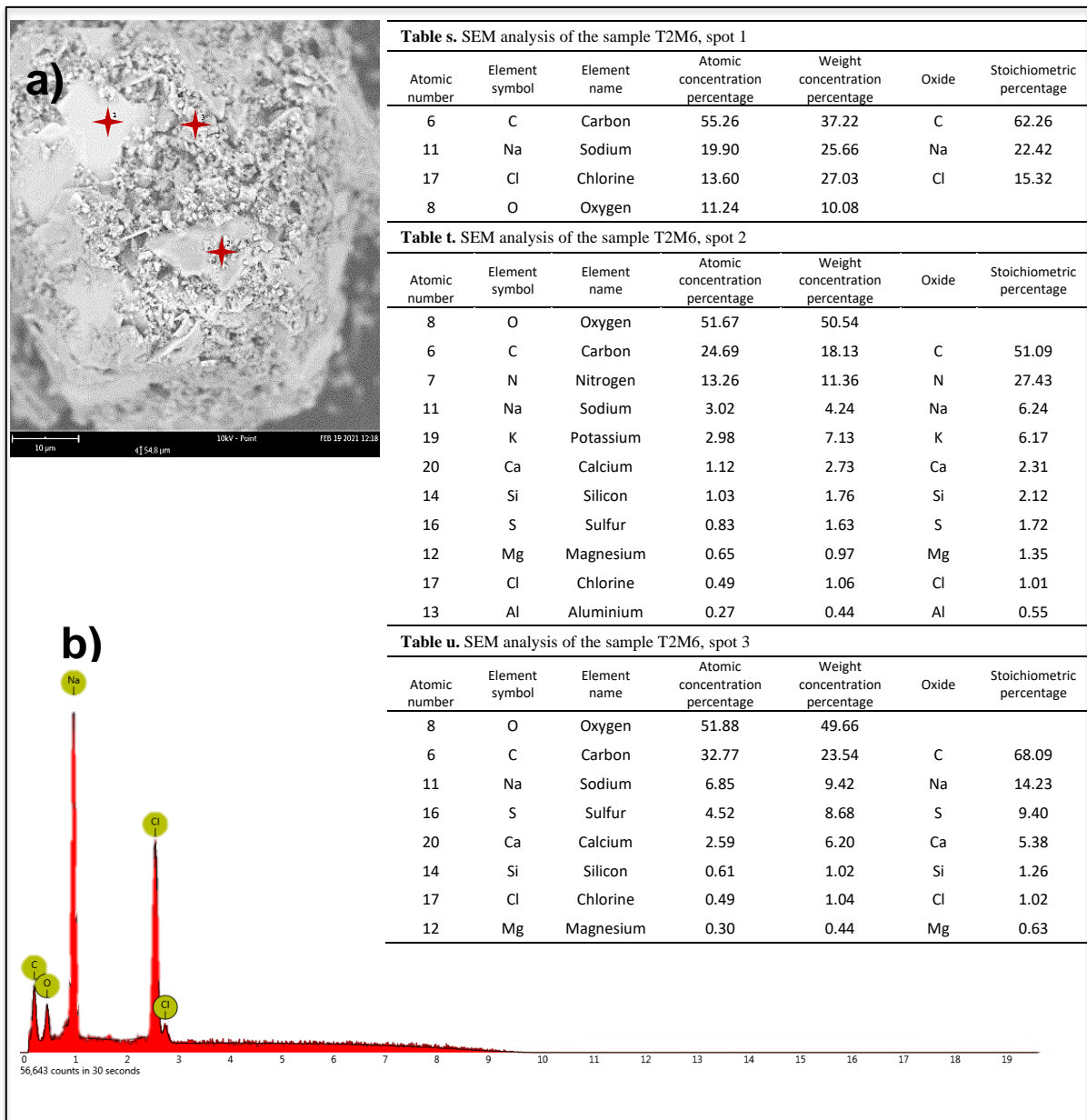| Atomic number	Element symbol	Element name	Atomic concentration percentage	Weight concentration percentage	Oxide	Stoichiometric percentage
8	O	Oxygen	58.66	49.19		
7	N	Nitrogen	16.38	12.02	N	39.62
11	Na	Sodium	11.00	13.26	Na	26.61
16	S	Sulfur	8.65	14.54	S	20.93
20	Ca	Calcium	4.06	8.54	Ca	9.83
19	K	Potassium	1.07	2.20	K	2.59
14	Si	Silicon	0.17	0.25	Si	0.42

SC 10. a) SEM image of the spots of T8M24 sample surface; b) spectrum of the sample whose elements are given in Table ab,ac,ad,ae and af.
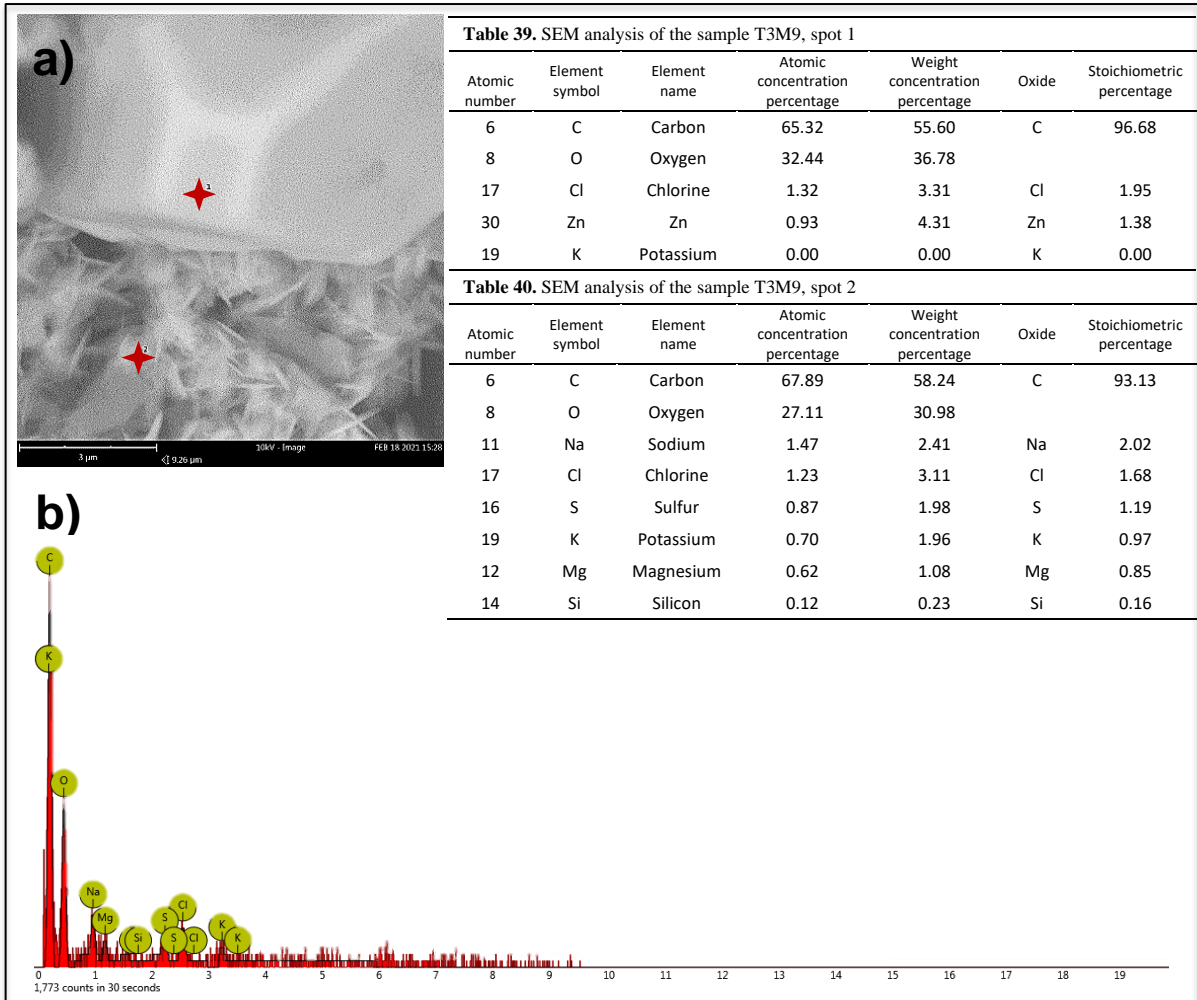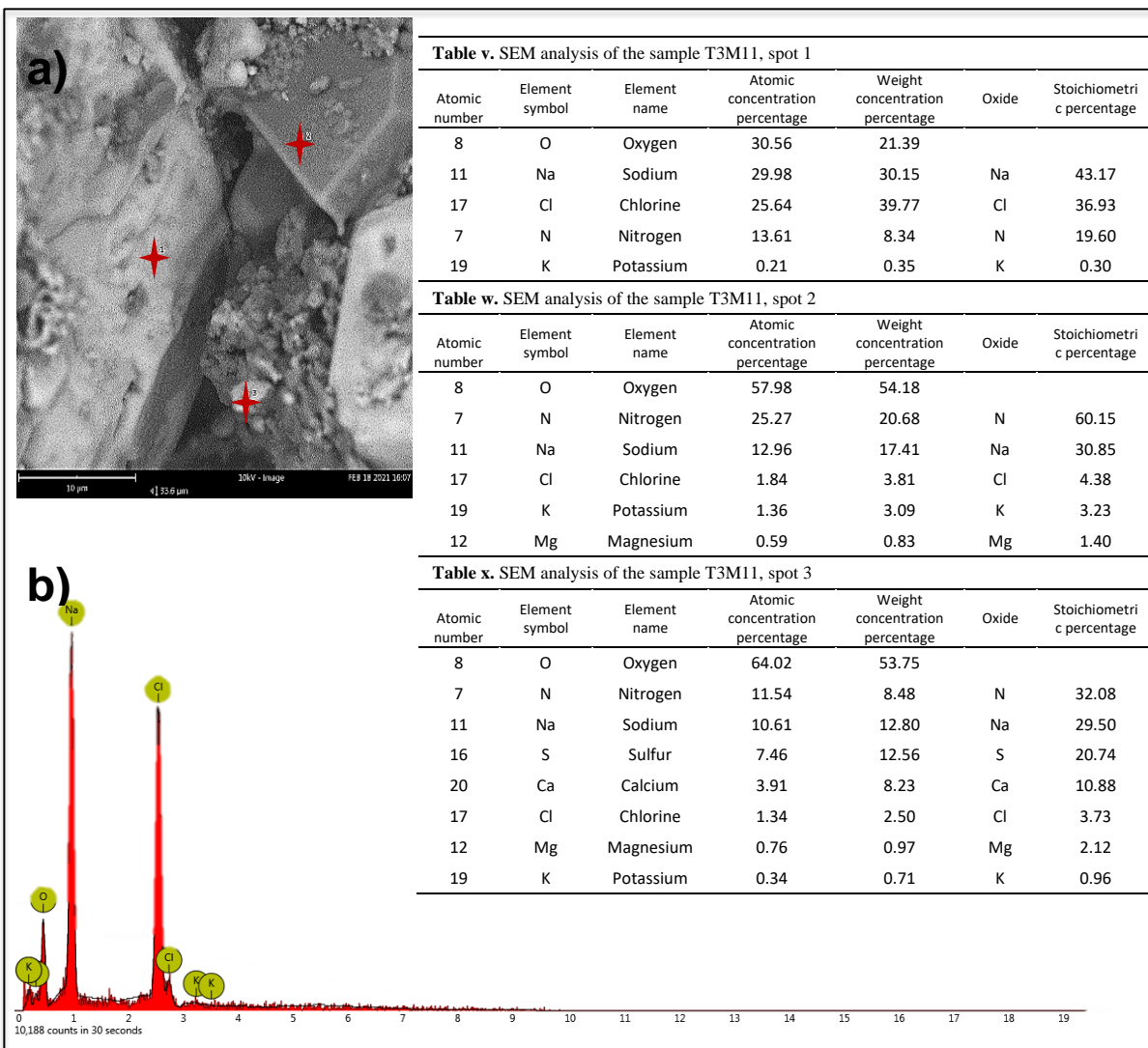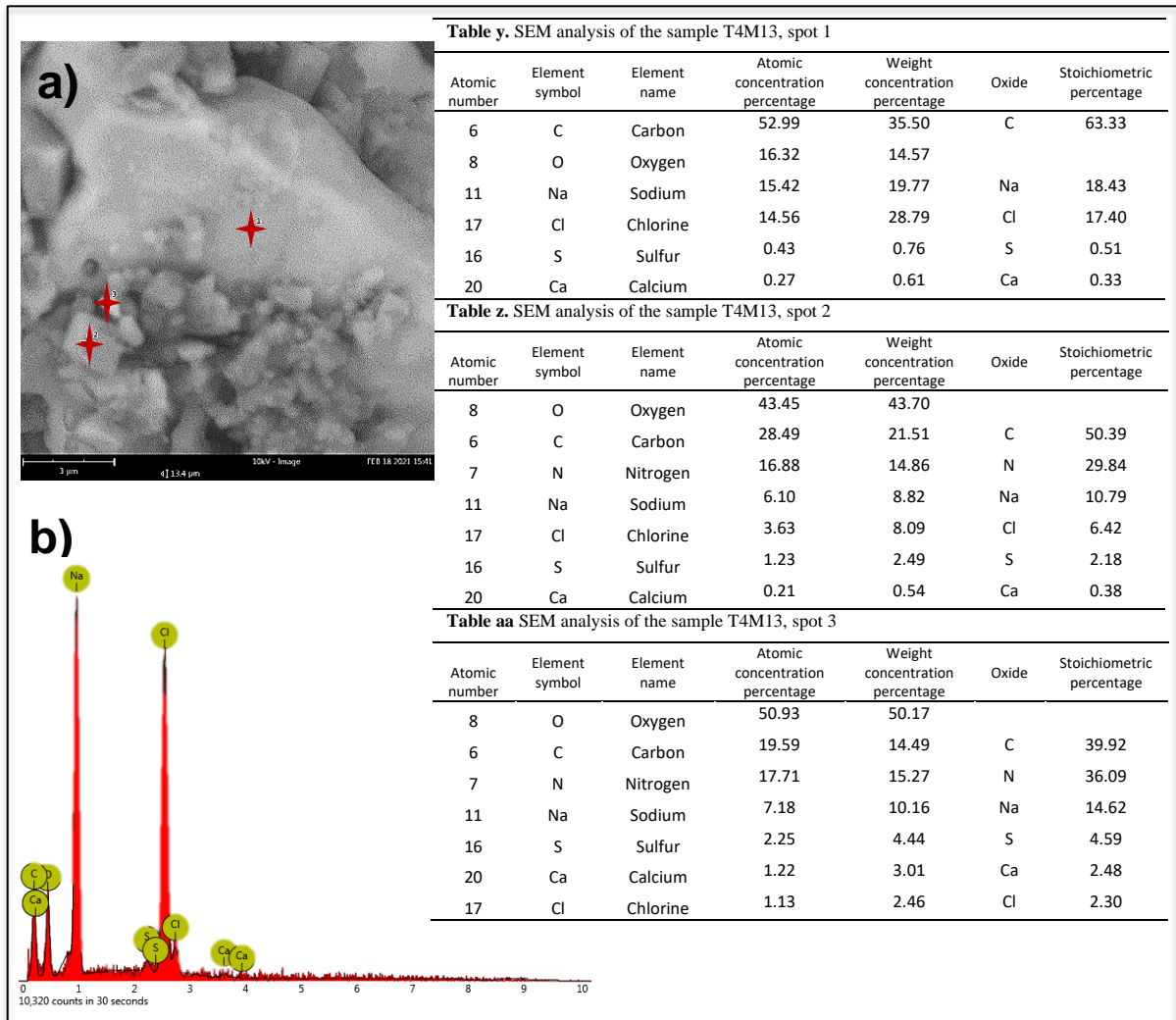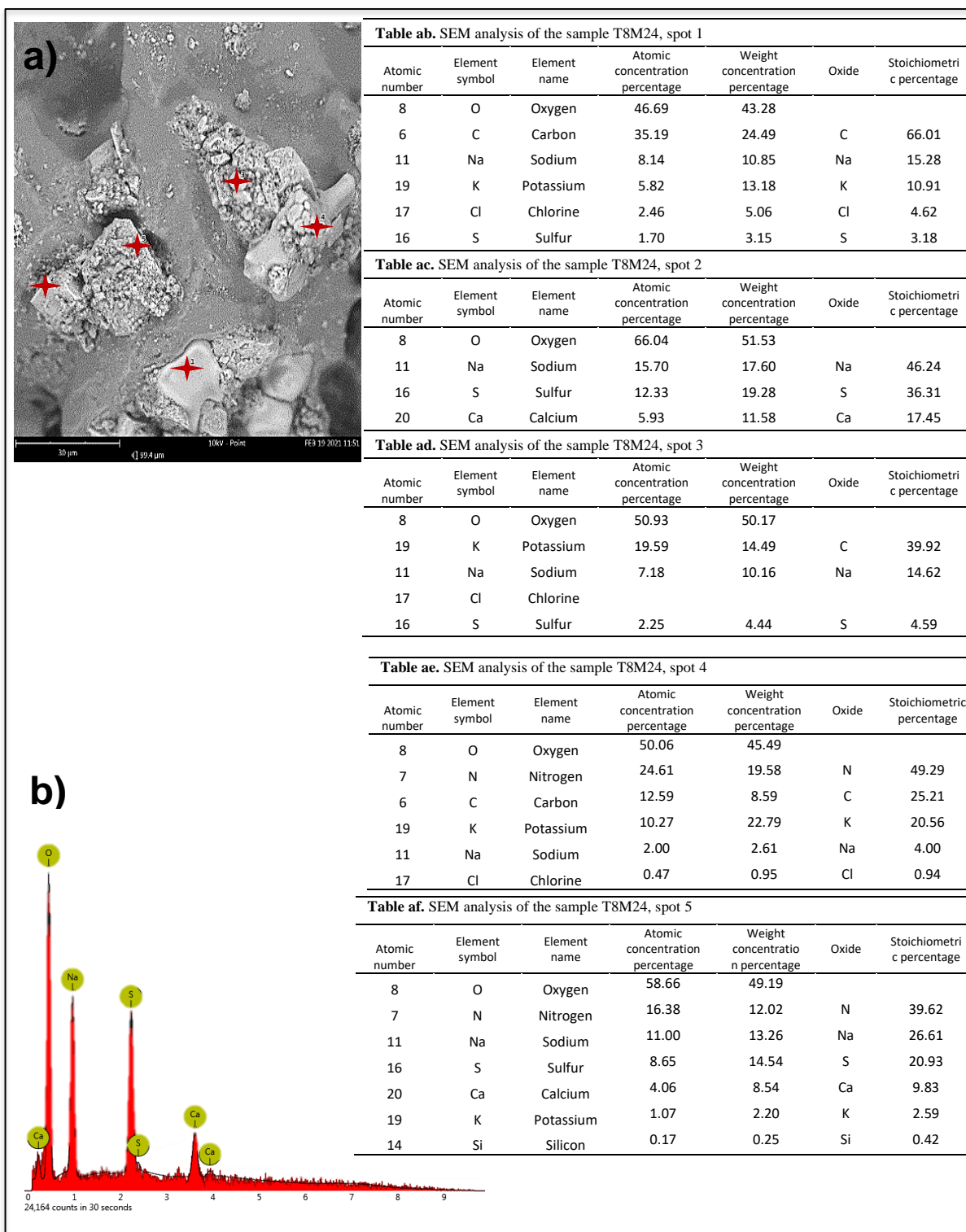
Table ag. SEM analysis of the sample T11M33, spot 1

Atomic number	Element symbol	Element name	Atomic concentration percentage	Weight concentration percentage	Oxide	Stoichiometric percentage
8	O	Oxygen	69.28	54.98		
11	Na	Sodium	13.37	15.25	Na	43.53
16	S	Sulfur	11.45	18.21	S	37.28
20	Ca	Calcium	5.62	11.17	Ca	18.30
14	Si	Silicon	0.27	0.38	Si	0.89

Table ah. SEM analysis of the sample T11M33, spot 2

Atomic number	Element symbol	Element name	Atomic concentration percentage	Weight concentration percentage	Oxide	Stoichiometric percentage
8	O	Oxygen	61.73	55.23		
7	N	Nitrogen	19.73	15.45	N	51.55
11	Na	Sodium	9.97	12.82	Na	26.05
16	S	Sulfur	4.81	8.62	S	12.56
20	Ca	Calcium	2.72	6.09	Ca	7.10
12	Mg	Magnesium	0.40	0.54	Mg	1.05
19	K	Potassium	0.38	0.82	K	0.99
14	Si	Silicon	0.27	0.42	Si	0.70

Table ai. SEM analysis of the sample T11M33, spot 3

Atomic number	Element symbol	Element name	Atomic concentration percentage	Weight concentration percentage	Oxide	Stoichiometric percentage
8	O	Oxygen	66.10	58.89		
7	N	Nitrogen	15.84	12.36	N	46.74
11	Na	Sodium	9.19	11.77	Na	27.11
16	S	Sulfur	4.31	7.70	S	12.72
20	Ca	Calcium	2.34	5.22	Ca	6.90
19	K	Potassium	1.00	2.17	K	2.94
12	Mg	Magnesium	0.69	0.93	Mg	2.03
17	Cl	Chlorine	0.32	0.63	Cl	0.94

SC 11. a) SEM image of the spots of T11M33 sample surface; b) spectrum of the sample whose elements are given in Table ag, ah and ai.